

Light dark matter searches with the NEWS-G experiment

Ioannis Katsioulas

Universite Paris-Saclay

CEA Saclay



University of Birmingham, June 29, 2018

ioannis.katsioulas@cea.fr



The dark matter conundrum

Observations of Zwicky 85 years ago

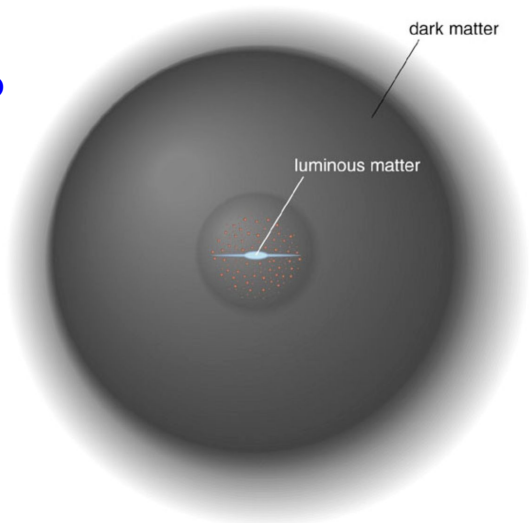
Die Rotverschiebung von extragalaktischen Nebeln
von F. Zwicky.
(16. II. 33.)

"The Redshift of Extragalactic Nebulae",
published in German in Helvetica Physica
Acta in 1933



"In a spiral galaxy, the ratio of dark-to-light matter is about a factor of ten. That's probably a good number for the ratio of our ignorance-to-knowledge. We're out of kindergarten, but only in about third grade."

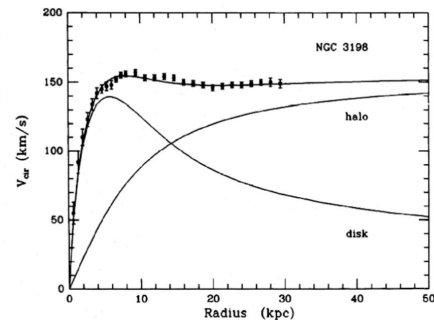
Vera Rubin



-What should it be from
astrophysical constraints:

- Mostly "Cold"
- Non-Baryonic
- "Weakly" interacting
- $\Omega_x h^2 = 0.1186 \pm 0.002$
- Stable or $\tau_x \gg \tau_U$

No Standard Model particle matches
the criteria



Dark matter detection

PHYSICAL REVIEW D

VOLUME 31, NUMBER 12

15 JUNE 1985

Detectability of certain dark-matter candidates

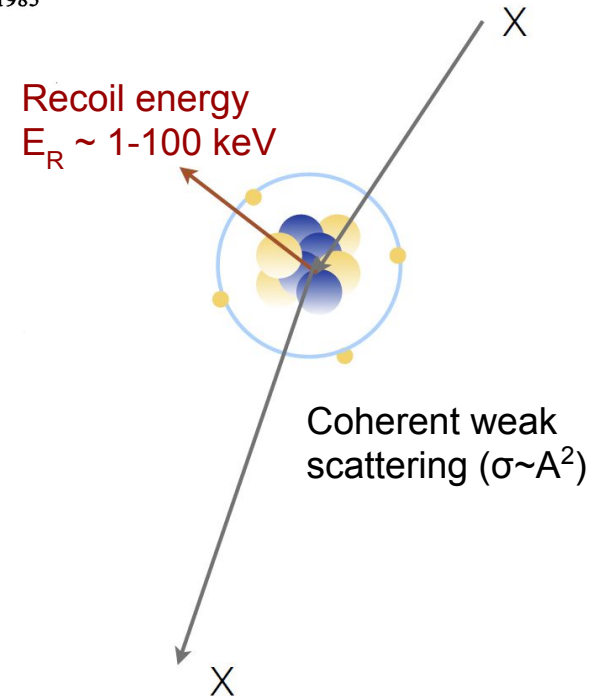
Mark W. Goodman and Edward Witten

Joseph Henry Laboratories, Princeton University, Princeton, New Jersey 08544

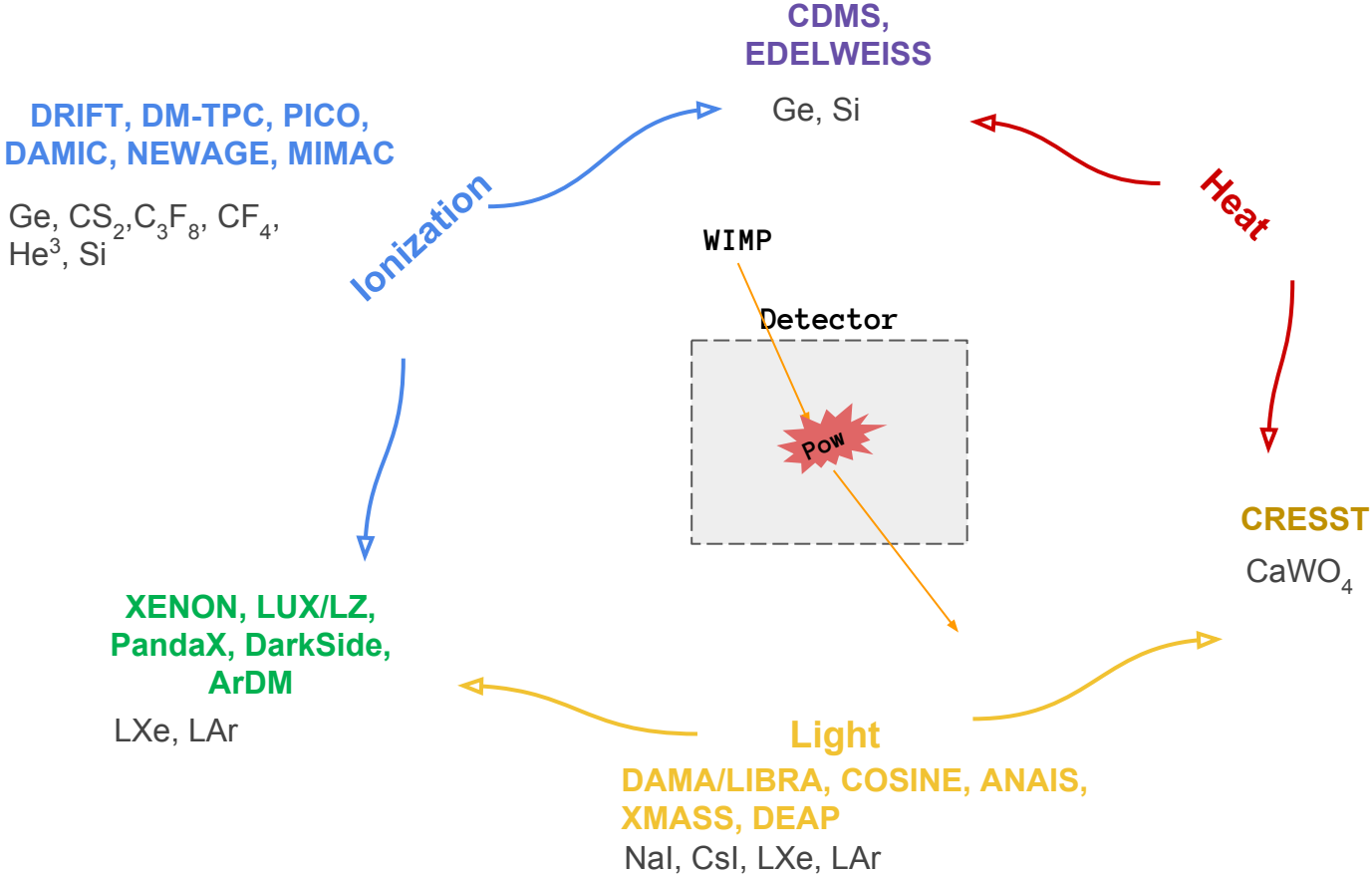
(Received 7 January 1985)

We consider the possibility that the neutral-current neutrino detector recently proposed by Drukier and Stodolsky could be used to detect some possible candidates for the dark matter in galactic halos. This may be feasible if the galactic halos are made of particles with coherent weak interactions and masses $1-10^6$ GeV; particles with spin-dependent interactions of typical weak strength and masses $1-10^2$ GeV; or strongly interacting particles of masses $1-10^{13}$ GeV.

“WIMP miracle” \Rightarrow Relic abundance explained by a massive particle ($10 \text{ GeV}/c^2$ - few TeV/c^2) interacting through weak scale interaction with baryonic matter

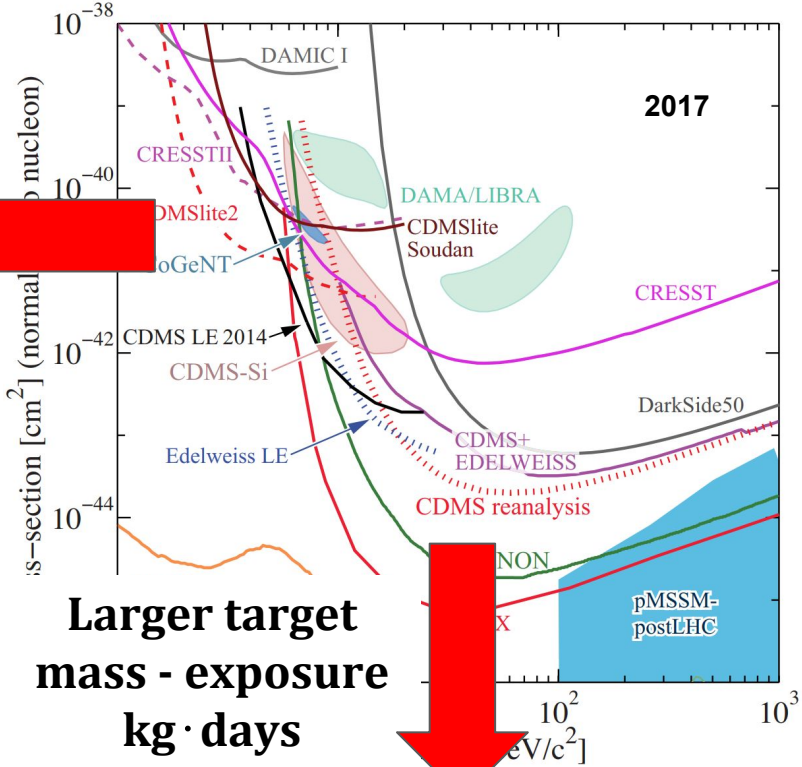
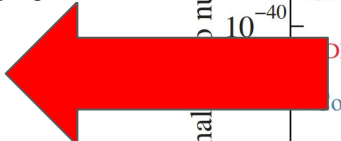


State of the art for dark matter detectors

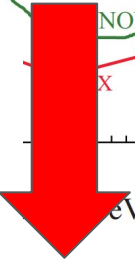


Status of dark matter searches

Detectors with a lower threshold

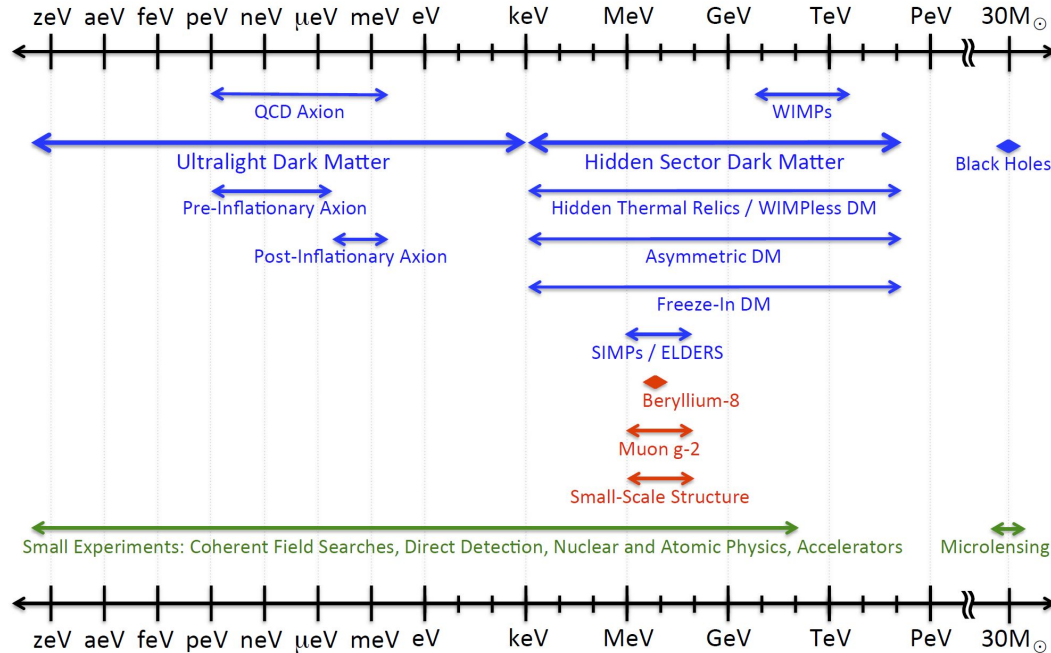


Larger target mass - exposure
kg · days



J. Feng and J. Kumar, "The WIMPless Miracle: Dark Matter Particles without Weak-scale Masses or Weak Interactions."

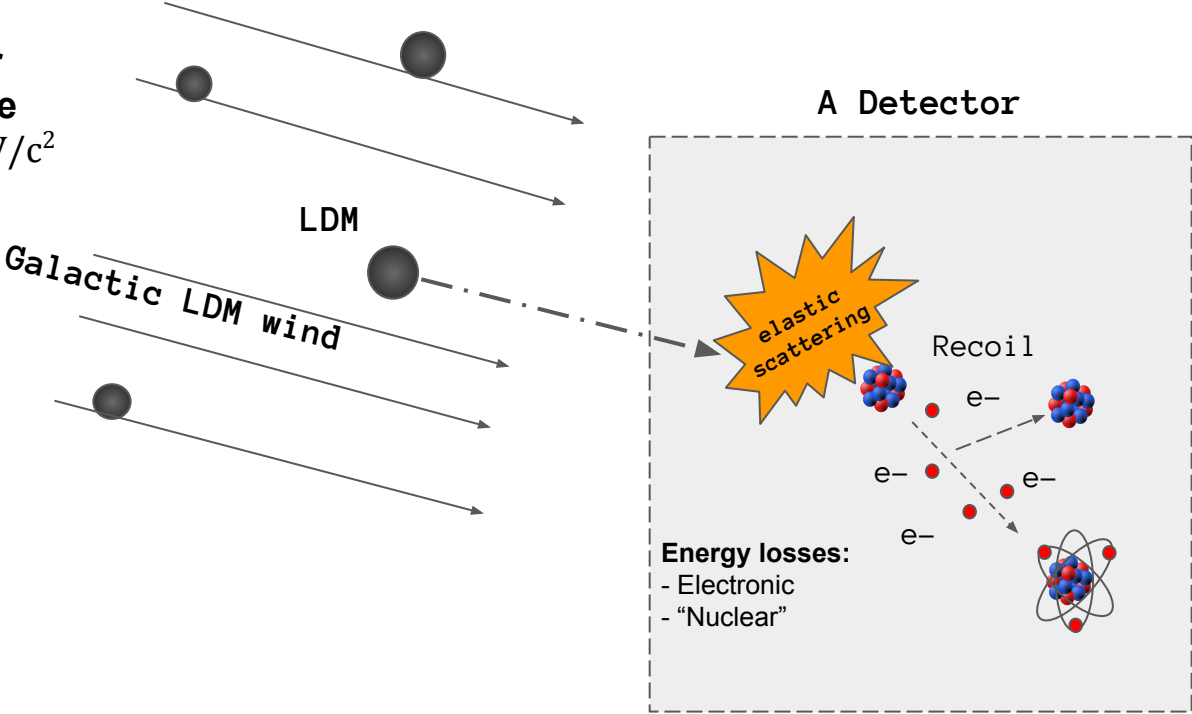
Dark Sector Candidates, Anomalies, and Search Techniques



Direct detection of light dark matter

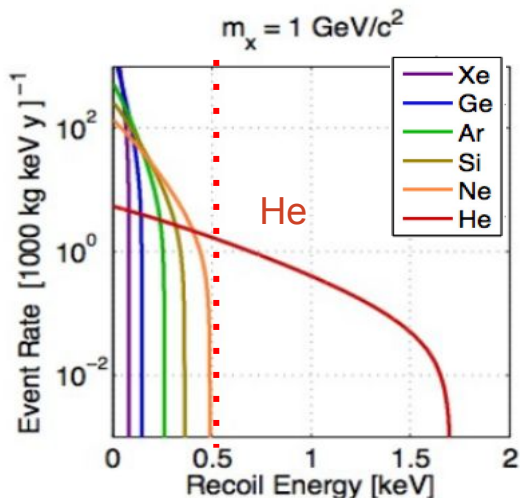
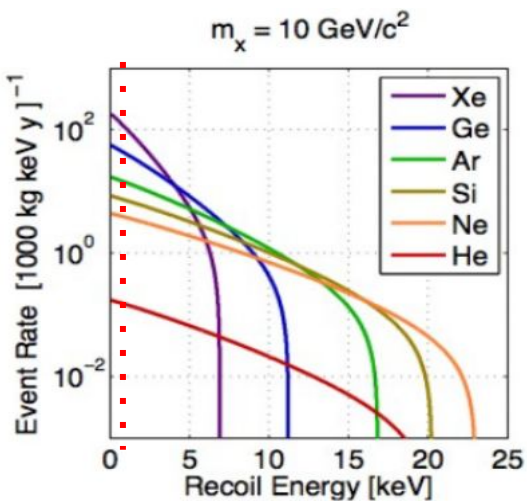
Detection through ionization - An example

**Light Dark Matter
(LDM) Mass range**
 $0.1\text{GeV}/c^2$ - few GeV/c^2



Comparison between heavy and light targets - A

Kinematics



- If we have $E_R = 500 \text{ eV}$ recoil induced by LDM particle of $M_\chi = 1 \text{ GeV}/c^2$

$$u_{min} = \sqrt{\frac{2 \cdot E_R}{r \cdot M_\chi}}$$

Minimum relative WIMP velocity to produce a recoil of E_R

$$E_R \rightarrow u_{min} \begin{cases} 1790 \text{ km/s for Xe target} \\ 1340 \text{ km/s for Ge target} \\ 1000 \text{ km/s for Ar target} \end{cases}$$

WIMP escape velocity $\sim 540 \text{ km/s}$

500 eV

Light Projectile + light target \Rightarrow Better kinematical match

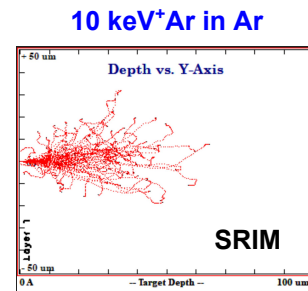
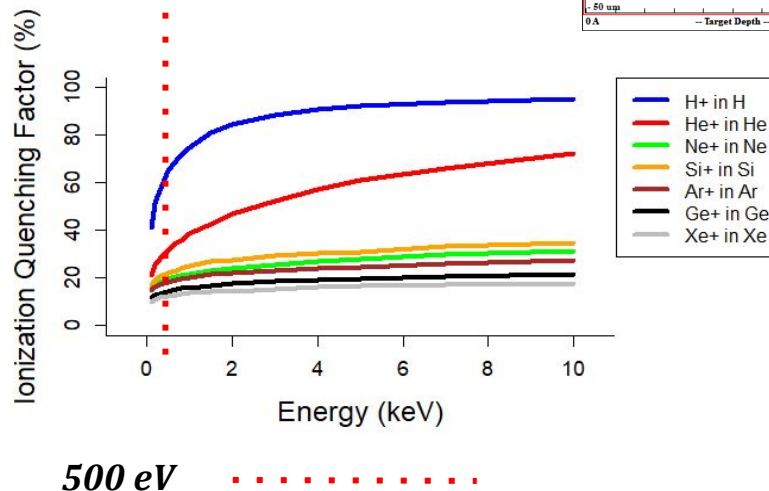
Comparison between heavy and light targets - B

Ionization quenching

Quenching factor (q_f) is defined as the fraction of the kinetic energy of an ion that is dissipated in a medium in the form of ionization electrons and excitation of the atomic and quasi-molecular states.

Detection energy threshold required due to quenching

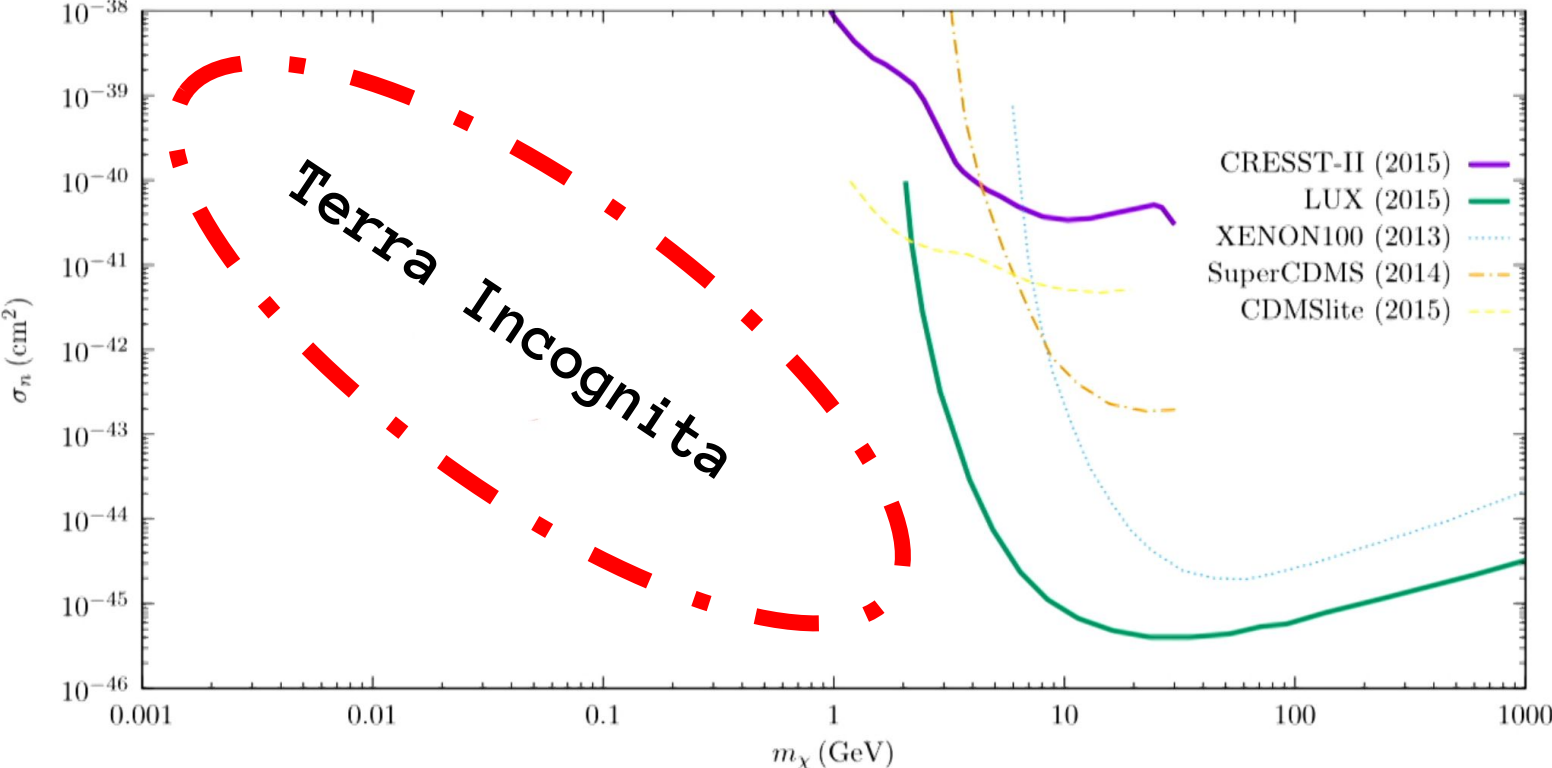
Target	Threshold (eV)
Xe	50
Ge	58
Ar	74
He	105



Light Projectile + light target \Rightarrow Less demanding detector threshold

Direct detection of light dark matter

No searches available in this region





Use light targets for dark matter searches?

Hydrogen, Helium \Rightarrow Gases (NTP) \Rightarrow Gaseous detector ???

Spherical Proportional Counter (SPC)

Fun fact

Old LEP RF cavities

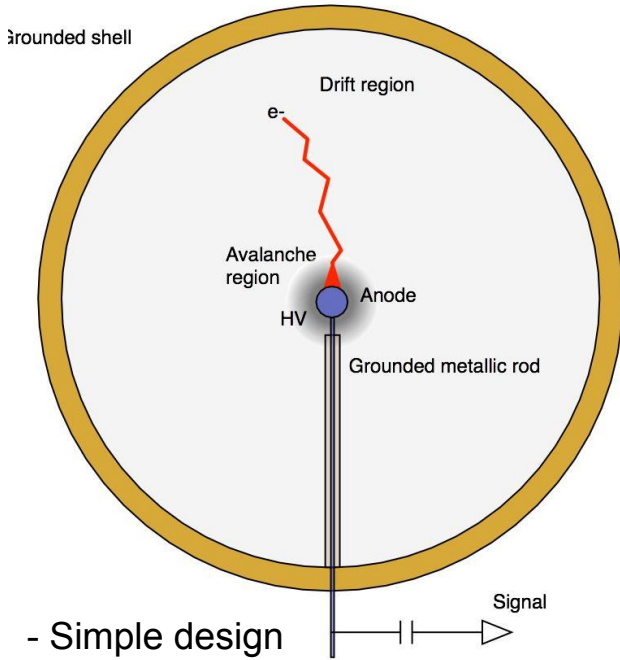


Spherical gaseous detectors



*In the picture:
I.Giomataris, G.Chapak*

The structure of the SPC



- Simple design
- Single readout

Electric field

Strong dependence on the radius

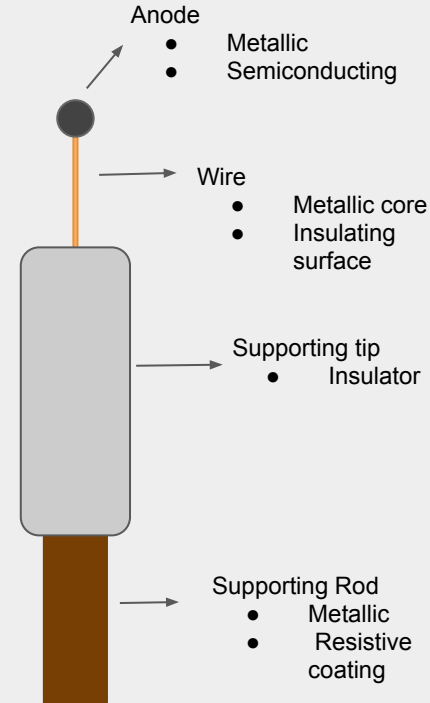
$$E(r) = \frac{V_0}{r^2} \frac{r_A r_C}{r_C - r_A} \approx \frac{V_0}{r^2} r_A$$

r_A = anode radius
 r_C = cathode radius

Natural division of the volume in two

- Drift volume
- Multiplication volume

The "Sensor"

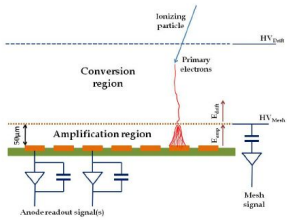


Advantage of spherical geometry - A

$C \sim$ Electronic noise
 \uparrow Electronic noise \uparrow Threshold

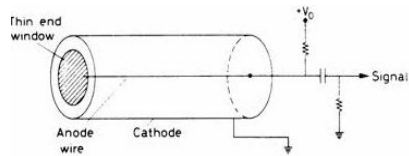
Capacities for a 1 m³ detector in different geometries

Parallel Plate



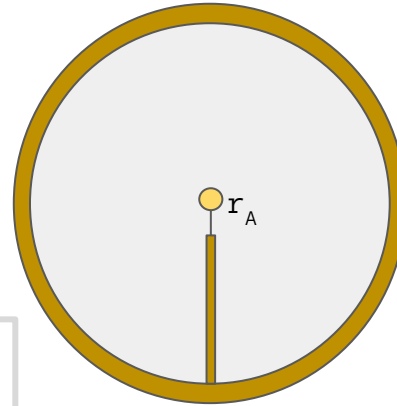
$$C = \epsilon_0 \frac{S}{d} \approx 3500 \text{ pF}$$

Cylindrical



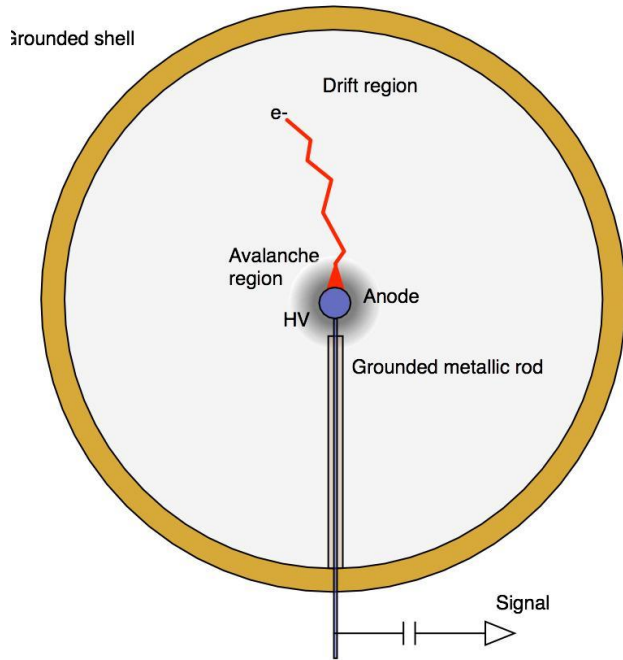
$$C = 2\pi\epsilon_0 \frac{L}{\ln(b/a)} \approx 115 \text{ pF}$$

Spherical



$$C \approx 4\pi\epsilon_0 r_A \approx 1.5 \text{ pF}$$

Advantage of spherical geometry - B



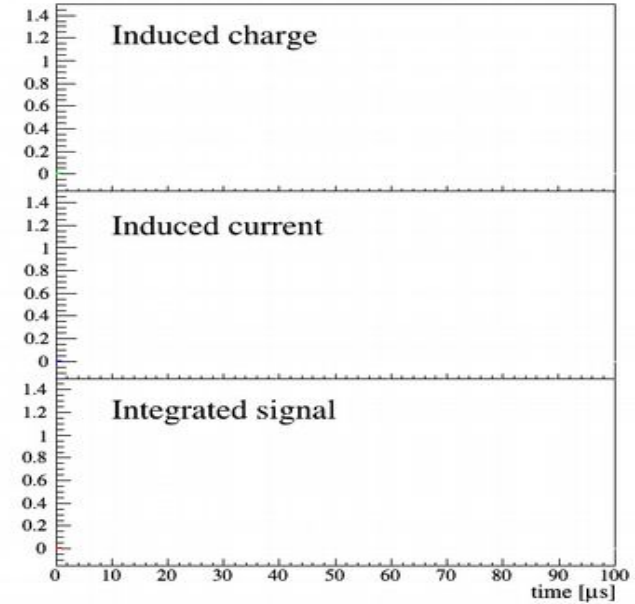
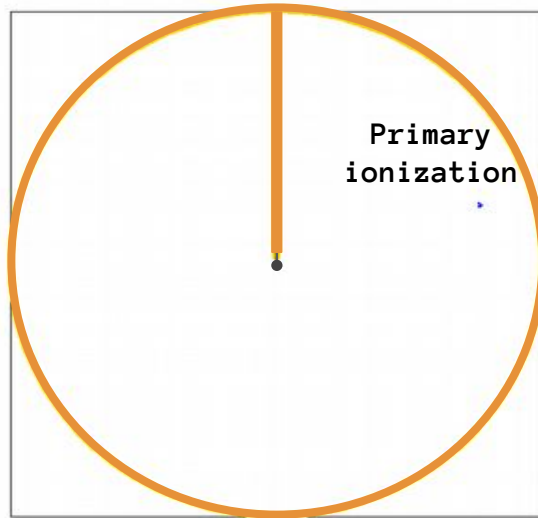
Advantages of the spherical geometry

- Lowest surface to volume ratio
- Sustains higher pressure
- Robustness (anode \varnothing 1 mm - 6.3 mm)

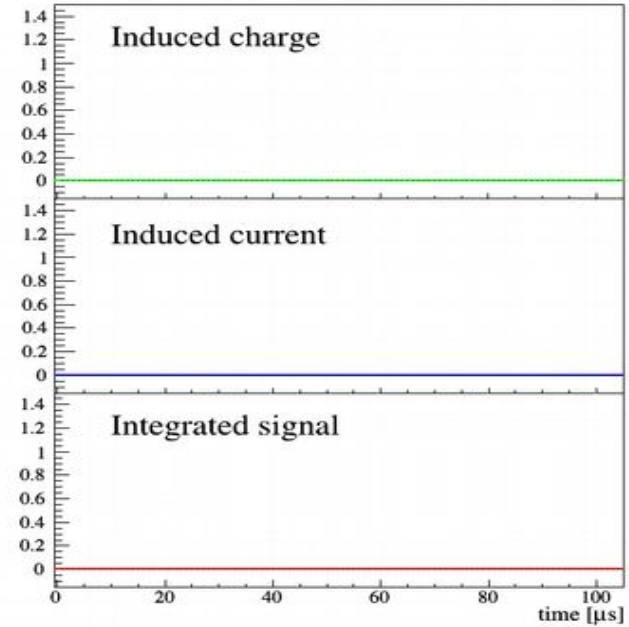
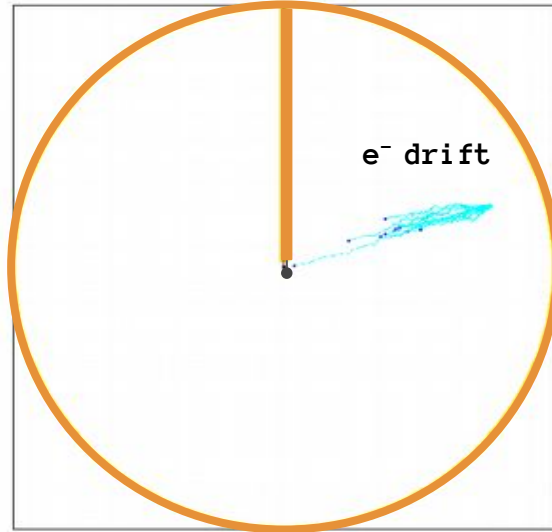
Built solely by radiopure materials

- Vessel made of Cu (~tens of kg)
- Rod made of Cu (~hundreds of gr)
- **All the rest less than weigh < 1 g**

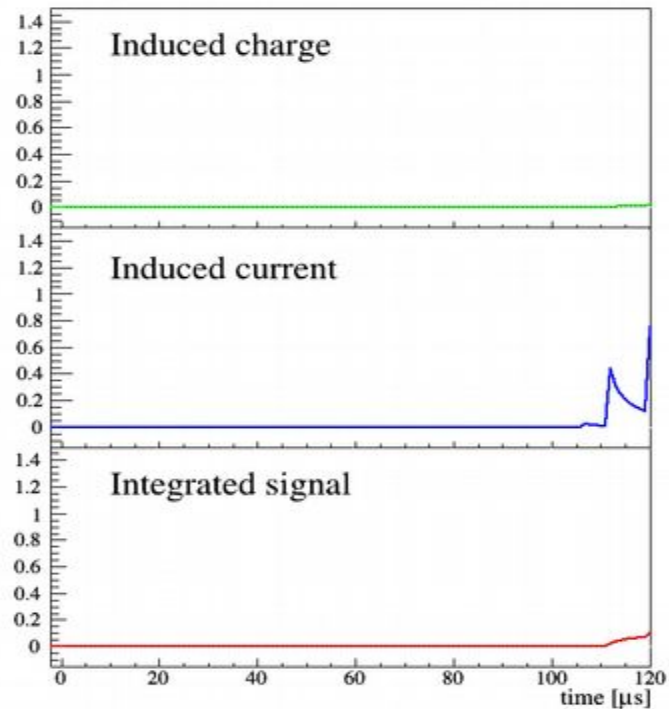
Pulse production



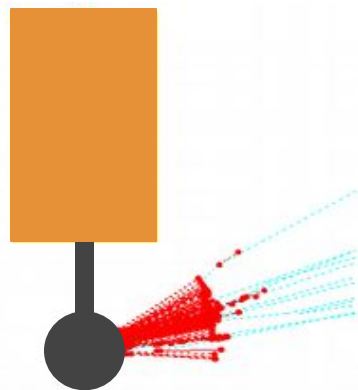
Pulse production



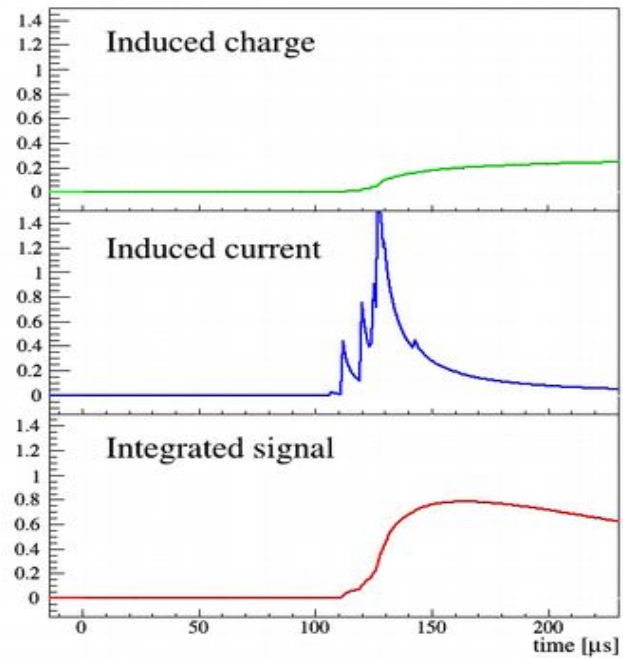
Pulse production



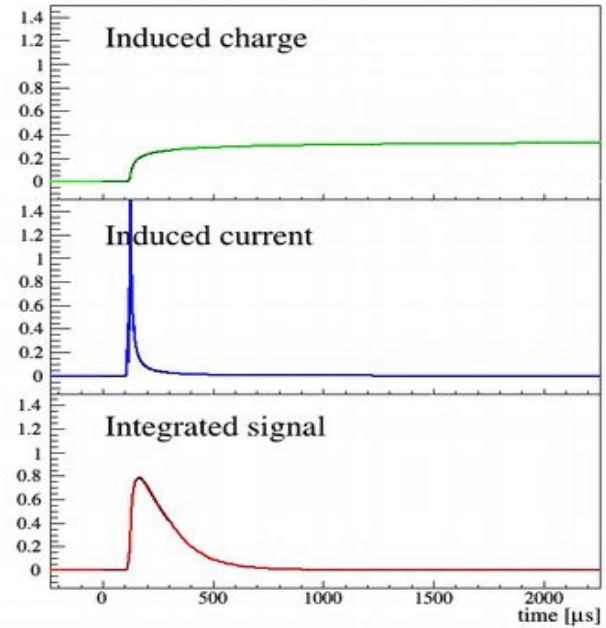
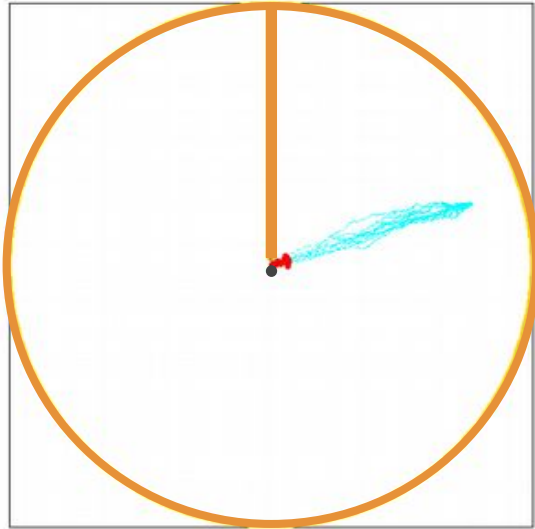
Pulse production



Drift of slow moving ions



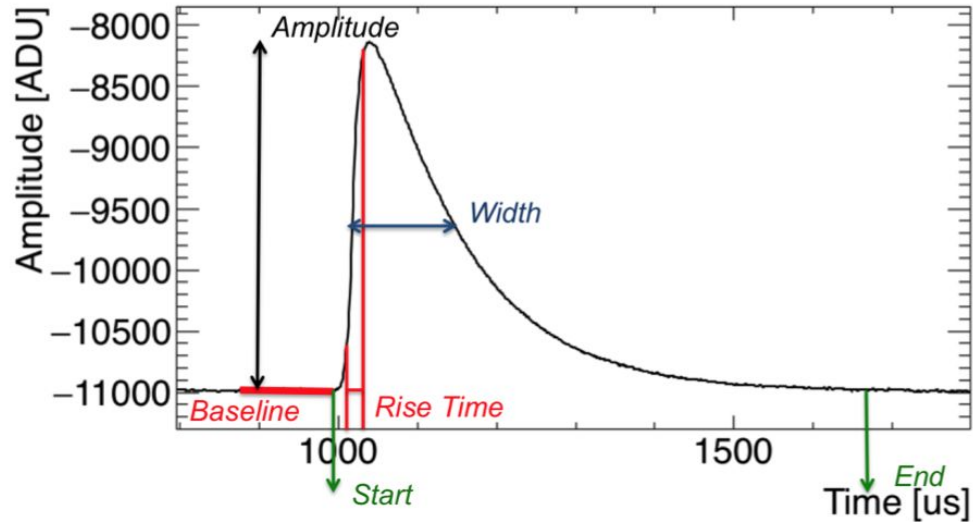
Pulse creation



Induced Pulses

Pulse Shape Analysis (PSA) parameters

Long Tail Pulse



Rise time & Width \propto Drift time dispersion

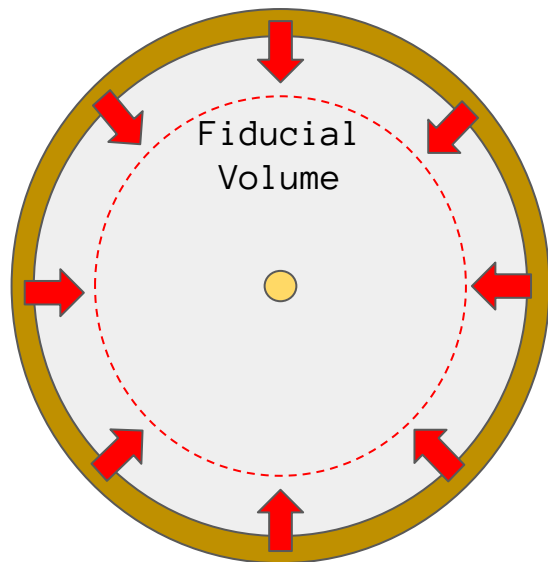
Basic Parameters

- Baseline
- Noise
- Amplitude (Pulse Height)
- Rise time
- Width
- Integral
- Number of peaks

A lot of information
hiding in the pulse
shape

Background rejection capabilities-A

Fiducialization



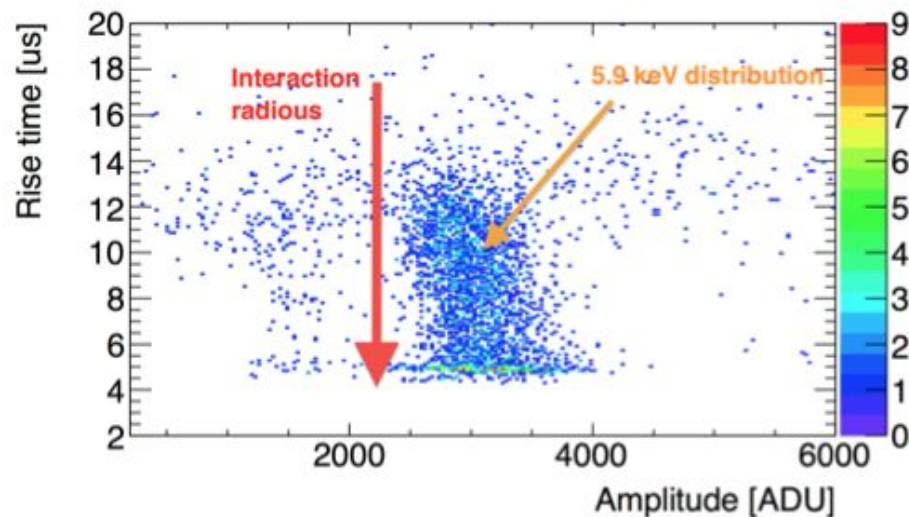
Background comes from the materials of the vessel

 **Surface**

Primary e- drift time dispersion

$$\sigma(r) \propto (r/r_{\text{sphere}})^3$$

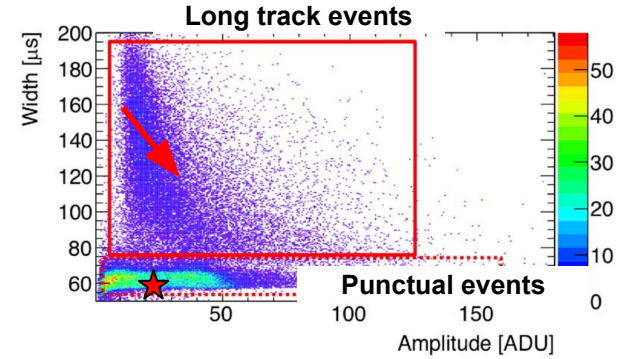
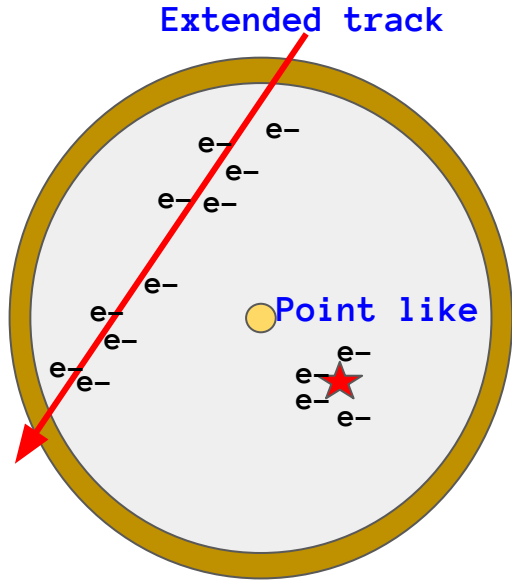
5.9 keV X-rays line



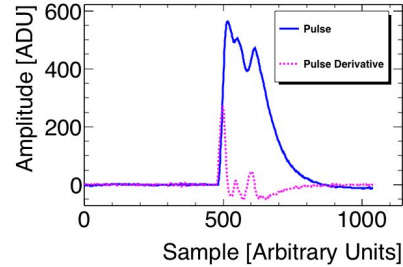
Rise time → Δt between 90% - 10% of pulse height

Background rejection capabilities-B

Event discrimination

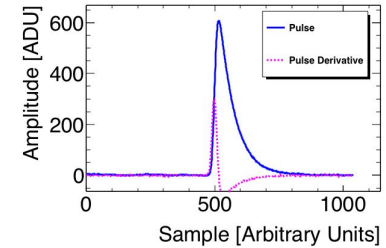


Muon pulse



Amplitude = 575 ADU
Width (FWHM) = 155.5 μs
Rise time = 18.2 μs

^+Ar pulse



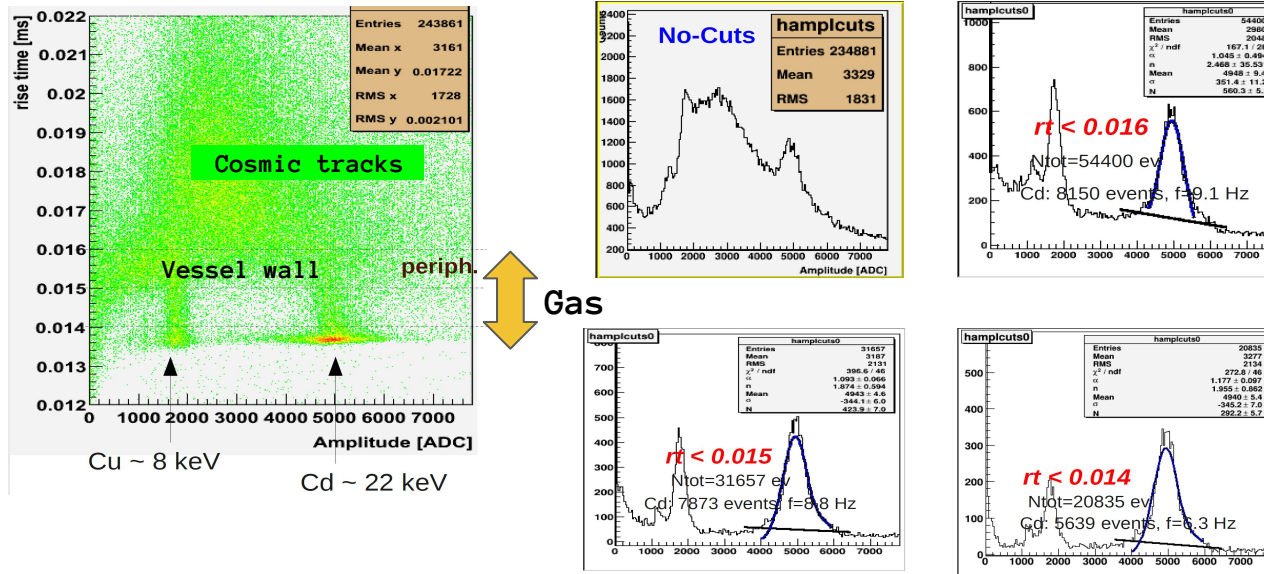
Amplitude = 606 ADU
Width (FWHM) = 63.4 μs
Rise time = 16.3 μs

Illustration of the basic analysis principle

^{109}Cd source

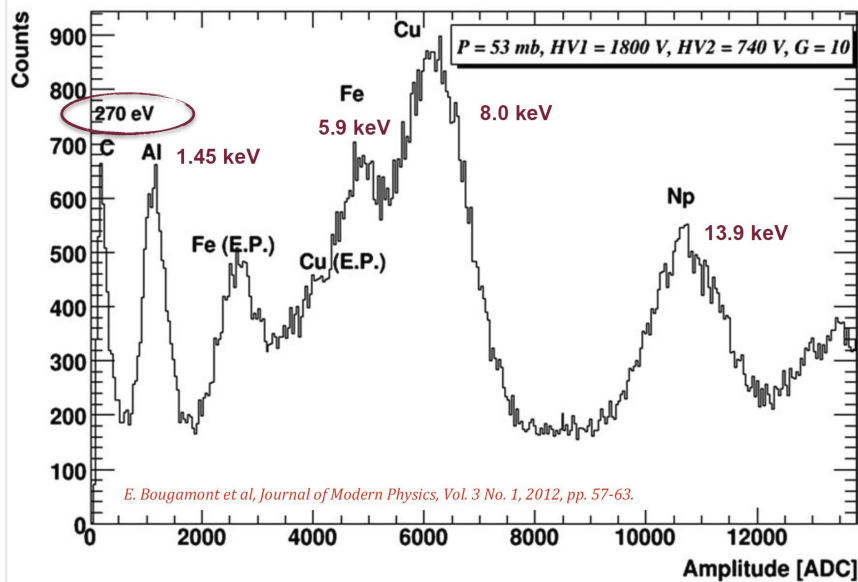
Irradiation through 200 μm Al window

P = 100 mb, Ar-CH₄ (2%)



Efficiency of the cut in $rt \rightarrow \sim 70\%$ signal (Cd line)
Significant background reduction

Low energy detection capabilities of a large volume SPC



SPC \varnothing 130 cm

Gas: Ar+2%CH₄

Detection of fluorescence X-rays

$^{241}\text{Am} \rightarrow ^{237}\text{Np} + ^4\text{He} + 5.6 \text{ MeV}$

Lines

Al \rightarrow 1.45 keV

Cu \rightarrow 13.93 keV

$^{237}\text{Np} \rightarrow 13.93 \text{ keV}(L_{\alpha}) 17.60 \text{ keV}(L_{\beta})$

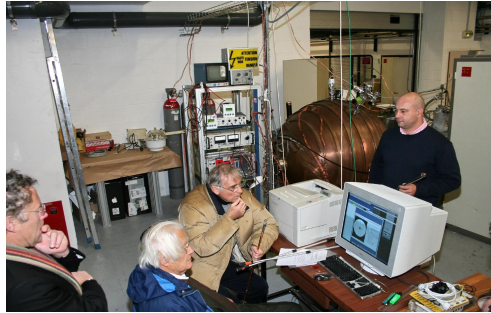
-Energy threshold at the single electron level

The spherical detector around the globe

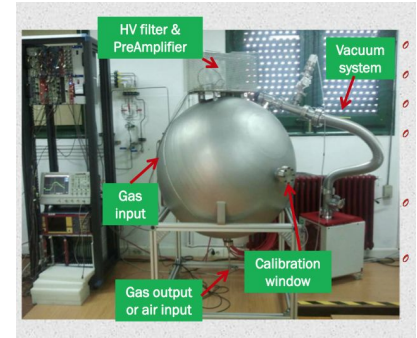
LSM, Modane



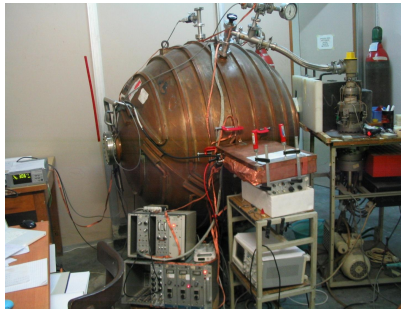
CEA Saclay



University of Saragoza



University of Thessaloniki



Queen's University



University of Tsinghua



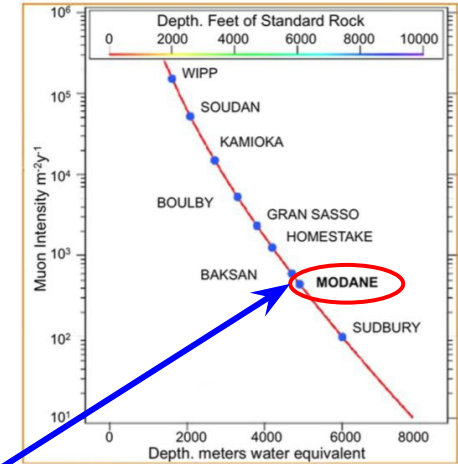
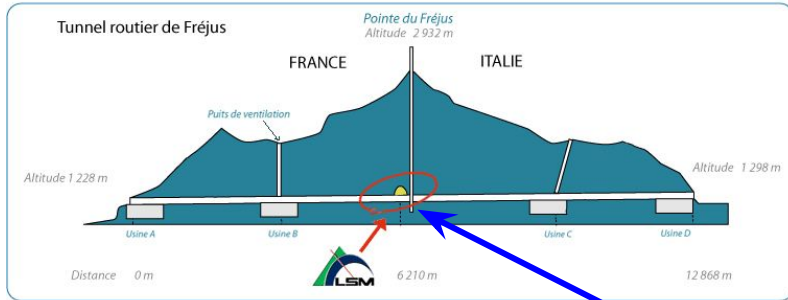
Also joining University of Bordeaux and very soon University of Birmingham

The SEDINE detector at LSM - A

One of the deepest and “quietest” laboratories in the world



Laboratoire Souterrain de Modane



4800 wme
5 $\mu/m^2/day$

The SEDINE detector at LSM - B

A competitive detector and a testing ground for NEWS-G / SNO

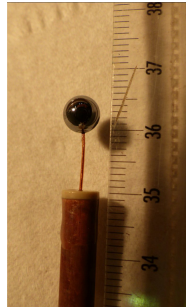
Vessel

Ø 60cm copper

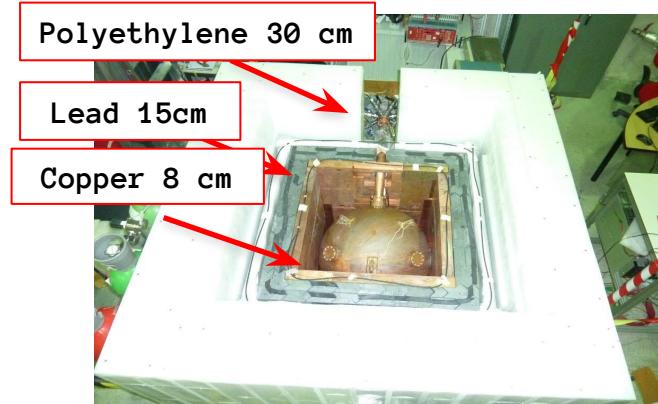


Sensor

Ø 6.3mm Si

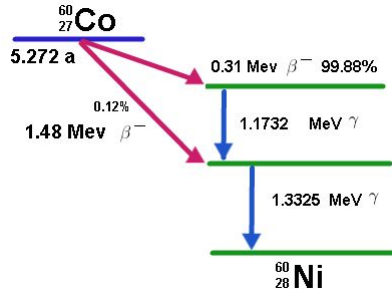


Shielding



- Copper vessel (Ø 60 cm)
- Equipped with a 6.3 mm Ø sensor
- Chemically cleaned several times for Radon deposit removal

Main background sources for LSM detector



^{60}Co Contamination of 1 mBq/kg
BG Rate = $0.3\text{-}0.5 \text{ keV}^{-1}\text{kg}^{-1}\text{day}^{-1}$

Solution: Limit time exposure on ground for pure copper.

^{210}Pb , ^{210}Bi Contamination of 1 nBq/kg

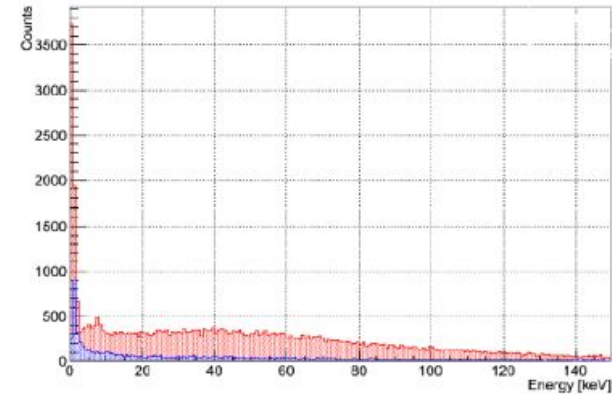
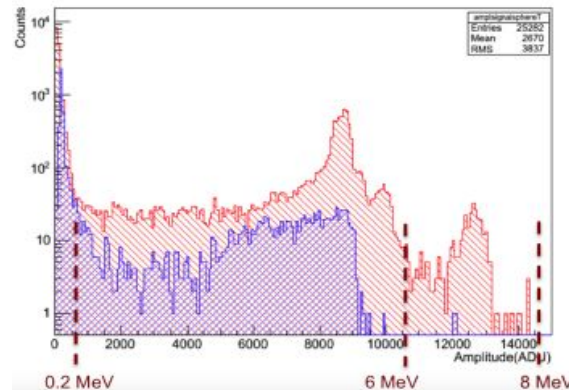
BG Rate = $0.1 \text{ keV}^{-1}\text{kg}^{-1}\text{day}^{-1}$

Competitive BG levels

Solution: Chemical cleaning

Effect of cleaning:

- High energy events 180 mHz
=> $\sim 2 \text{ mHz}$
- Low energy events 400 mHz
=> $\sim 20 \text{ mHz}$



WIMP search run data

Target: Ne+0.7%CH₄ at 3.1 bar
→ 280 gr target mass

Duration: 42 days in sealed mode

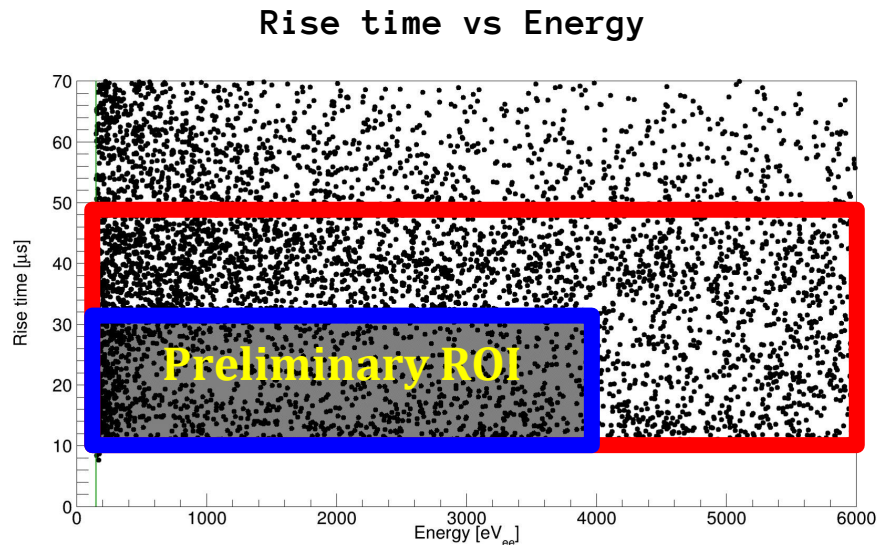
Dead time: 20.1%

Exposure: 9.6 kg*days (34.1 live-days x 0.28 kg)

Trigger threshold: 35 eVee (~100% efficient at 150 eVee)

Analysis threshold: 150 eVee (~720 eVnr)

Calibration: ³⁷Ar gaseous source, 8 keV Cu fluorescence, AmBe neutron source



Sideband region used together with simulations to determine the number and distribution of expected events in preliminary ROI

Simulating the detector response

Modeling the rise time vs energy response

Electric field

- Field map from COMSOL

Drift of primary electrons

- Magboltz drift parameters

Quenching factor

- Parametrization derived from SRIM

Avalanche

- Polya distribution estimation using Garfield++

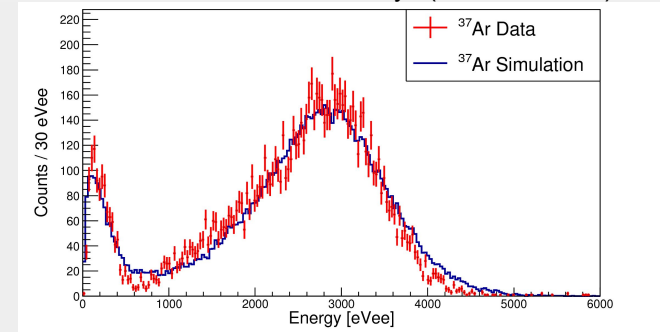
Simulated pulses

- Ion induced current preamplifier response
- Noise templates taken from the pretraces of real pulses

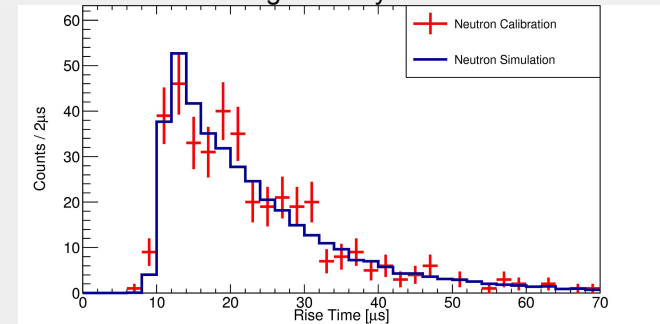
Same trigger algorithm and processing as used for real pulses

Validation

^{37}Ar gaseous source
2.82 keV and 270 eV X-rays (K and L shells)



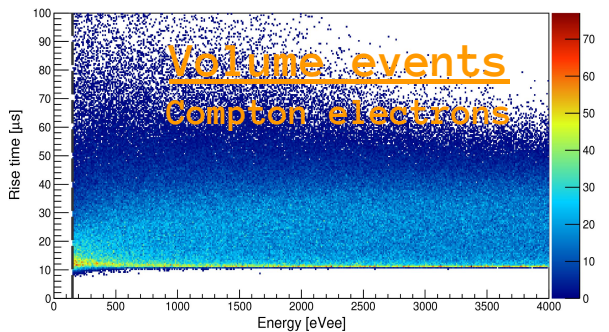
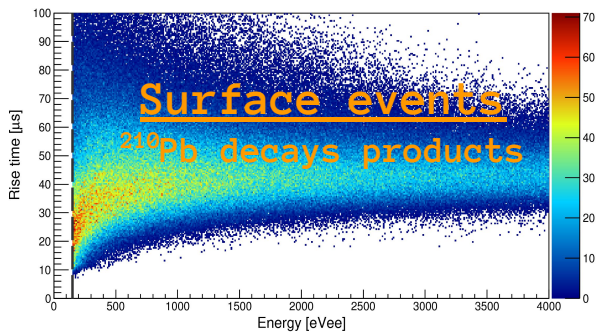
^{241}Am - ^9Be neutron source
Nuclear recoils homogeneously distributed in the volume



Analysis of the WIMP run data

Analysis methodology - BDT

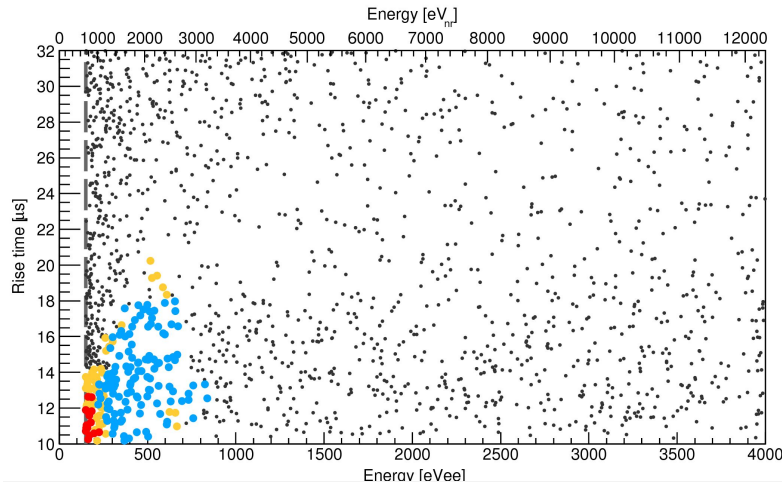
Background modeling



Trained with
simulated WIMP
and background
events

BDT

Mass dependent selection for 8 WIMP masses

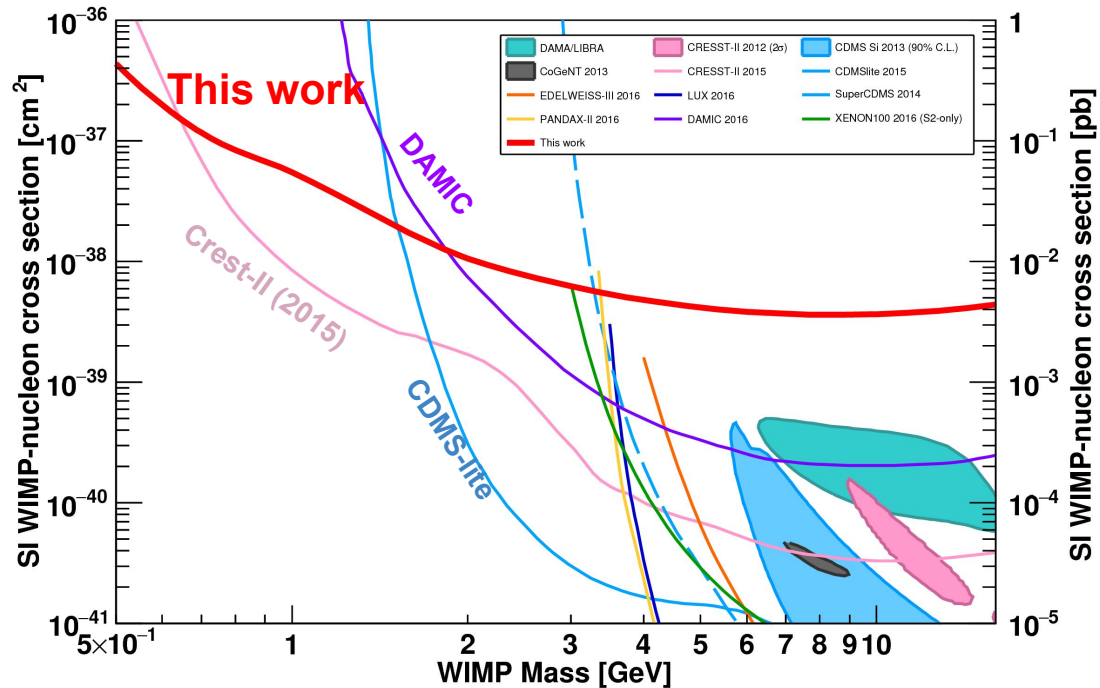


1620 events recorded in the preliminary ROI

- Failed any of the BDT cuts
- pass the BDT cut for $0.5 \text{ GeV}/c^2$: 15 events
- pass the BDT cut for $16 \text{ GeV}/c^2$: 123 events
- pass the BDT cut for other masses

First results of NEWS-G with SEDINE

[NEWS-G collaboration, Astropart. Phys. 97, 54 \(2018\), doi: 10.1016/j.astropartphys.2017.10.009](https://doi.org/10.1016/j.astropartphys.2017.10.009)



Exclusion at 90% confidence level (C.L.) of cross-sections above $4.4 \cdot 10^{-37} \text{ cm}^2$ for a $0.5 \text{ GeV}/c^2$ WIMP

Limit set on spin independent WIMP coupling with standard assumptions on WIMP velocities, escape velocity and with quenching factor of Neon nuclear recoils in Neon calculated from SRIM

NEWS-G current status & developments

Preparing the He physics run

Gas quality

Testing gas mixtures of He/CH₄

- High pressure operation (Penning)
- Hydrogen rich target

Upgrading gas system

- Tightness
- Filtering
- Gas recirculation
- Residual Gas Analyzer monitoring

Sensor developments

Aims

- High pressure operation
- High gain
- Increased stability
- Low radioactivity

Techniques

- Resistive technologies
- 3D printing technologies
- FEM simulations

Quenching factor measurements

- Ion / electron beam (LPSC, France)
- Neutron beam (TUNL, USA)

Study of the detector response

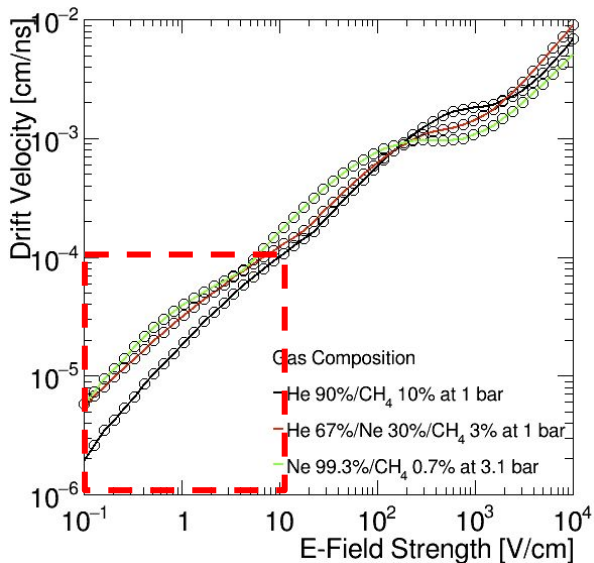
Solid state laser (213 nm)

- drift time measurements
- parametrization of the avalanche process

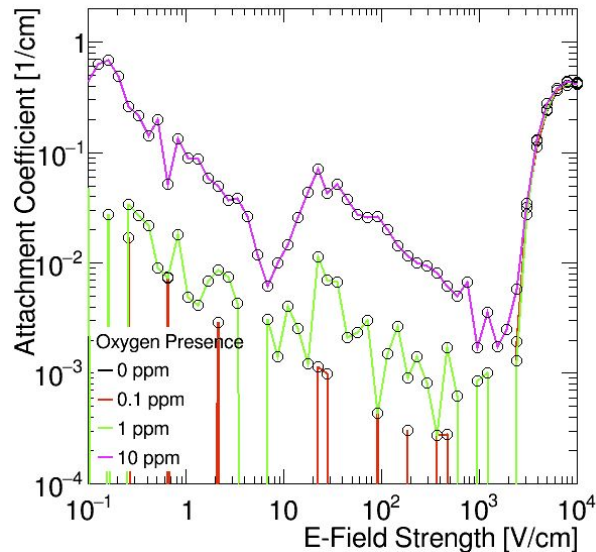
Experience operating with a He mixture

Sensitivity to contaminants - Attachment

Drift velocity of e^-



Attachment coefficient vs E-field magnitude



Range of low E-field - - - -

Gas quality - A

Required purity ~ ppb

He BIP®

O ₂	< 10	ppb
H ₂ O	< 20	ppb
CO+CO ₂	< 0.5	ppm
THC (as CH ₄)	< 100	ppb
N ₂	< 1	ppm

Experts® Gases

Ar BIP®

O ₂	< 10	ppb
H ₂ O	< 20	ppb
CO+CO ₂	< 100	ppb
THC (as CH ₄)	< 100	ppb
N ₂	< 1	ppm

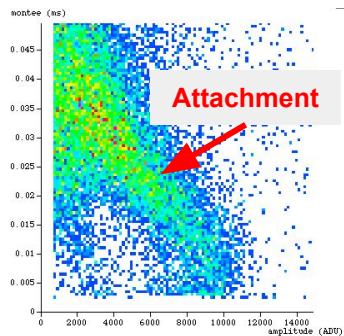
Experts® Gases

Gas quality - B

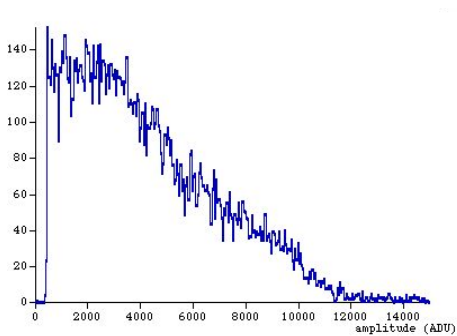
Gas filtering

He/CH4 (90/10)
600 mbar
HV1=1820 V
HV2=+225 V
Ball Φ 2 mm
No OXISORB

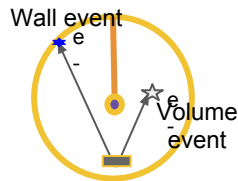
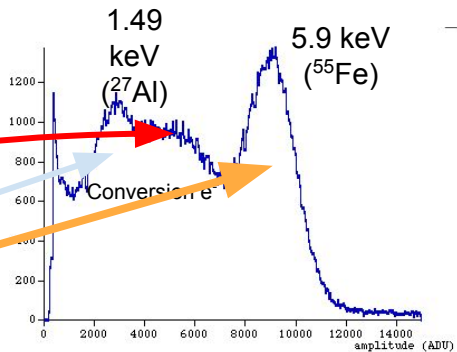
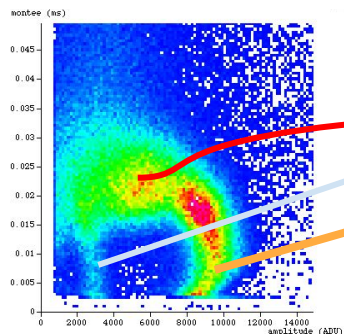
Rise time vs Amplitude 2D Histo



Amplitude 1D Histo



He/CH4 (90/10)
600 mbar
HV1=1840 V
HV2=+300 V
Ball Φ 2 mm
OXISORB



Improvements

Vacuum conditions

1.E-4 mbar \rightarrow 1.E-5 mbar \rightarrow 1.E-6 mbar

Leak Rate \approx 1.4E-6 mbar*L/s

\Rightarrow Not a dramatic effect

Gas quality

Contaminants \sim ppm

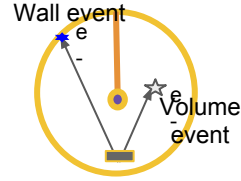
\downarrow
Oxisorb \sim 100 ppb

\Rightarrow **Big improvement**

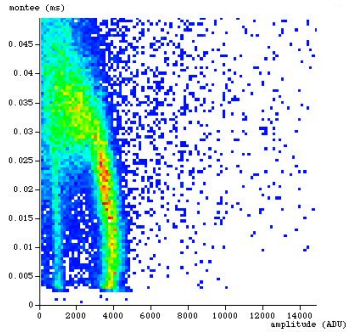
Increased drift velocity results in less attachment

Gas quality - C

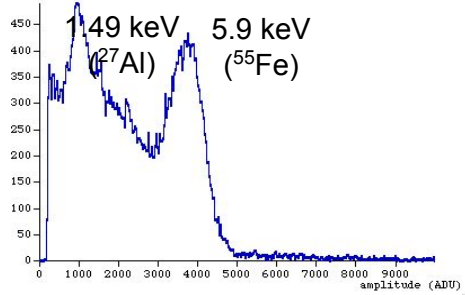
Removing sources of outgassing



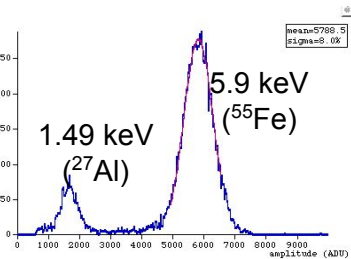
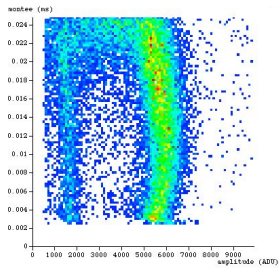
Rise time vs Amplitude 2D Histo



Amplitude 1D Histo



No cuts



After Cuts

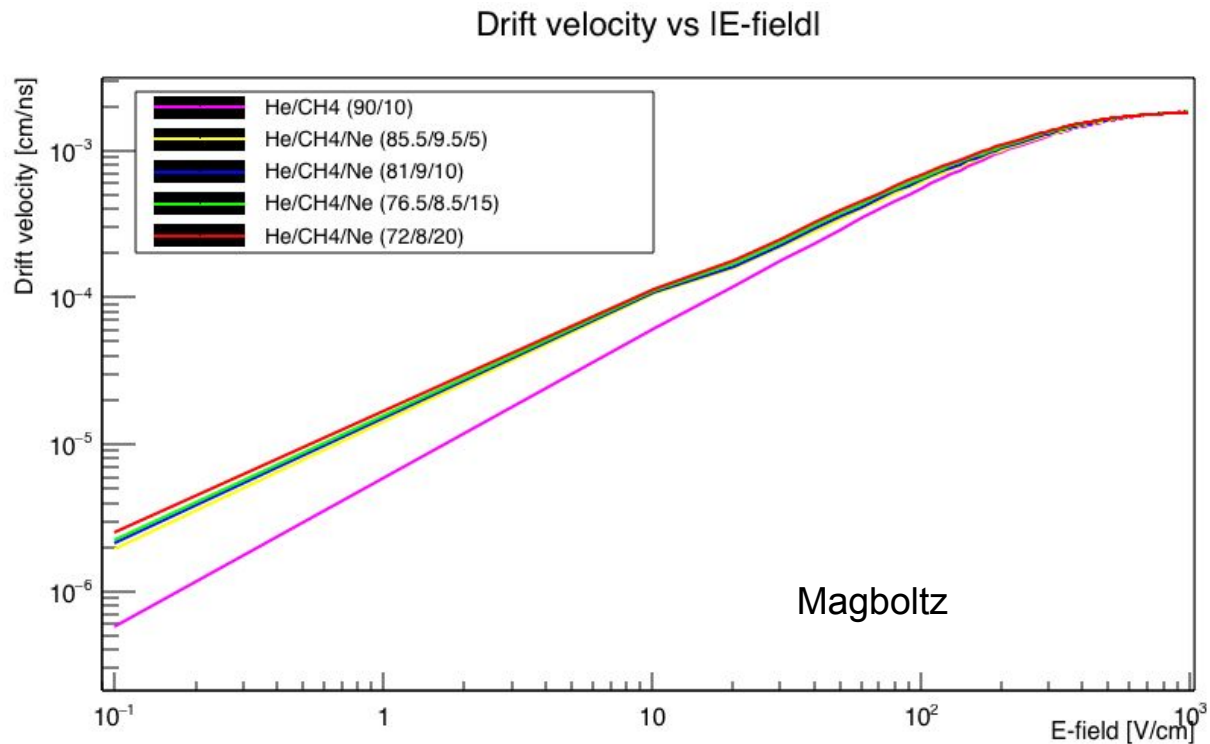
Risetime [2,25] μ s

Result

- The whole signal is $< 25 \mu$ s (before $< 35 \mu$ s)
- Resolution at 6 keV (σ) $\sim 8\%$ (instead $\sim 10\%$)
- Resolution at 1.49 keV (σ) $\sim 17.2\%$ (instead $\sim 22\%$)
- Clear separation between conversion e- events and volume events

Drift velocity increment

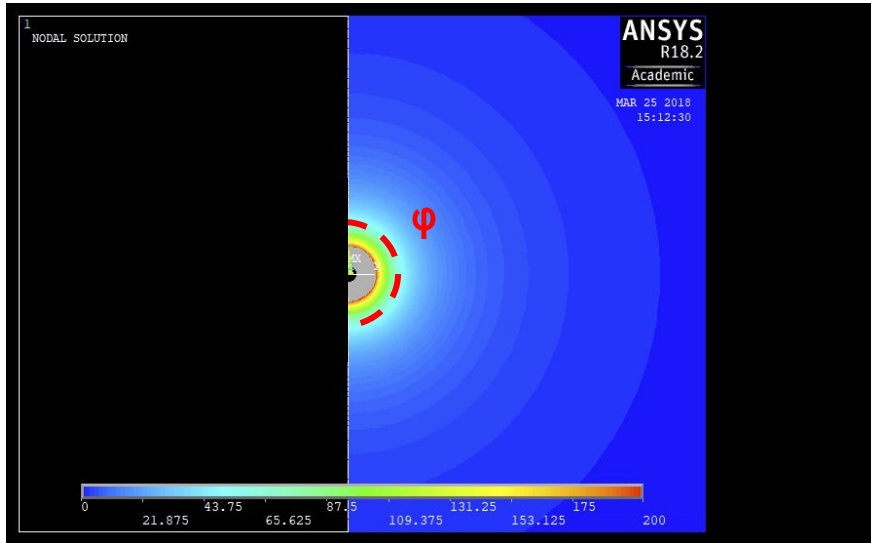
The effect of adding a third noble gas



Sensor influence on the E-field

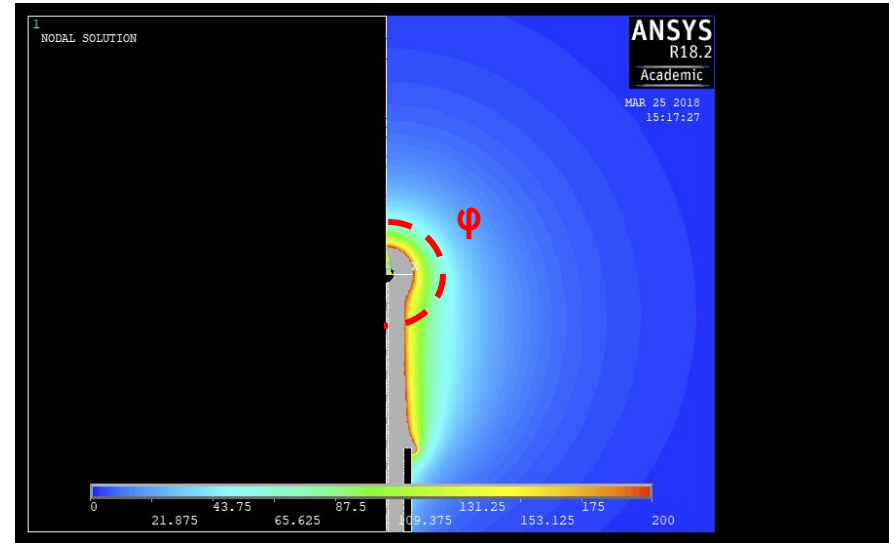
Electric field magnitude dependence on the azimuthal angle (ϕ) - Inhomogeneous response

The ideal case



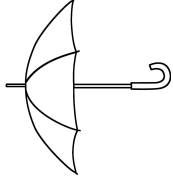
- A floating ball with a HV applied on its surface

The reality



- A ball connected to a wire through which the HV is applied on the ball.
- The wire - ball structure is supported by a grounded rod.

The umbrella

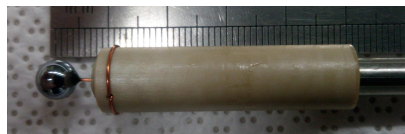
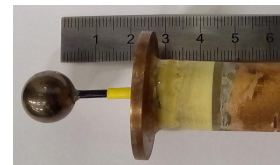
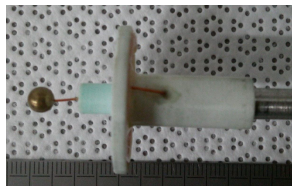


Material used: Copper, Brass, Steel, Iron, PE, PEEK, Teflon, Kapton, Plexiglass, Si, Araldite

Introduction of a secondary correction electrode

Goals:

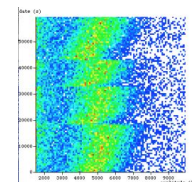
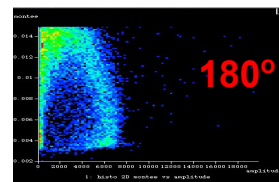
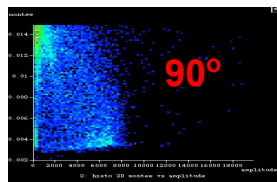
- Homogeneous field
- Limited discharges
- Operation in high pressure
- Stability



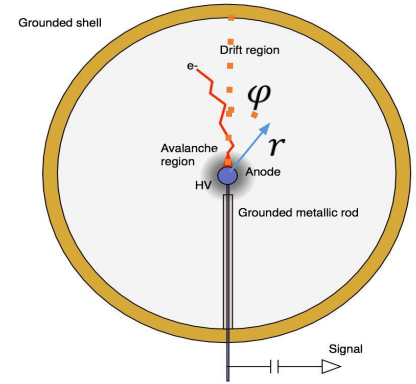
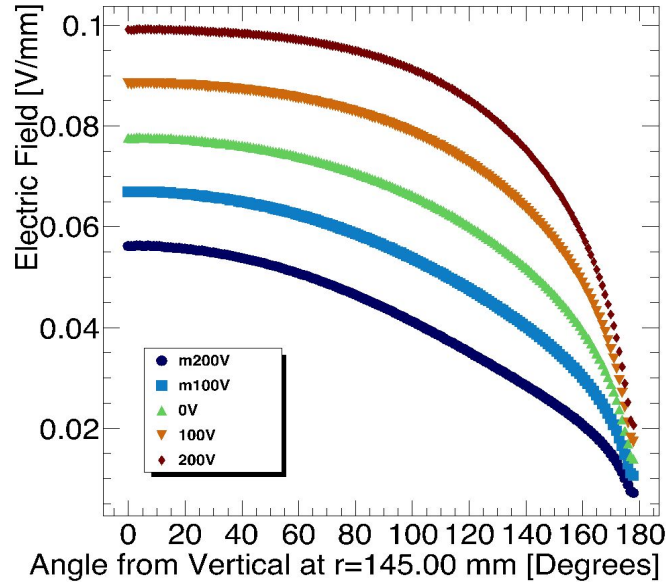
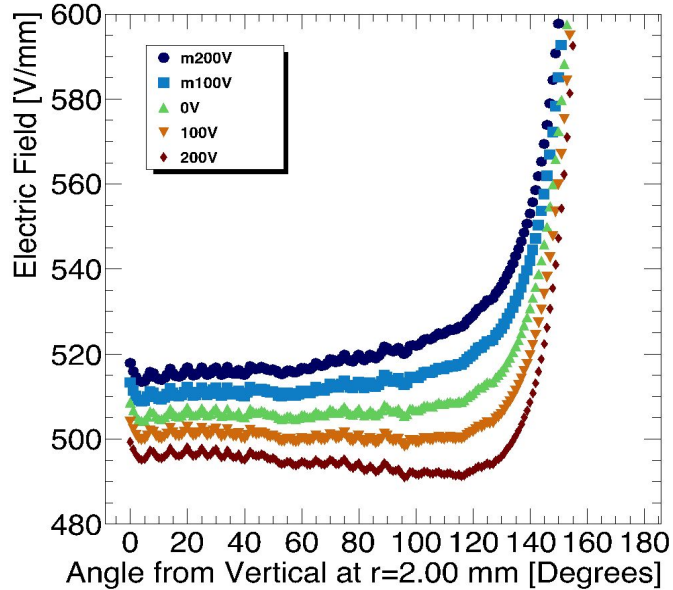
Inhomogeneous response

Instability

Possible issues

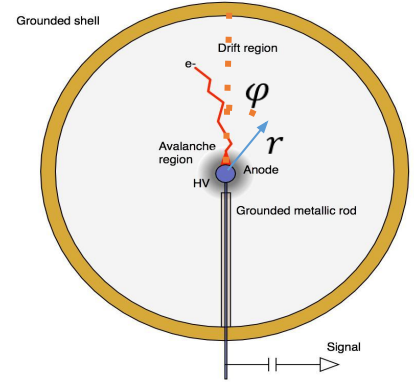
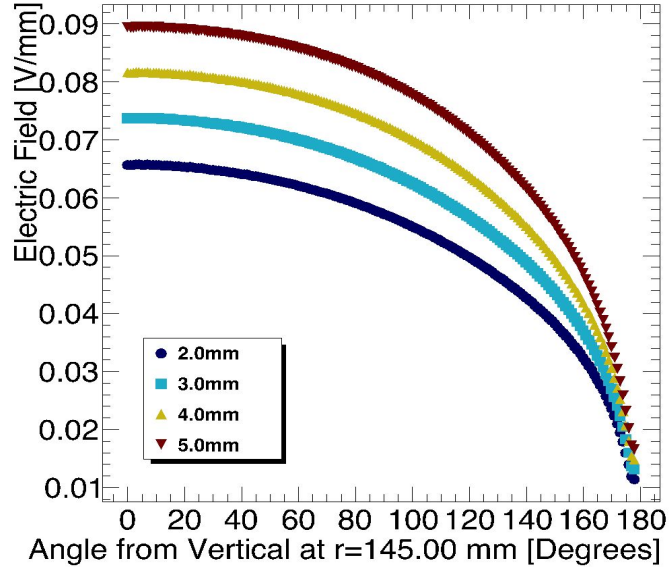
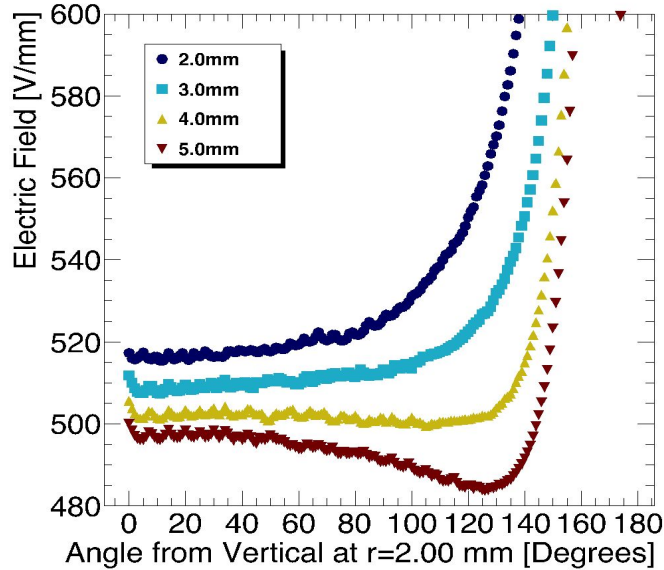


Sensor Design: Umbrella Voltage



$r_A = 1$ mm
 $r_C = 150$ mm
 $V_A = 2000$ V
Separation = 3.5 mm

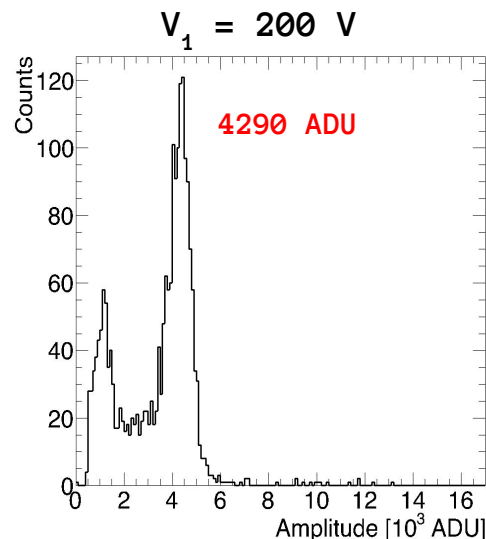
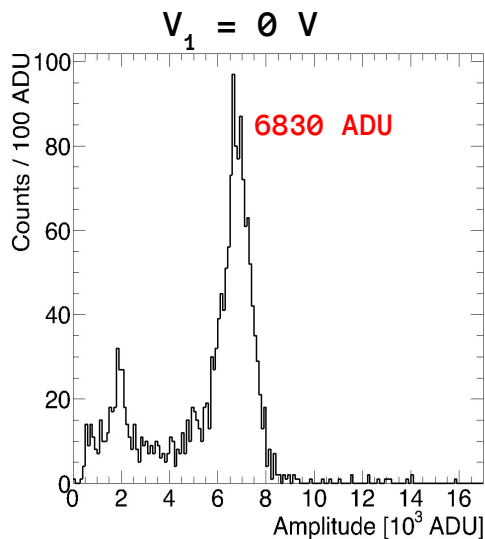
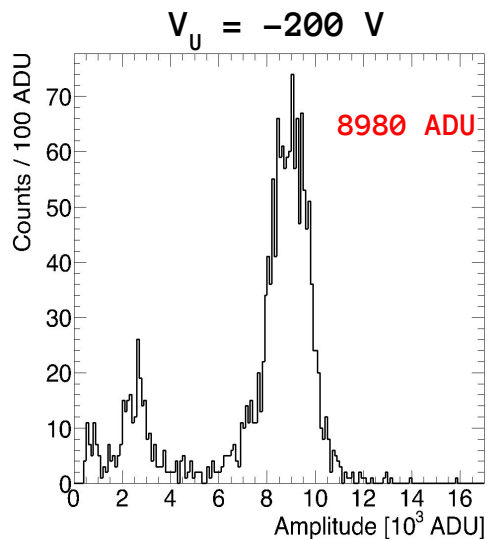
Sensor Design: Anode-Umbrella Separation



$$\begin{aligned} r_A &= 1 \text{ mm} \\ r_C &= 150 \text{ mm} \\ V_A &= 2000 \text{ V} \\ V_U &= 0 \text{ V} \end{aligned}$$

Sensor Design: Measurements

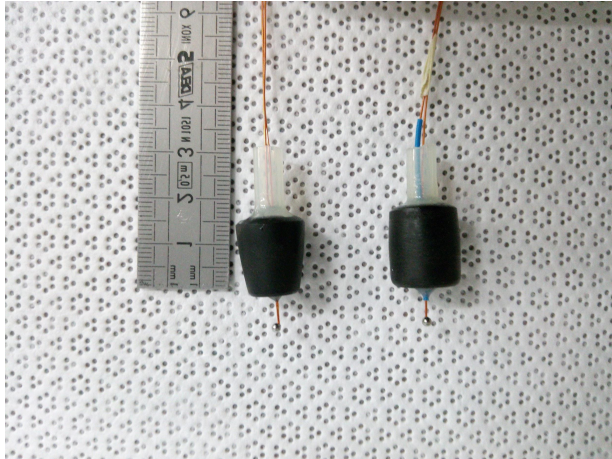
- Fe55 Source – 5.9 keV x rays
- 30 cm diameter test sphere operating at 600 mbar of He + 10% CH₄
- Anode Diameter = 2 mm, Separation = 3.5 mm



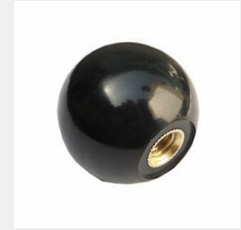
Gain reduced by presence of positive voltage on umbrella - electric field near anode reduced

The resistive umbrella

Bakelite Prototypes

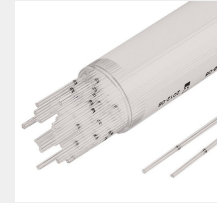


Glass Prototype



Bakelite

Chemical Formula:
 $(C_6-H_6-O.C-H_2-O)_x$



Soda - lime glass

Chemical composition*:
70% SiO_2 (glass) +
15% Na_2O (soda) +
9% CaO (lime) +
Other

*there are a lot different compounds

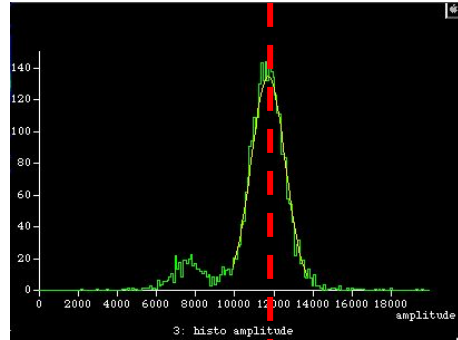
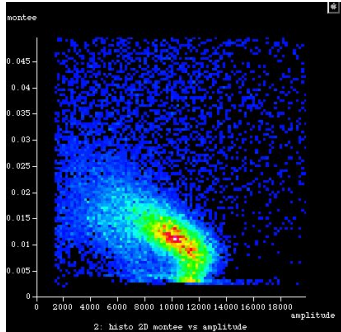
Advantages:

- Volume Resistivity $10^{10} \Omega \cdot cm - 10^{12} \Omega \cdot cm$
- Compact and homogeneous material
- Minimized insulating surface

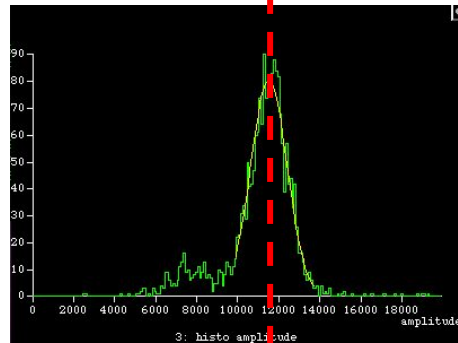
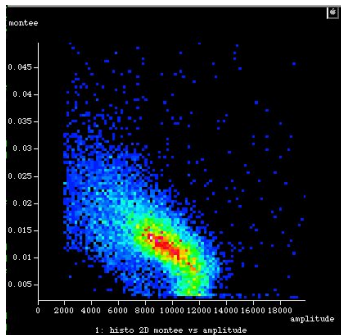
Performance of the resistive umbrellas - A

Homogeneous response

He+9%CH₄+7%Ar
730 mbar
Anode Φ 2 mm

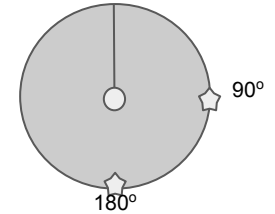


180°



90°

⁵⁵Fe source position



The difference in gain between the two positions is close to the statistical error

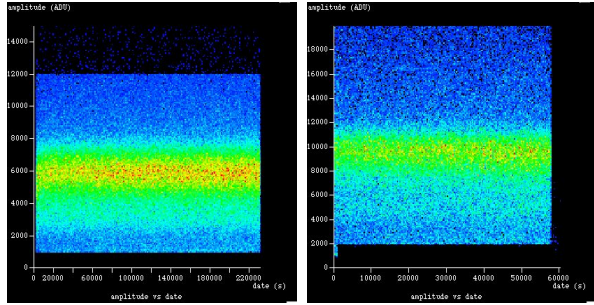
Rise time vs Amplitude

Amplitude

Performance of the resistives umbrellas - B

Pulse Height (ADU)

Stability

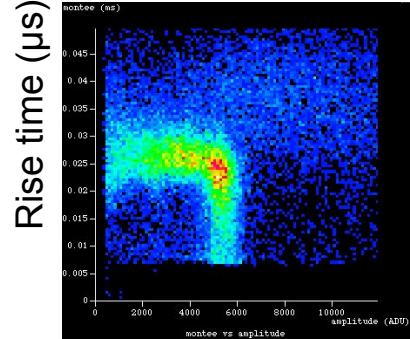


Time (s)

Ball: $\Phi 2$ mm steel
 Gas: He+30%Ar+7%CH₄
 P = 715 mbar
 HV1 = 1830 V
 HV2 = 0 V

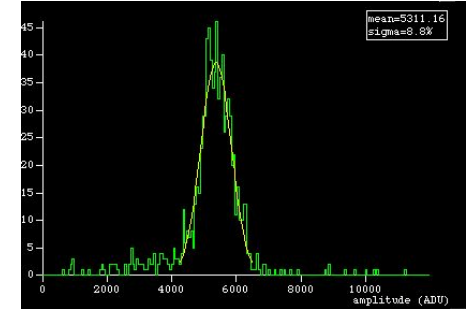
Ball: $\Phi 2$ mm steel
 Gas: He+10%Ar+2.5%CH₄
 P = 1880 mbar
 HV1 = 2300 V
 HV2 = 0 V

Resolution



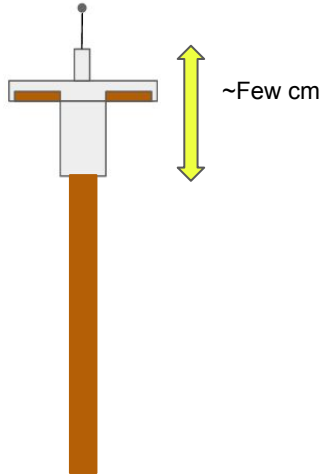
Pulse Height (ADU)

Ball: $\Phi 3$ mm steel
 Gas: He+30%Ar+3%CH₄
 P = 1000 mbar
 HV1 = 2300 V
 HV2 = 0 V

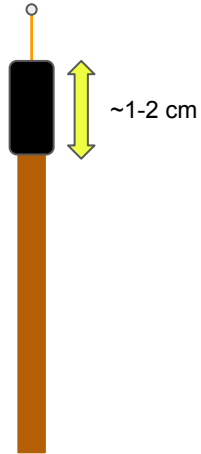


Iron fluorescence (~ 6.4 keV)

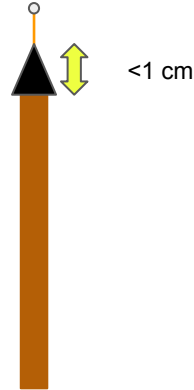
Evolution of the sensor “umbrellas”



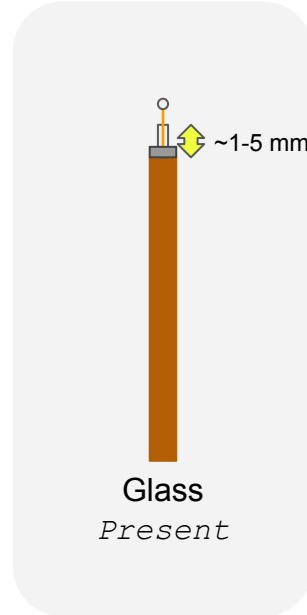
Classic “umbrella”
< 2016



Bakelite Version 1
2017 first half



Bakelite Version 2
2017 second half



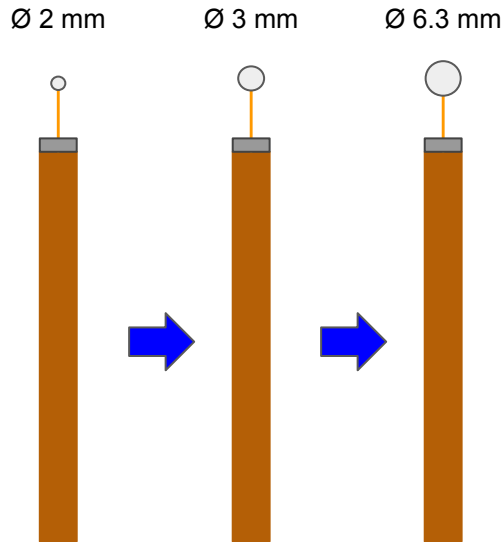
Glass
Present

Evolution targets:

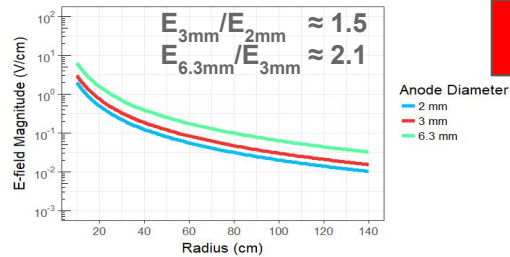
- Precision
- Easy construction
- Low mass
- **Detector stability**
- **Homogeneous response**
- **Low radioactivity**

The multiball sensor - ACHINOS

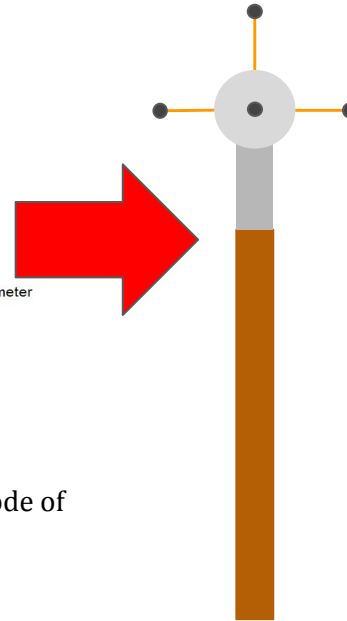
Dealing with the low electric field magnitude (~ 1 V/cm) at large detectors



The idea: Use multiple balls placed in the same potential instead



Comparison of E-field strength for anode of different radii vs the radius



$$E(r) = \frac{V_0}{r^2} r_1 \quad \text{Electric field dependence on the radius}$$

AIM:

1. Operation in high pressure
2. Build larger volume detectors

Conundrum:

Both Gain and Drift time are a function of E/P

$$\ln M = \int_{E(r^1)}^{E(r^2)} a(E/P) \frac{dE}{E}$$

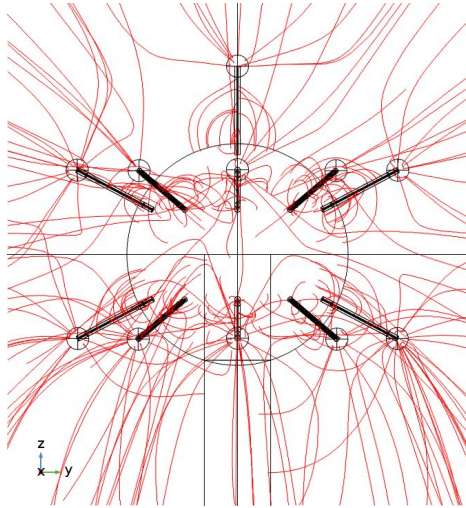
$$v_{drift} = \mu \frac{E}{P}$$

The elegant solution - ACHINOS

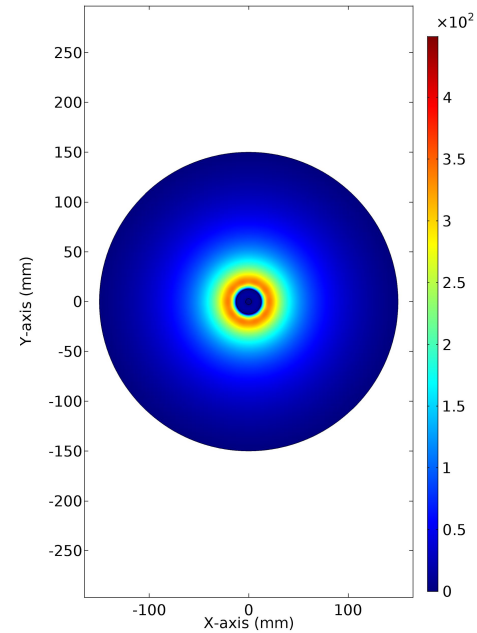
- Decoupling Gain - Drift
- Tunes Volume electric field
- Anodes can be read out individually

Study of the Electric field using FEM software

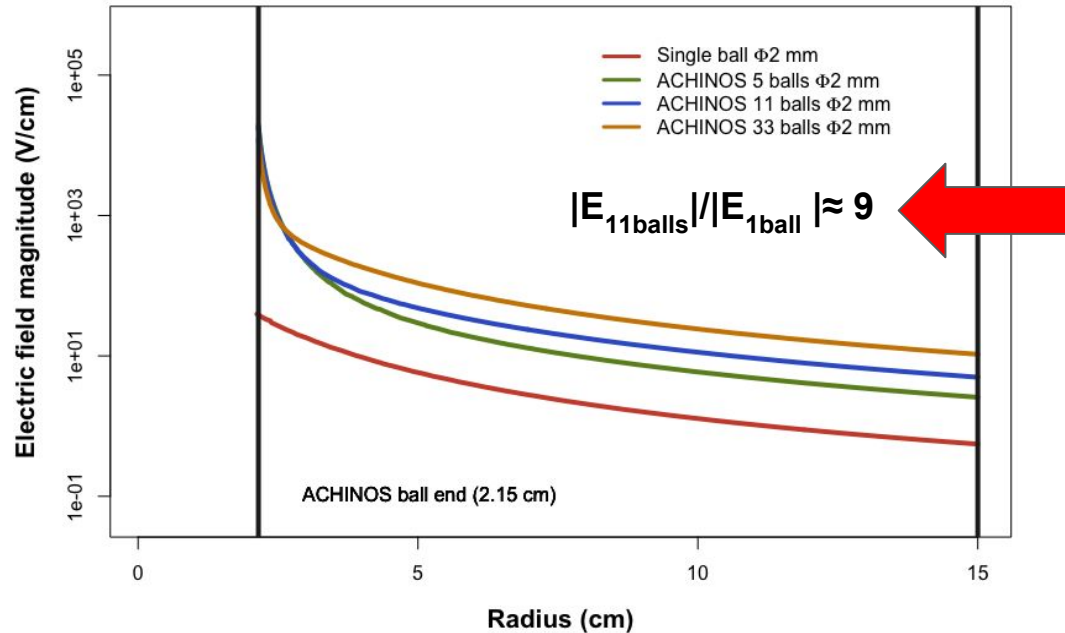
Field lines close close to the central structure



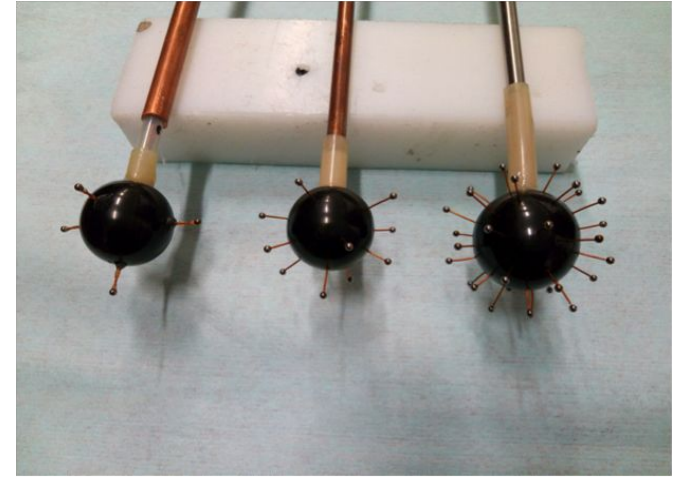
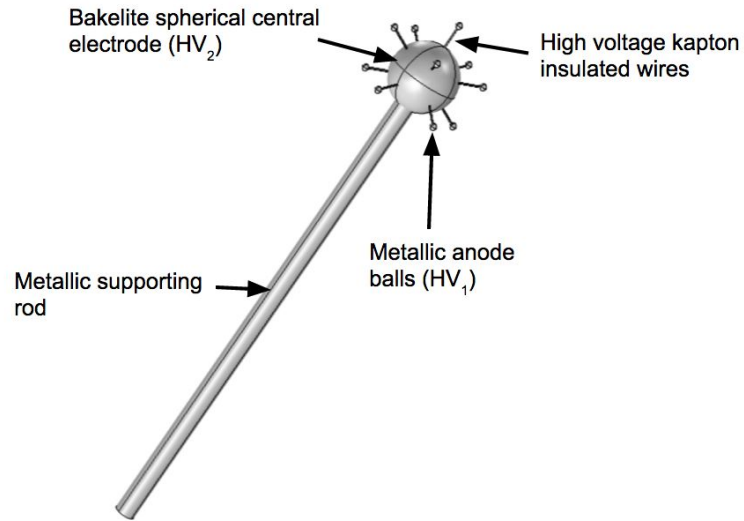
Creation of collective iso-potentials



Electric field magnitude with ACHINOS



The first ACHINOS prototypes

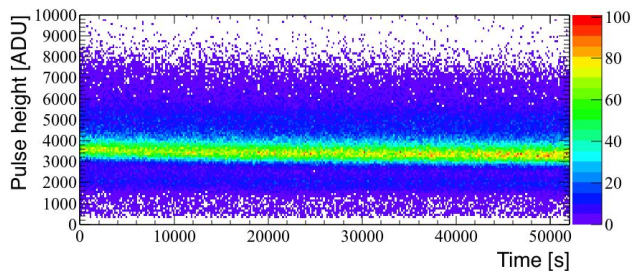


Composition:

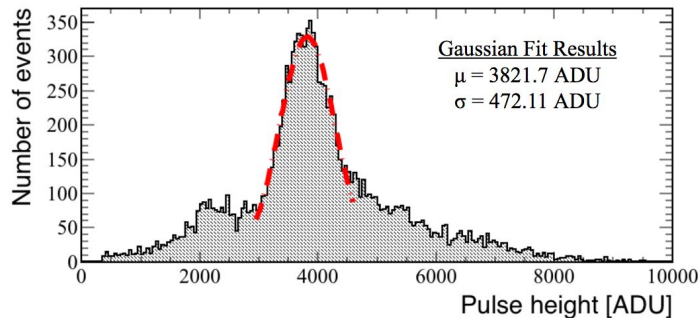
- 5, 11, or 33 balls
- Anode \varnothing 2 mm
- Placed in a virtual spherical surface
- Set in the same HV1
- Bias electrode made of bakelite (resistive) HV2

Positive results with the first prototypes

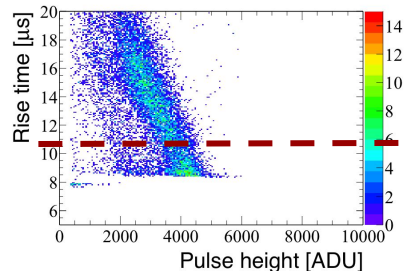
Stability in terms of sparking



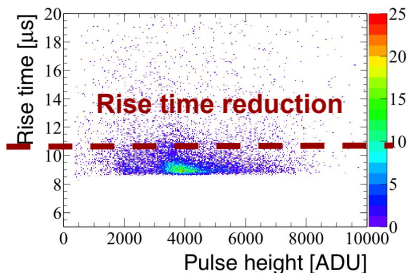
Measurement of the 5.9 keV line



Rise time vs Pulse height Single ball



Rise time vs Pulse height 11-balls



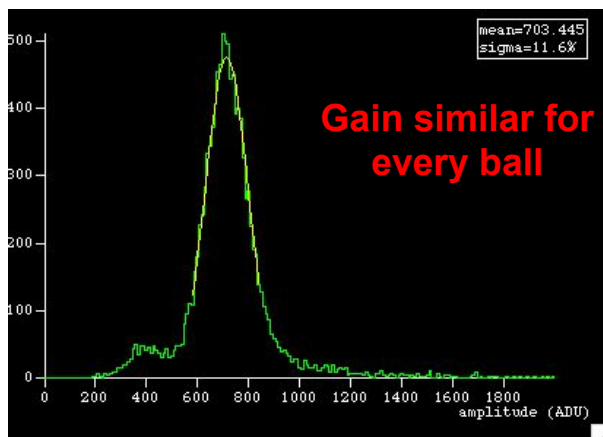
Conditions:

- Gas Mixture: He:Ar:CH₄ (80:11:9)
- Pressure: 640 mbar
- HV1 = 2015 V, HV2 = -200 V

Preliminary results with the 2nd gen prototypes

On going study of the 2nd gen prototypes

Measurement of the 5.9 keV ^{55}Fe X-ray line



Conditions:

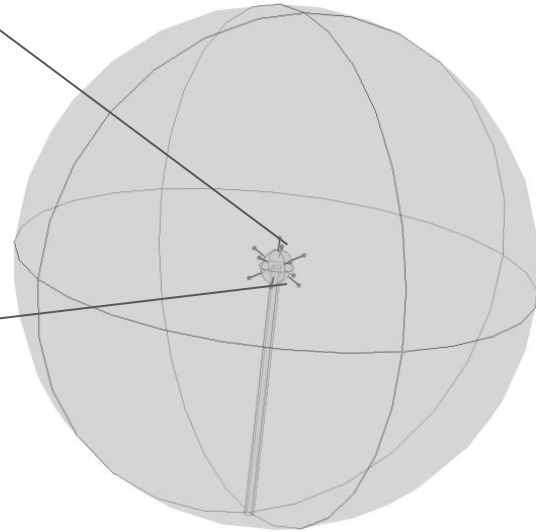
- Gas Mixture: He:Ar:CH₄ (56:37:7)
- Pressure: 455 mbar
- HV1 = 1100 V, HV2 = -100 V



Prospects

- Alternate coatings such as copper power/glue
- More compact design of the 3D printed support structure
- Anode balls of $\varnothing 1$ mm
- Operation in higher pressure
- Operation in high gain

Why such a weird name



ACHINOS = Sea urchin = Αχινός

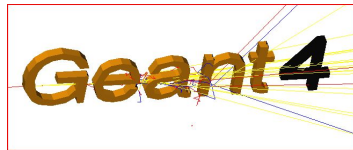


Development of detailed simulation methods to model the detector response

The power of combining state-of-the art software

Software for the simulation of particle passage through matter

- Build geometry
- Transport of particles
- Particle interaction
- Generation-Transport of secondaries
- ...
- Energy deposition in the ROI



Software for the simulation of gaseous detectors

- Drift of charges
- Diffusion
- Avalanche
- Signal Induction
- Electronics

Garfield
Garfield++



Software based on FEM

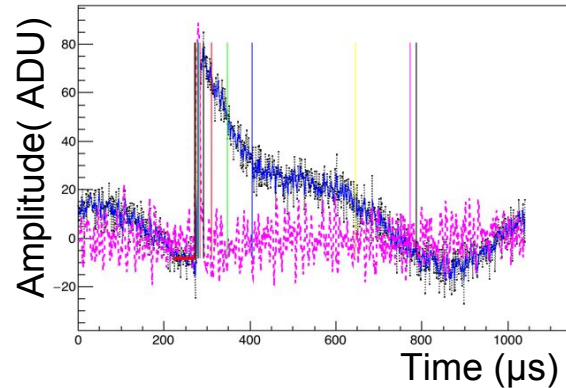
- Electric Field
- Magnetic Field
- Particle tracks



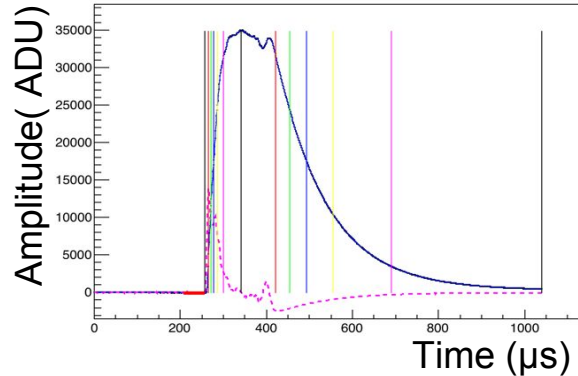
Simulated detector response

Examples of simulated pulses treated with the same analysis algorithm as real pulses

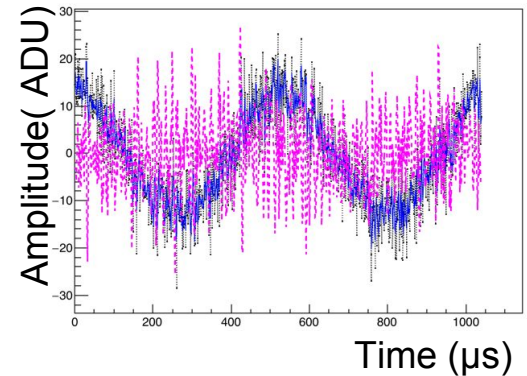
Surface e- extracted by a 5.9 keV X-ray



Atmospheric Muon



No pulse - only noise



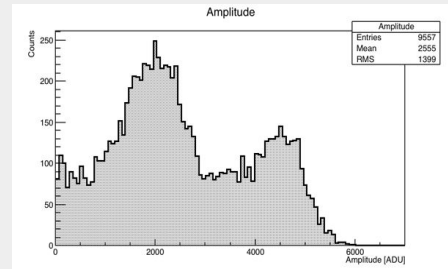
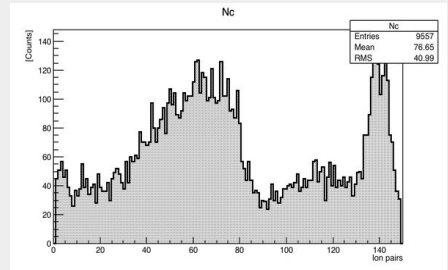
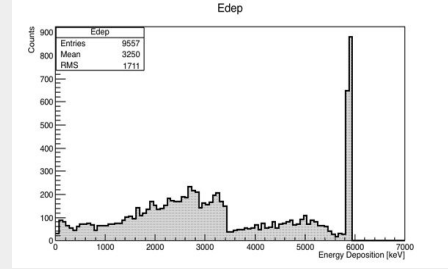
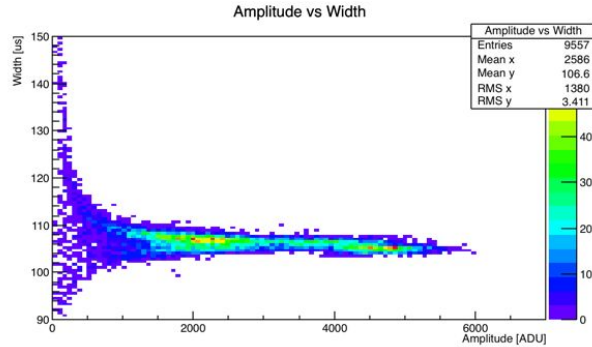
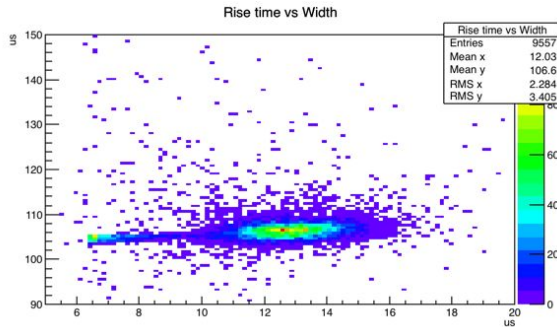
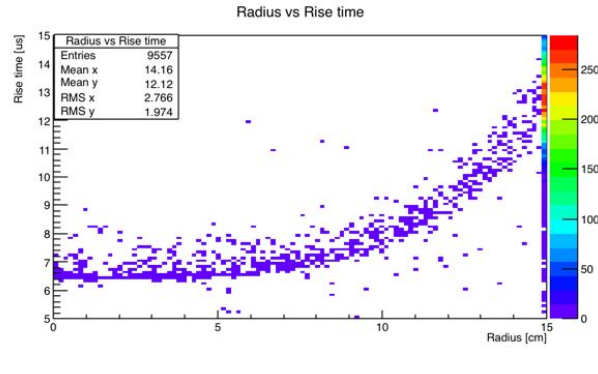
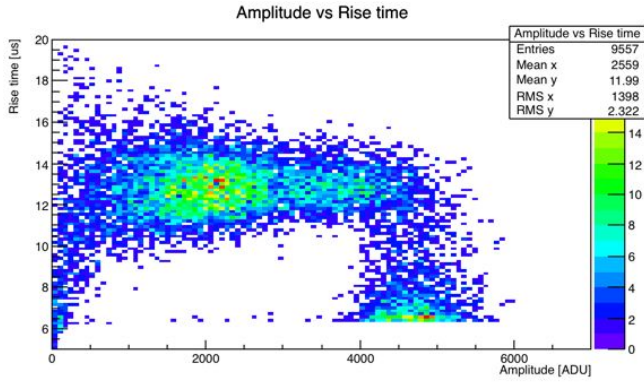
He+10%CH4 @ 1 bar

Irradiation of the volume with an 5.9 keV ⁵⁵Fe source

An illustration of the method

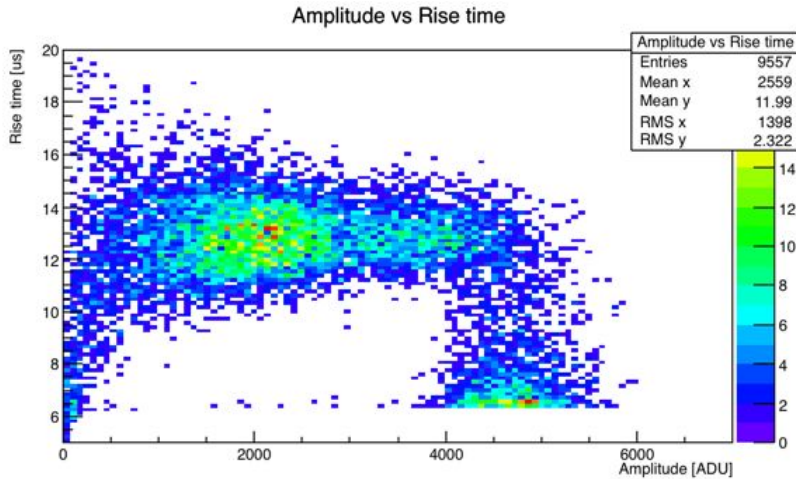
Assumed an $\tau=100 \mu\text{s}$ for our preamp with $g=0.45\text{mV/fC}$ and 50 ADU/mV 2800 V applied on Φ 3mm anode

From the initial interaction to the detector response

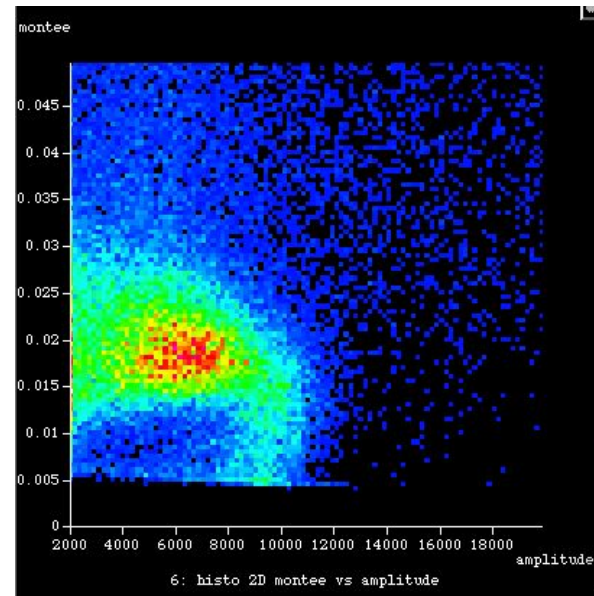


A qualitative comparison with the experiment

Simulation



Experiment

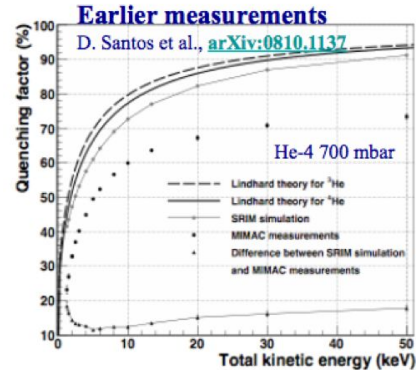
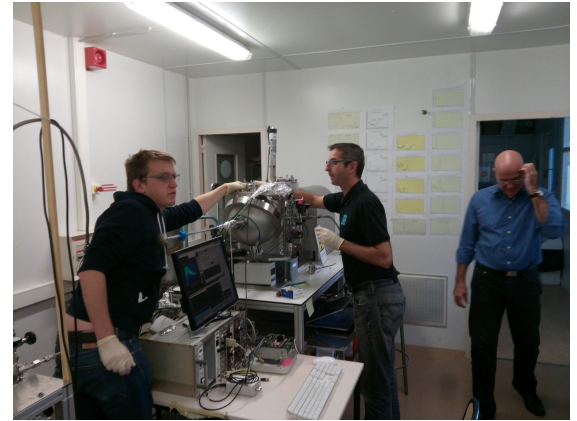


Detector: Spherical Proportional Counter (SPC)

Source: ^{55}Fe X-ray (5.9 keV)

Gas: He/CH₄ at 500 mbar

Quenching factor measurements at LPSC Grenoble



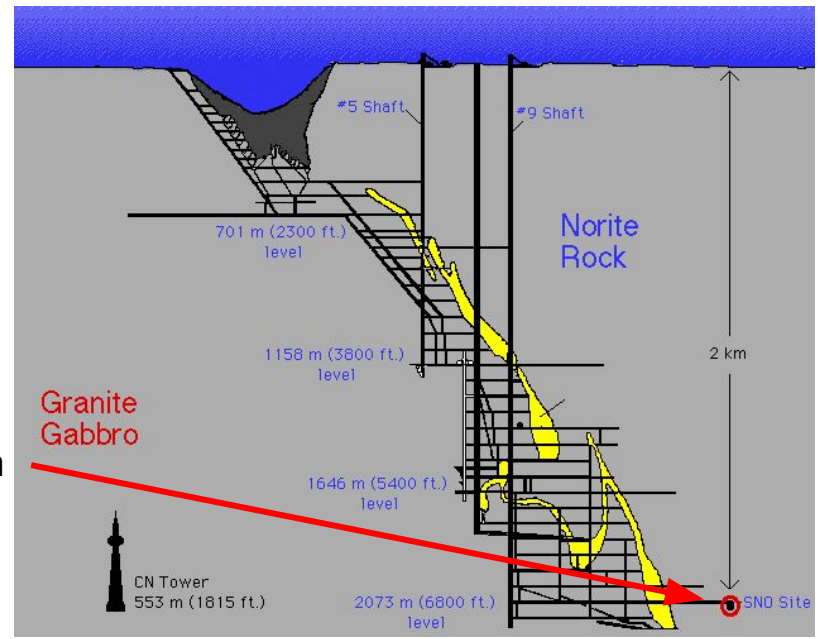
Electrons and ions are passing through a 1 μm in diameter hole to enter in the gaseous volume of the SPC !!!

- “High” flux environment ($\sim 10^{10} \text{cm}^{-2}\text{s}^{-1}$)
- Very low energy threshold ($< 100 \text{eV}$)

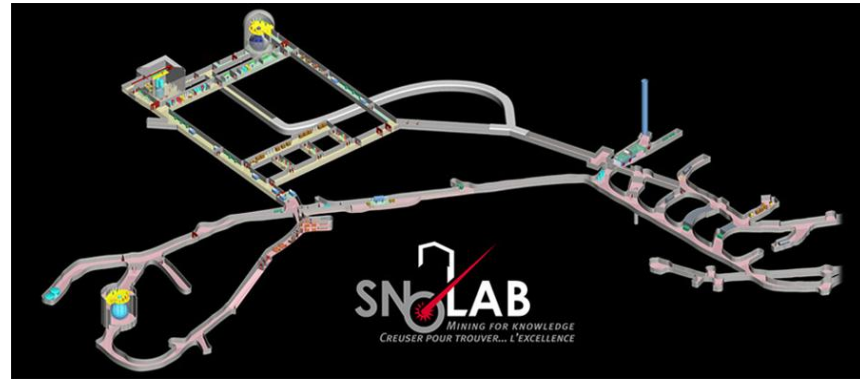
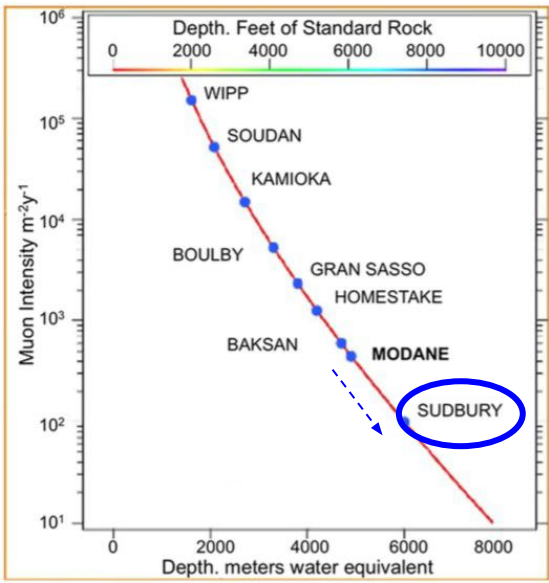
NEWS-G at SNOLAB

The underground laboratory in the Sudbury, Canada

Deeper underground
0.25 $\mu\text{m}^2/\text{day}$
~8x lower μ flux than LSM



Practically, at 2 km is the deepest clean room in the world



NEWS-G at SNOLAB

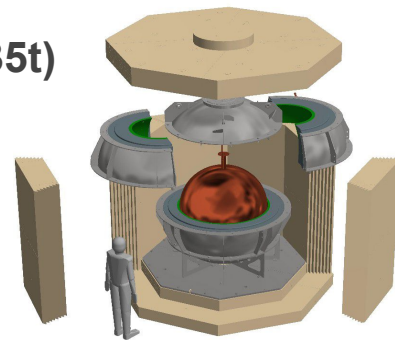
The new and improved setup

Copper vessel (140 cm \varnothing , 12 mm thick)

- Low activity copper (C10100)
 - 7 to 25 $\mu\text{Bq/kg}$ Th
 - 1 to 5 $\mu\text{Bq/kg}$ of U
- Electropolishing & Electroplating

Upgraded compact shielding (35t)

- 40 cm PE + Boron sheet
- 22 cm VLA Pb (1 Bq/kg ^{210}Pb)
- 3 cm archaeological lead
- Airtight envelope to flush pure N (against Rn)



Hemispheres built in France, stored at LSM before welding



Glove box for Radon free rod installation



Estimated background

Simulation done with 12mm thick 140cm diam copper sphere full with 99% Ne 1%CH4, 11.43 kg of gas

Source Position	Mass (kg) or Surface (cm ²)	Source	evts/kg/day/[(μBq/kg) or (nBq/cm ²)]	contamination units	evts/kg/day < 1ke
CopperSphere	627.83 kg	Co60	0.0018	30 μBq/kg	0.054
CopperSphere	627.83 kg	U238	0.0036	3 μBq/kg	0.011
CopperSphere	627.83 kg	Th232	0.0049	12.9 μBq/kg	0.063
InnerSurface	57255 cm ²	Pb210	0.012	0.16 nBq/cm ²	0.002
ArchLead	2108.95 kg	U238	0.001	61.8 μBq/kg	0.062
ArchLead	2108.95 kg	Th232	0.0011	9.13 μBq/kg	0.010
Rod	0.0931721 kg	Co60	2.95E-007	30 μBq/kg	0.000
Rod	0.0931721 kg	U238	1.81E-006	3 μBq/kg	0.000
Rod	0.0931721 kg	Th232	2.11E-006	12.9 μBq/kg	0.000
Wire	2.66005e-05 kg	Co60	1.48E-010	31000 μBq/kg	0.000
Wire	2.66005e-05 kg	U238	2.12E-009	300000 μBq/kg	0.001
Wire	2.66005e-05 kg	Th232	1.42E-009	50000 μBq/kg	0.000
Wire	2.66005e-05 kg	K40	5.41E-010	1660000 μBq/kg	0.001
LabArea		T1208/K40			0.076

Total 0.279

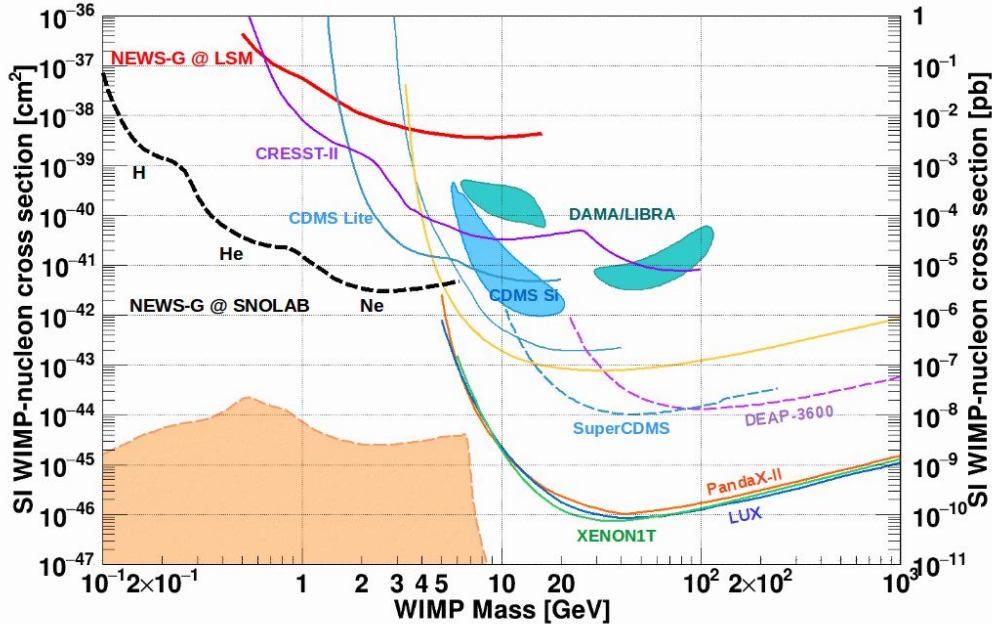
Copper

Internal surface
Lead shield

External BG with SNO
Flux

NEWS-G at SNOLAB

Projected sensitivity



*100 kg.days, 200eVee ROI above threshold at 1 electron.
(Not accounting for sensitivity improvement from resolution effects and RT cuts)*

The NEWS-G collaboration

- **Queen's University Kingston** – G Gerbier, P di Stefano, R Martin, G Giroux, T Noble, D Durnford, S Crawford, M Vidal, A Brossard, F Vazquez de Sola, Q Arnaud, K Dering, J Mc Donald, M Clark, M Chapellier, A Ronceray, P Gros, J Morrison, C Neyron 
 - Copper vessel and gas set-up specifications, calibration, project management
 - Gas characterization, laser calibration, on smaller scale prototype
 - Simulations/Data analysis
- **IRFU (Institut de Recherches sur les Lois fondamentales de l'Univers)/CEA Saclay** -I Giomataris, M Gros, C Nones, I Katsioulas, T Papaevangelou, JP Bard, JP Mols, XF Navick, 
 - Sensor/rod (low activity, optimization with 2 electrodes)
 - Electronics (low noise preamps, digitization, stream mode)
 - DAQ/soft
- **LSM (Laboratoire Souterrain de Modane), IN2P3, U of Chambéry** - F Piquemal, M Zampaolo, A DastgheibiFard 
 - Low activity archeological lead
 - Coordination for lead/PE shielding and copper sphere
- **Thessaloniki University** – I Savvidis, A Leisos, S Tzamarias 
 - Simulations, neutron calibration
 - Studies on sensor
- **LPSC (Laboratoire de Physique Subatomique et Cosmologie) Grenoble** - D Santos, JF Muraz, O Guillaudin 
 - Quenching factor measurements at low energy with ion beams
- **Pacific National Northwest Lab**– E Hoppe, DM Asner 
 - Low activity measurements, Copper electroforming
- **RMCC (Royal Military College Canada) Kingston** – D Kelly, E Corcoran 
 - 37 Ar source production, sample analysis
- **SNOLAB –Sudbury** – P Gorel 
 - Calibration system/slow control
- **University of Birmingham** – K Nikolopoulos, P Knight 
 - Simulations, analysis, R&D
- **Associated lab : TRIUMF** - F Retiere 
 - Future R&D on light detection, sensor



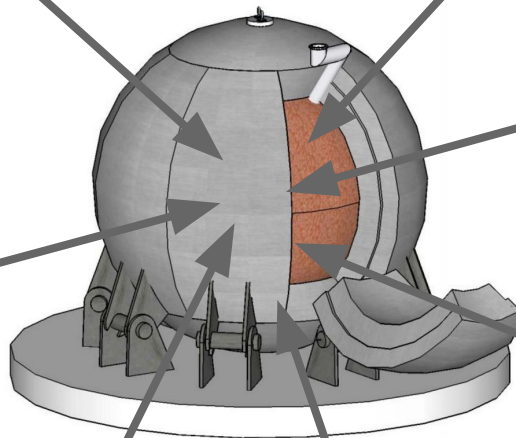
Thessaloniki, Greece 2018



Thank you very
much for your
attention

Additional material

NEWS-G SNO



Operation with different targets:
Ne, He, H

Operation with different pressures:
Tenths mbar - 10 bar

Operation with High Z medium (Xenon) to better determine the background

Resistive sensors:
High Gain

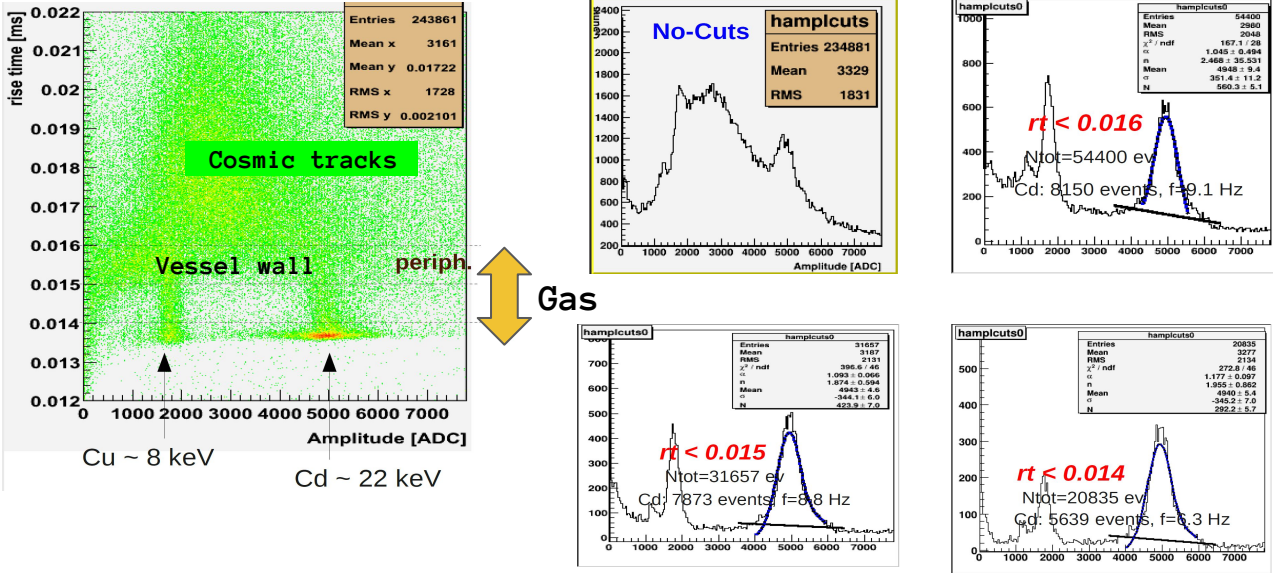
ACHINOS sensor:
Tuning volume electric field - High gain -
Multichannel readout

“Penning” Mixtures
Ne/CH₄ or He/CH₄ (99.3/0.7):
High pressure - High Gain -
Minimized voltages applied

Regular Mixtures
Ne/CH₄ or He/CH₄ (90/10):
Hydrogen rich gases

Illustration of the basic analysis principle

^{109}Cd source
 Irradiation through 200 μm Al window
 P = 100 mb, Ar-CH₄ (2%)



Efficiency of the cut in $rt \rightarrow \sim 70\%$ signal (Cd line)
Significant background reduction

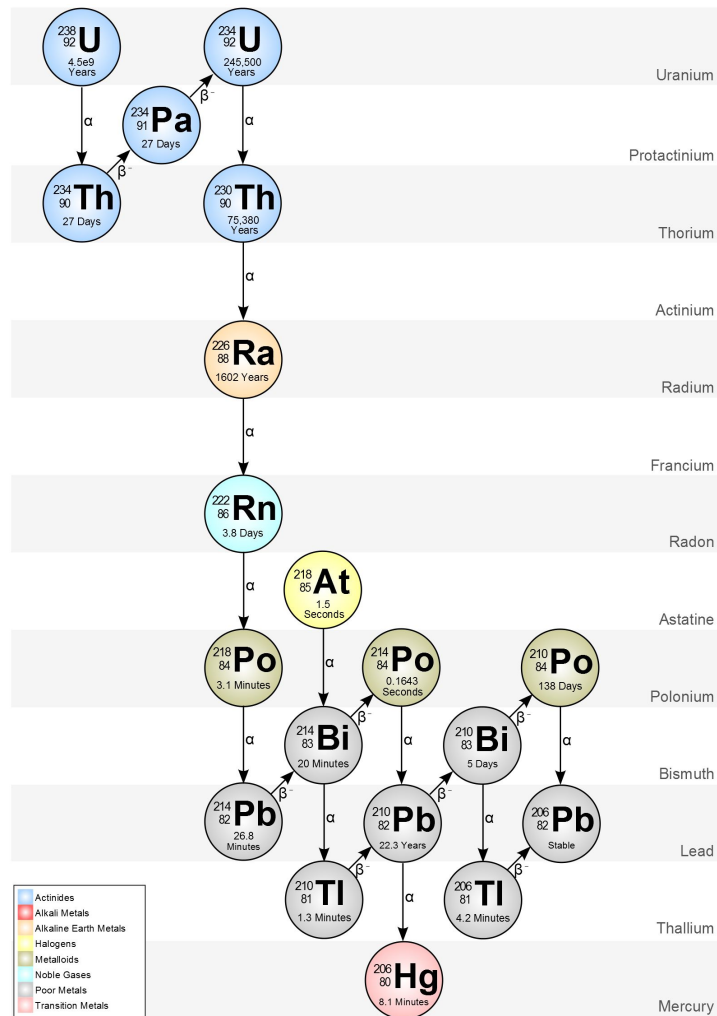


Table 1. Radiocarbon results. Material codes and protocols are described in Crann et al. (2017).

Lab ID	Submitter ID	Material	Mat. Code ^a	¹⁴ C yr BP	±	F ¹⁴ C	±	A (Bq/kg)	±
UOC-6176	Bakelite_NewsG	Bakelite	D	9334	35	0.3129	0.0014	69.52	0.47

	¹⁴ C	¹⁴ C
Bakelite	69,52 Bq/kg	69,52 mBq

Bq/kg

	BN_Graphite_Li ke		BN Spray_1		BN Spray_2		BN powder		BN_Diamond_Li ke	Bakaleite	
226Ra	2,22E+00	±7,47E-02	5,19E+00	±8,65E-01	1,34E+00	±1,90E-01	5,65E-02	±4,23E-02	<1,97E-01	2,78E+00	±0,120300
228Th	1,48E-01	±1,95E-02	1,20E+01	±9,54E-01	3,23E+00	±1,45E-01	7,79E-03	±1,74E-02	<1,10E-01	4,31E+00	±0,114112
210Pb	1,04E+00	±1,42E-01	1,73E+01	±3,53E+00	7,13E+00	±6,74E-01	6,72E-02	±3,56E-02	<6,23E-01		
238U	9,20E-01	±1,19E-01	2,04E+01	±3,46E+00	3,17E-02	±4,86E-03	1,31E-01	±9,76E-02	<4,20E-01		
137Cs	<0,02140		<9,77E-01		<2,92E-03		<6,89E-02		<1,39E-01		
40K	<0,433558		<6,01E+00		4,61E-01	±7,34E-02	<6,58E-01		<1,49E+00	1,36E+02	±2,448022
228Ra	<0,144085		1,49E+01	±2,66E+00	3,31E+00	±3,62E-01	3,31E+00	±0,362473 831	<4,76E-01	4,99E+00	±0,3117708

	Glass tube				Bakalite
	Bq/kg		Bq/m	Bq/tube	Bq/umbrella
226Ra	4,06	± 0,223	1,70E-04	1,54E-03	2,78 E-03
228Th	1,46	± 0,081	6,11E-05	5,55E-04	4,31 E-03
210Pb	3,28	± 0,467	1,38E-04	1,25E-03	
238U	3,02	± 0,371	1,27E-04	1,15E-03	
40K	1,3	± 0,410	5,48E-05	4,94E-04	1,36 E-01
228Ra	1,36	± 0,225	5,70E-05	5,17E-04	4,39 E-03

Glass tube dimension :

High : 100 mm

Radius_{ext} : 2mm

Thickness : 0.5 mm

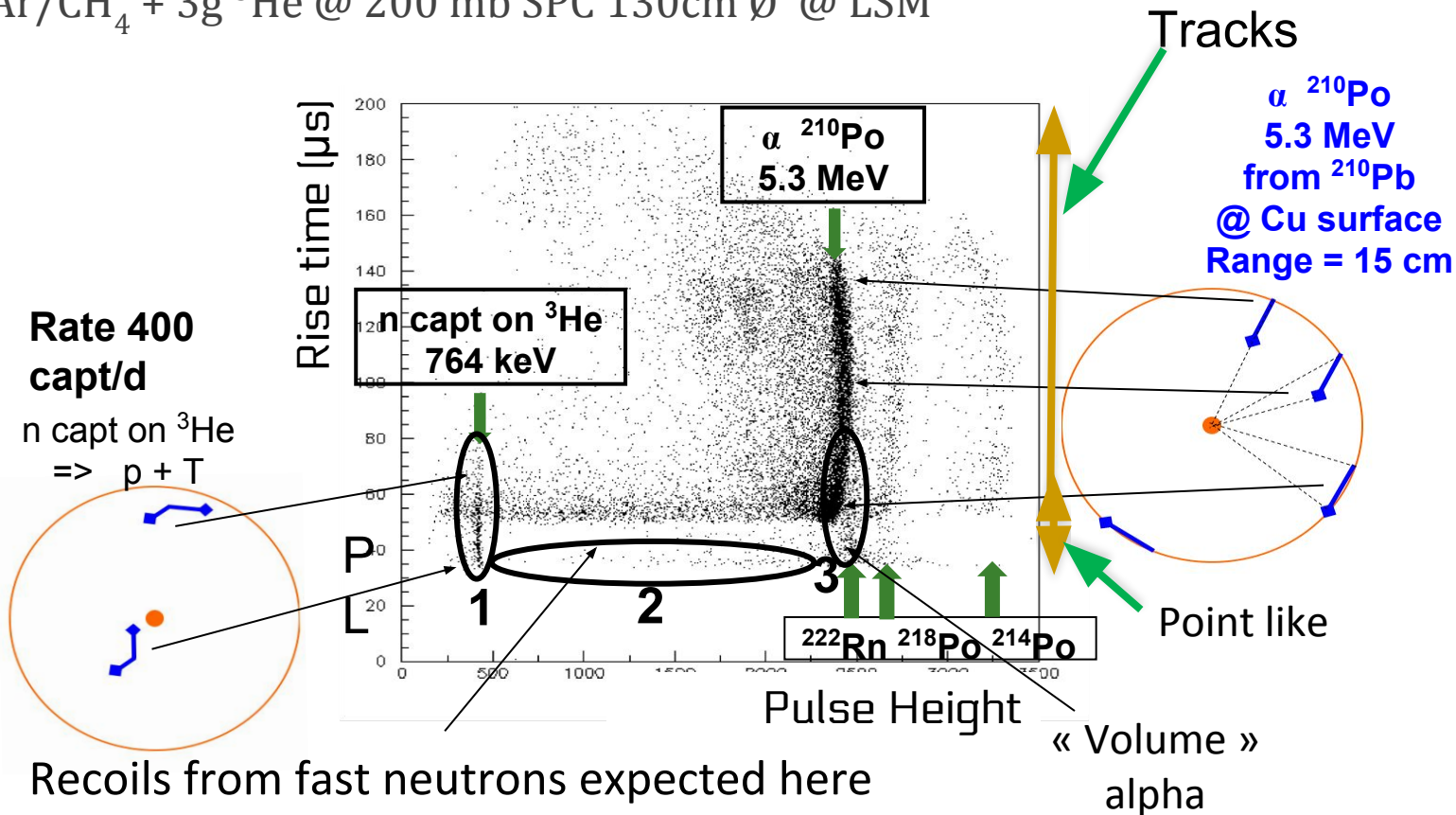
Weight : 0.38g

Bakalite conic umbrella :

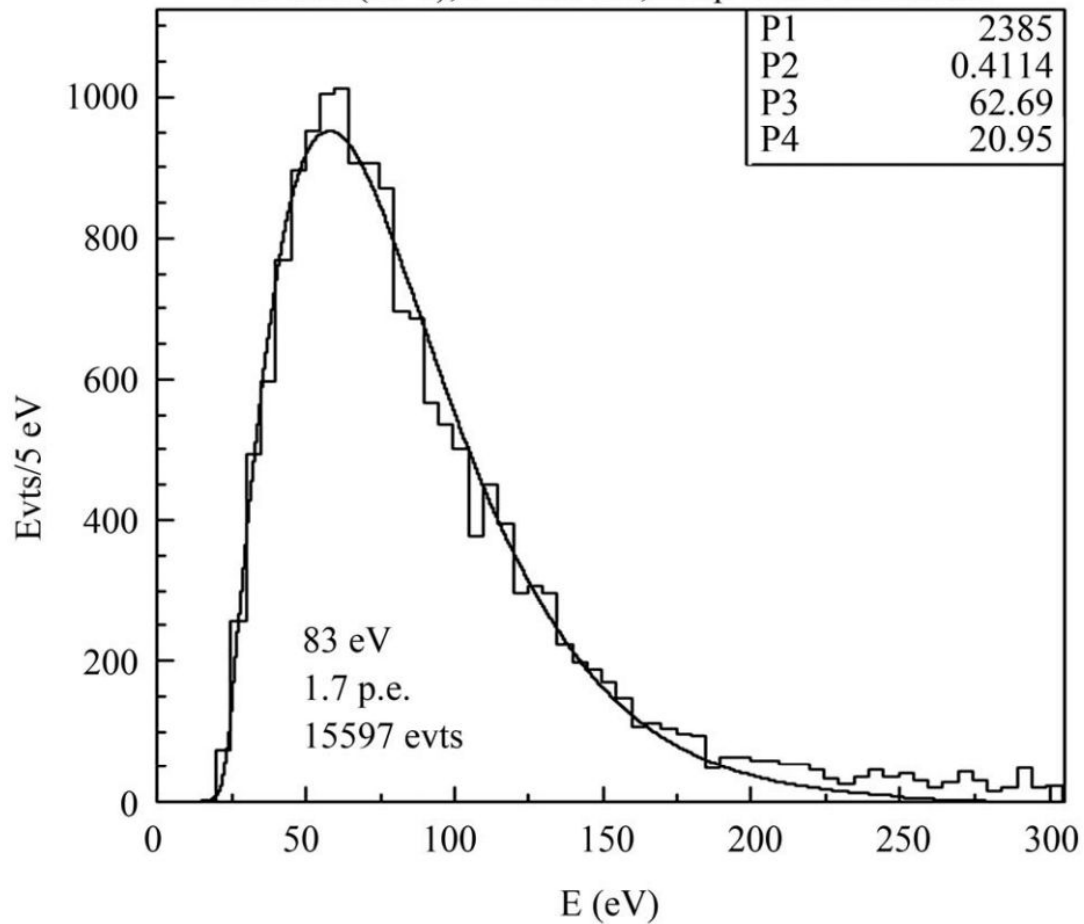
Weight : ≈ 1g

Illustration of particle identification – Background rejection

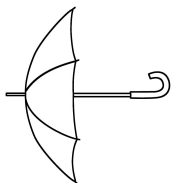
Run with Ar/CH₄ + 3g ³He @ 200 mb SPC 130cm Ø @ LSM



Ne-CH4(93-7), P = 100 mb, lamp with 3 attenuator

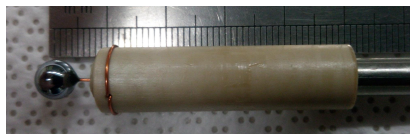
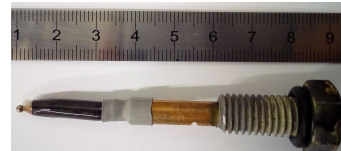
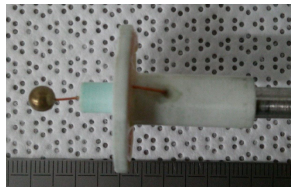


The umbrella



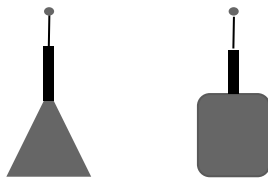
Material used: Copper, Brass, Steel, Iron, PE, PEEK, Teflon, Kapton, Plexiglass, Si, Araldite

Introduction of a secondary correction electrode

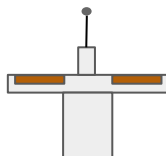


Goals:

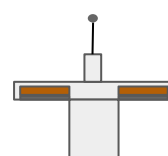
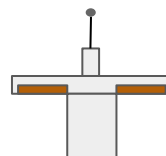
- Homogeneous field
- limited discharges
- operation in high pressure
- stability



Coaxial cable umbrella

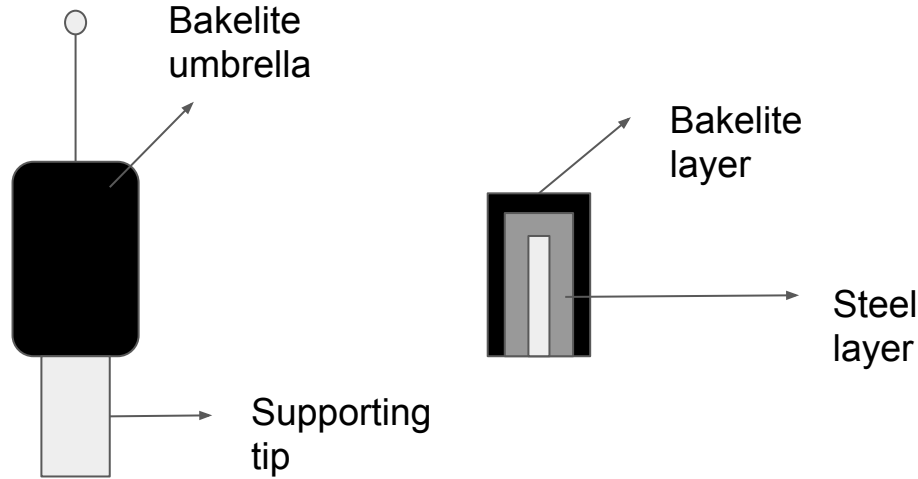


“Classical” umbrella



Kapton wire umbrella

The resistive umbrella



Advantages:

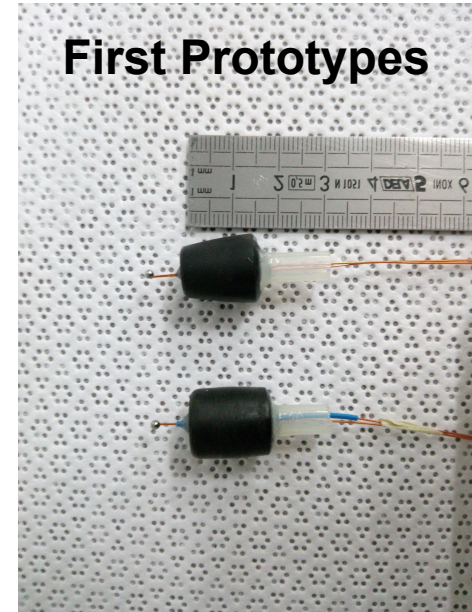
- Bakelite resistivity $\sim 10^{12} \Omega \cdot \text{cm}$
- Compact and homogeneous material
- Very good conduct between the steel (conducting) layer and the bakelite layer
- Minimized insulating surface

Bakelite

Chemical Formula:



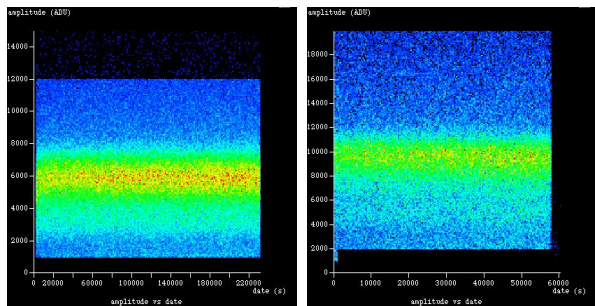
Thermosetting phenol formaldehyde resin, formed from a condensation reaction of phenol with formaldehyde.



"Glass" sensor prototype performance

Pulse Height (ADU)

Stability

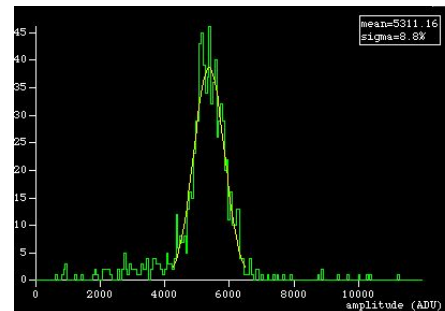
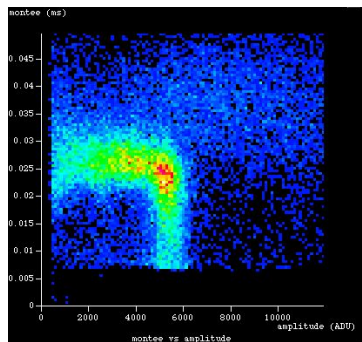


Time (s)

Ball: $\Phi 2$ mm steel
 Gas: He+30%Ar+7%CH₄
 P = 715 mbar
 HV1 = 1830 V
 HV2 = 0 V

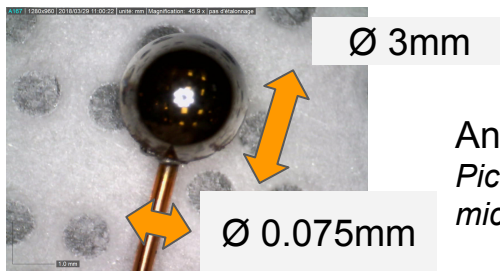
Ball: $\Phi 2$ mm steel
 Gas: He+10%Ar+2.5%CH₄
 P = 1880 mbar
 HV1 = 2300 V
 HV2 = 0 V

Resolution



Ball: $\Phi 3$ mm steel
 Gas: He+30%Ar+3%CH₄
 P = 1000 mbar
 HV1 = 2300 V
 HV2 = 0 V

Iron fluorescence (~ 6.4 keV)

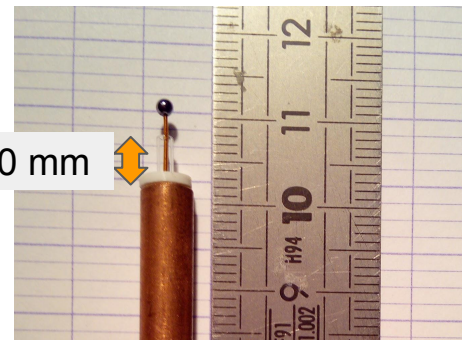


$\Phi 3$ mm

$\Phi 0.075$ mm

Anode micro-soldering
 Picture from digital
 microscope (x 45.9)

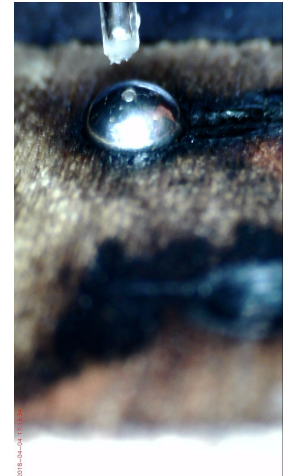
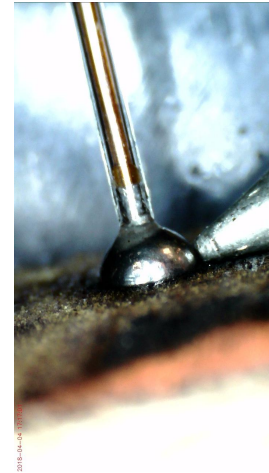
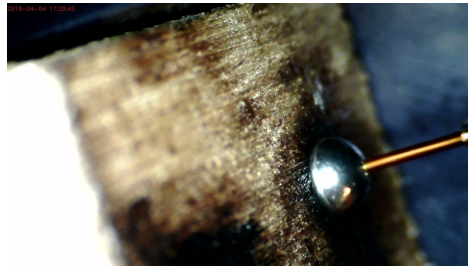
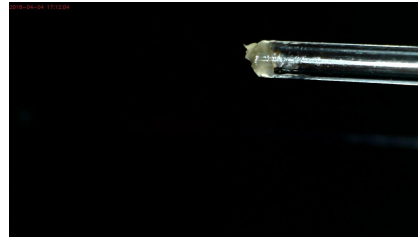
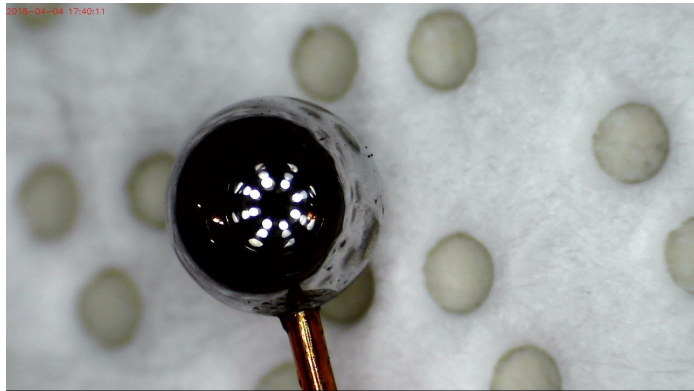
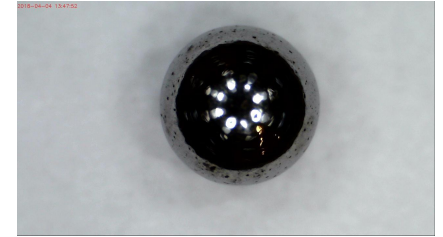
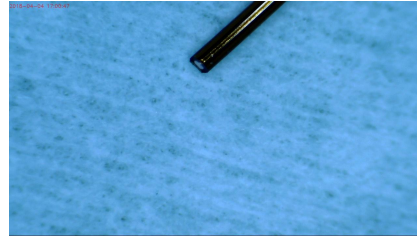
2-10 mm



The μ -soldered ball

Motivation

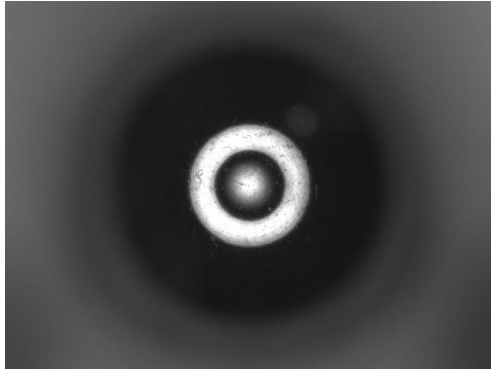
- Better sphericity
- Avoidance of ball deformations
- Field homogeneity



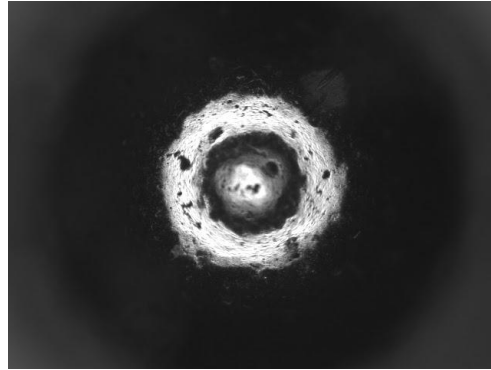
Control of ball quality

Checking diameter and surface smoothness

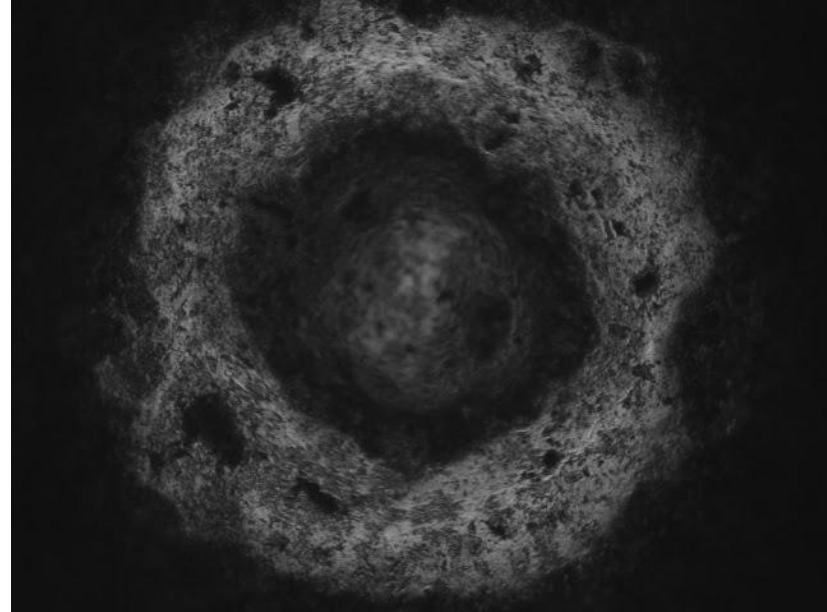
2 mm Inox ball



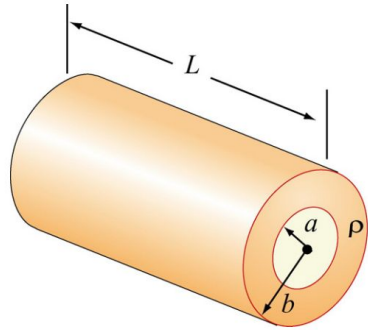
3 mm steel ball



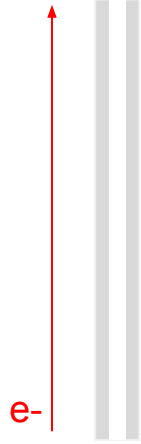
A closer look on a 3 mm ball



Metallized glass umbrella

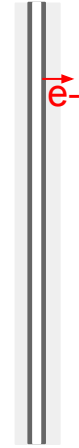


Hollow resistive cylinder

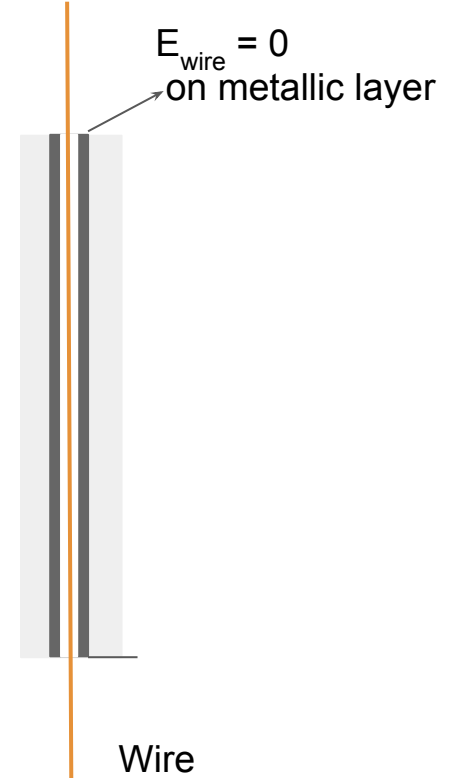


$$R = \frac{\rho L}{\pi(b^2 - a^2)}$$

Resistive cylinder with metallized inner surface

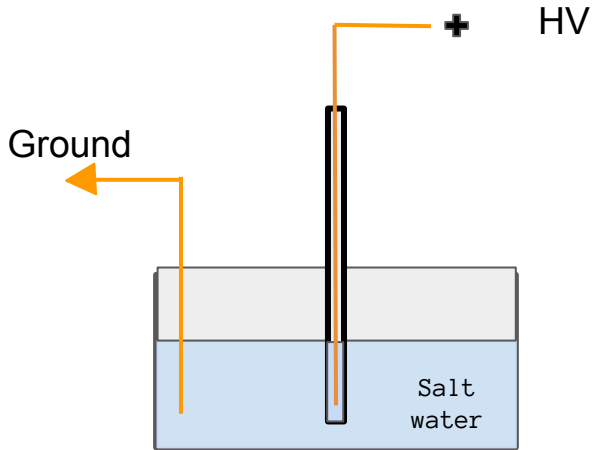


$$R = \frac{\rho}{2\pi L} \ln\left(\frac{b}{a}\right)$$

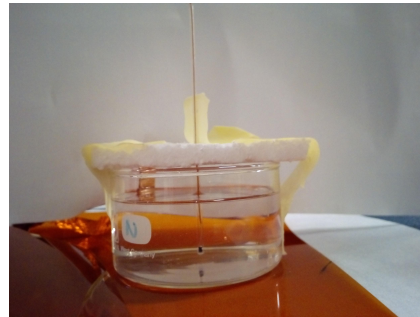


Properties of “Soda”-glass

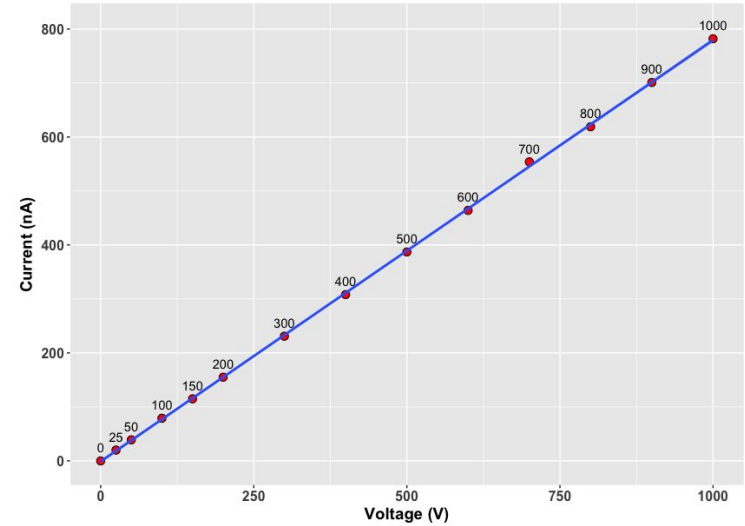
Resistivity - Activity - Density



Schematic



Real structure



Activity: 14.48 mBq/g

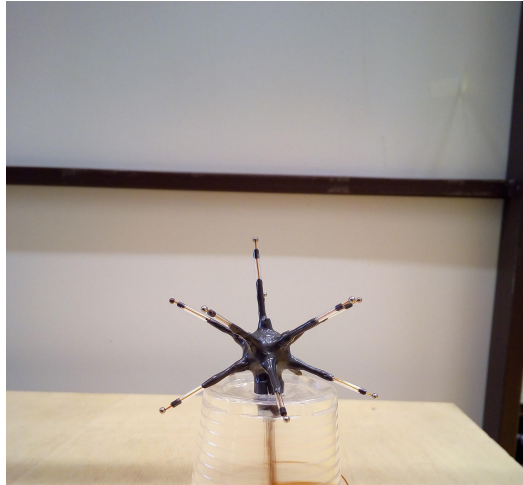
Density: 2.1-2.25 g/cm³

Measurement result

$$\rho = 5.05 \times 10^{10} \Omega \cdot \text{cm} \pm 26.6\%$$

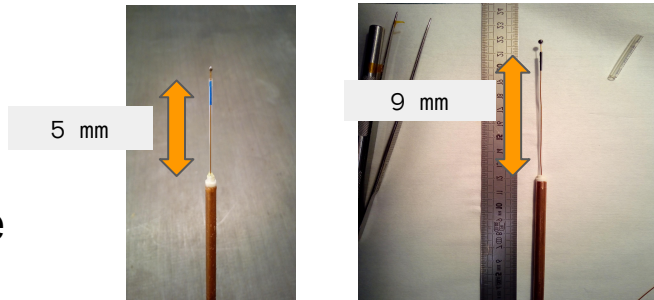
Second generation of prototypes under investigation

The new 11-ball ACHINOS modules based on 3D-printed supporting structures, coated with graphite-gluce layer (resistivities in the $10^6 \Omega \cdot \text{cm}$ - $10^{12} \Omega \cdot \text{cm}$) and glass tubes to extend the bias electrodes

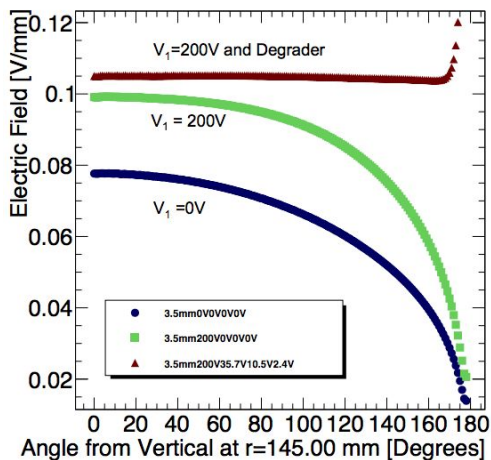


A new idea

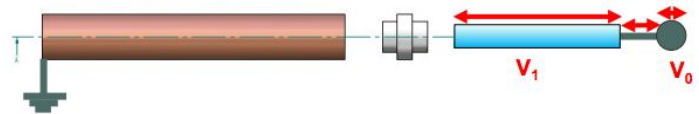
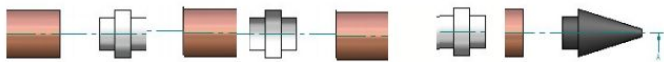
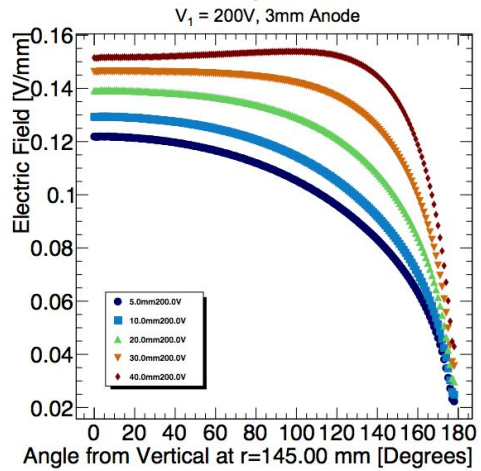
Improvement of the electric field in the far region of the detector



Degrader



Mini-Degrader

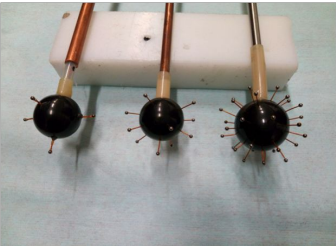
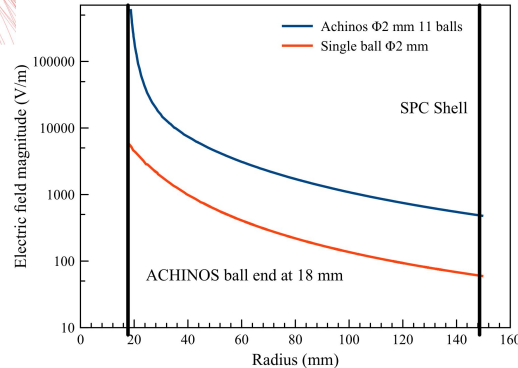
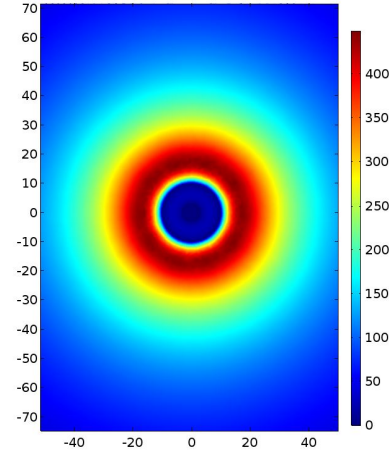
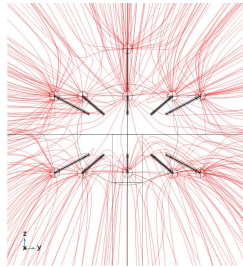
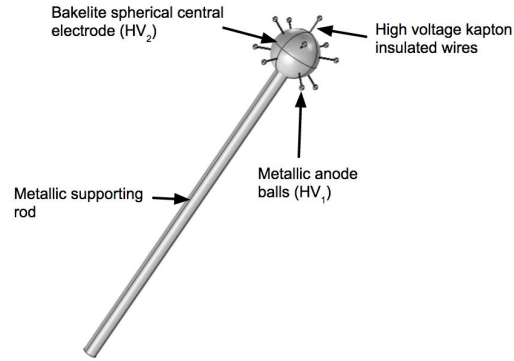


Figures from P.Knights recent presentation at IOP

A sensor upgrade

Sensor development - ACHINOS

If instead of one ball we use a number of them placed at equal distance on a sphere you can have the same gain but increased field at the outer region of the detector



AIM:

1. Operation in high pressure
2. Build larger volume detectors

Conundrum:

Both Gain and Drift time are a function of E/P

$$\ln M = \int_{E(r^1)}^{E(r^2)} a(E/P) \frac{dE}{E}$$

$$v_{drift} = \mu \frac{E}{P}$$

The elegant solution - ACHINOS

- Decoupling Gain - Drift
- Tunes Volume electric field
- Anodes can be read out individually

Possible improvements

- Construction method
- Testing of different geometries
 - Simulations
 - Prototypes
- Looking for the optimal number of anodes
 - Performance
 - Complexity
 - Noise
- Material for the bias electrode
 - Resistive coating
 - Bakelite
 - Thin layer of deposited carbon (<50 nm)

Glass bias electrodes



3D printed designs



Increased number of anodes

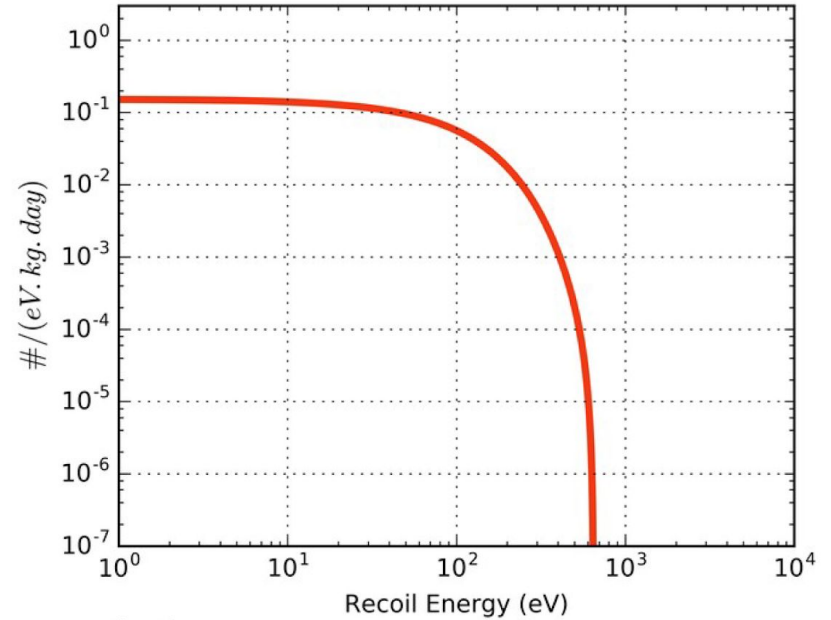
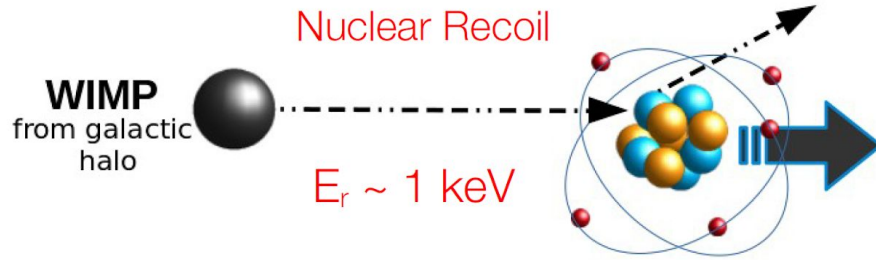


Resistive coatings



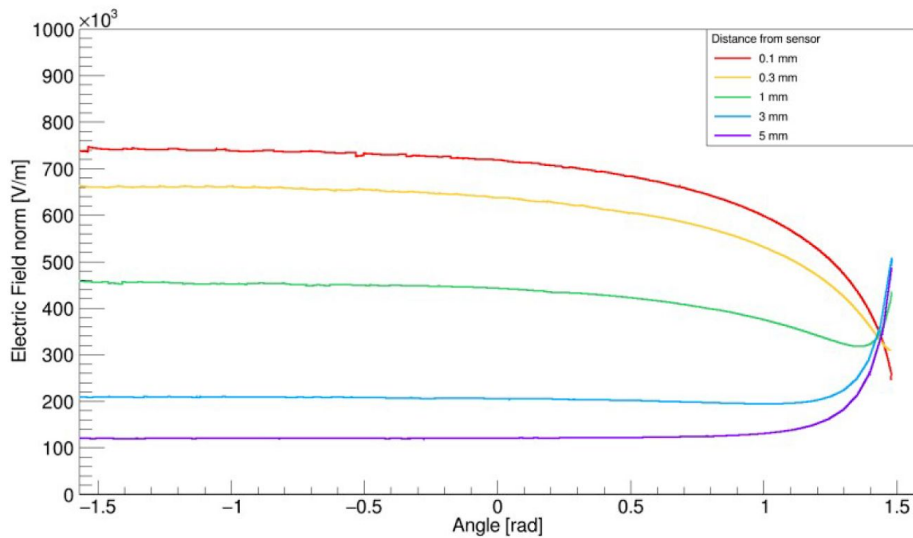
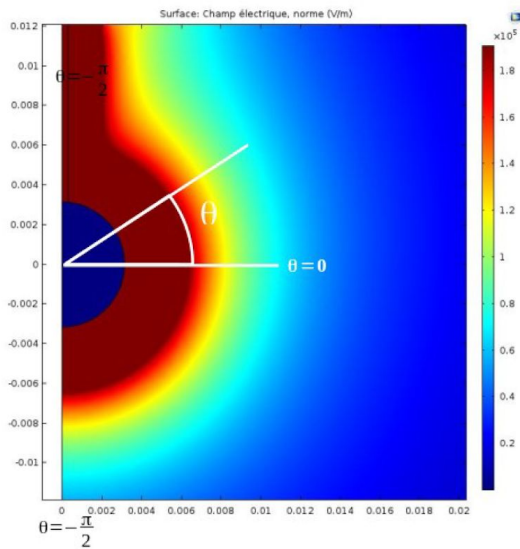
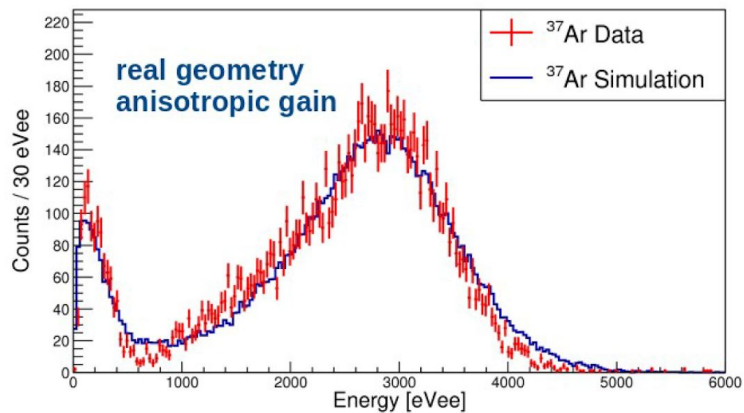
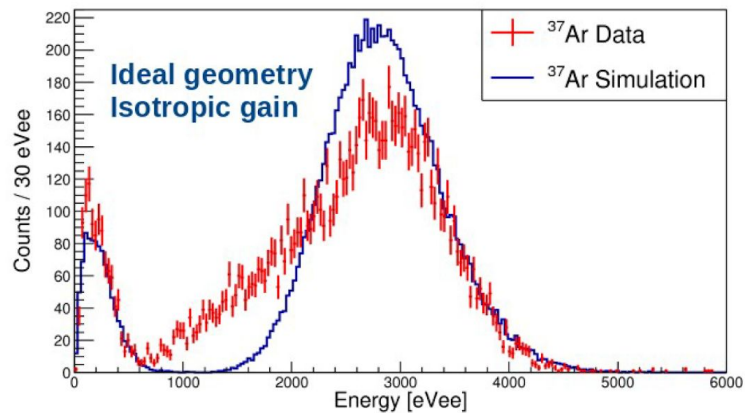
Neon, 1 kg.year, 1pb, 1 GeV WIMP

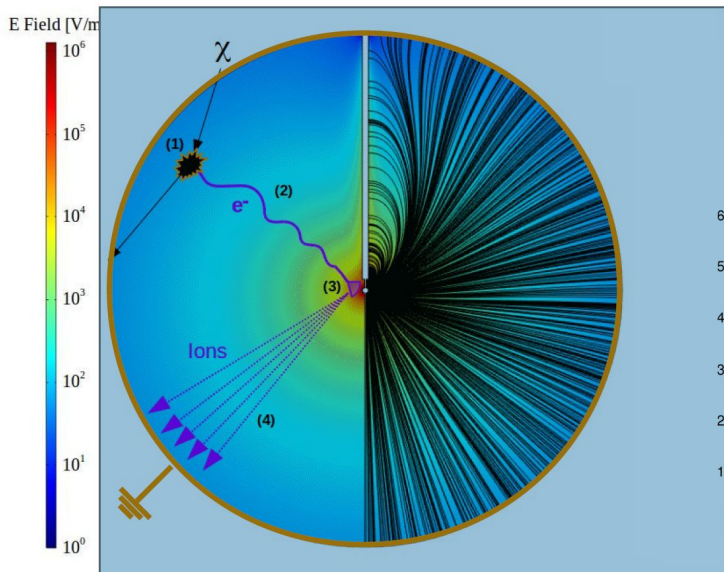
WIMP Recoil Spectrum



$$\frac{dR}{dE_r} = M_T \frac{\rho_0 \sigma_0}{2m_\chi m_r^2} F^2(E_r) \int_{v_{min}} \frac{f(\vec{v})}{v} d^3v$$

Schnee, R. W. (2009). Introduction to Dark Matter Experiments. In Theoretical Advanced Study Institute in Elementary Particle Physics. Boulder, Colorado, USA.



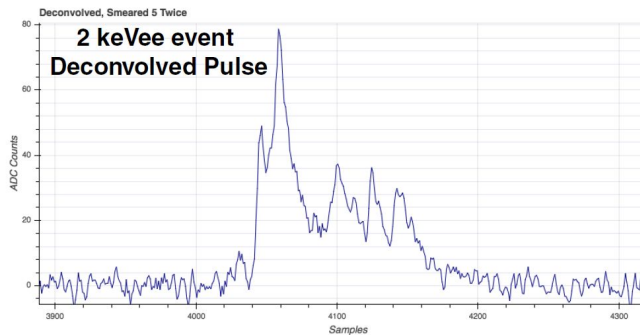
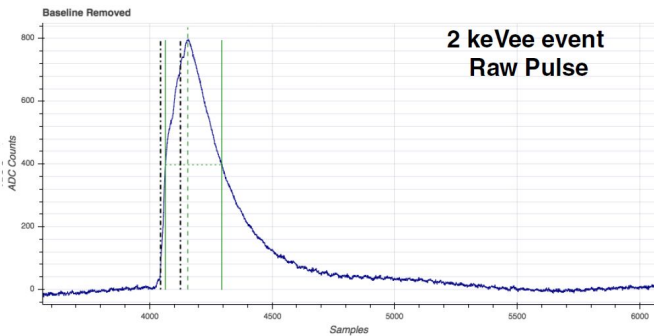
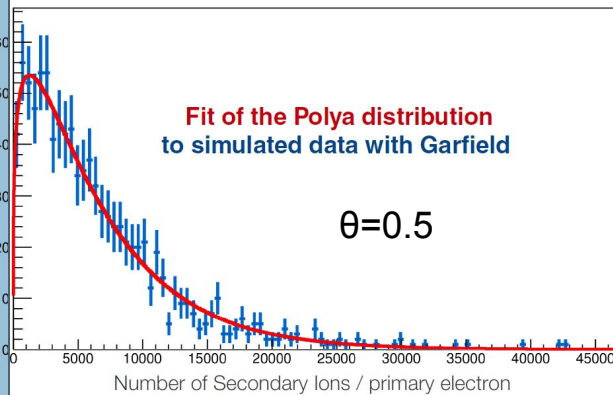


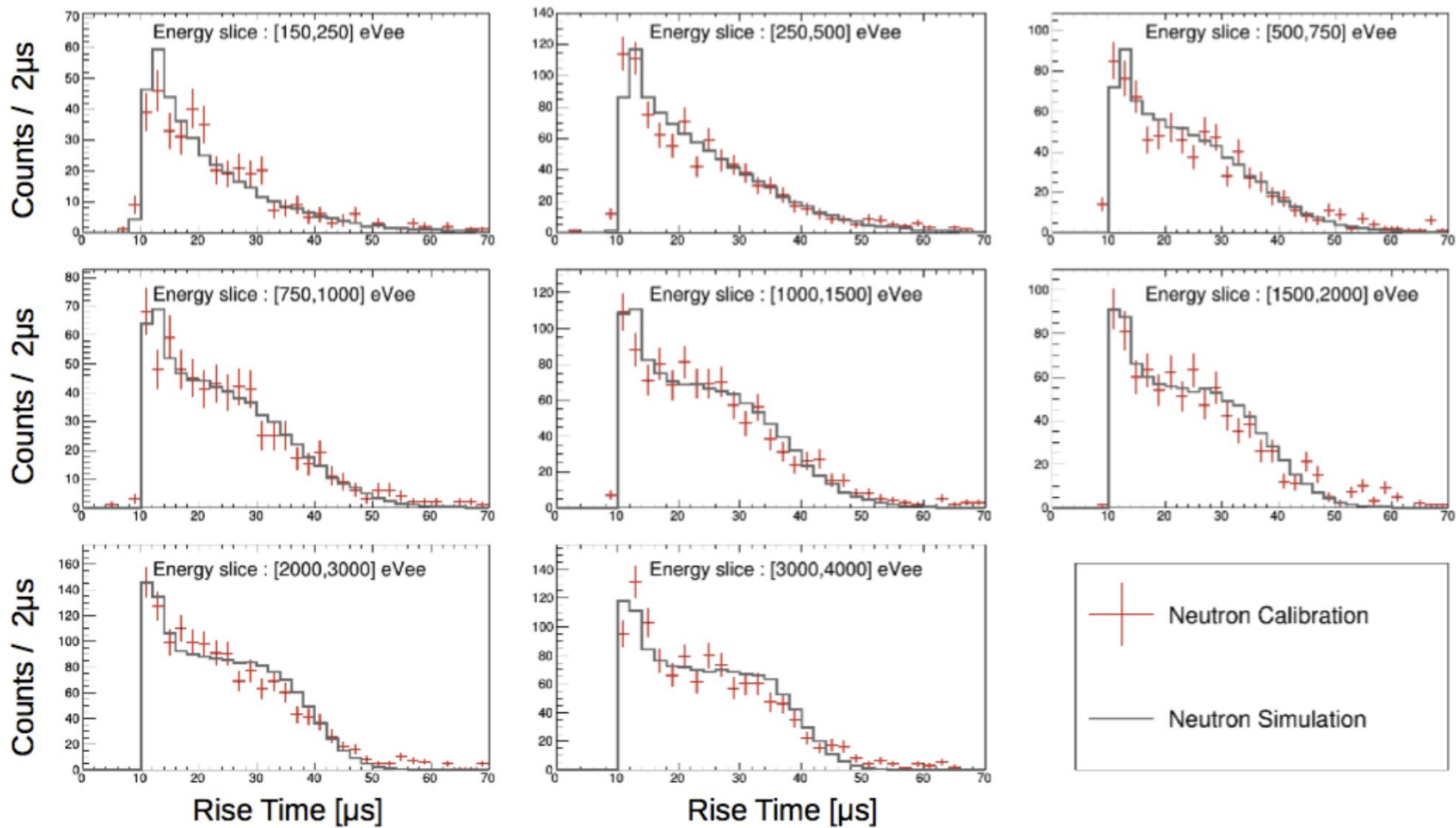
Avalanche process

$\langle \text{Gain} \rangle \sim 7000$ secondary ions / primary electron

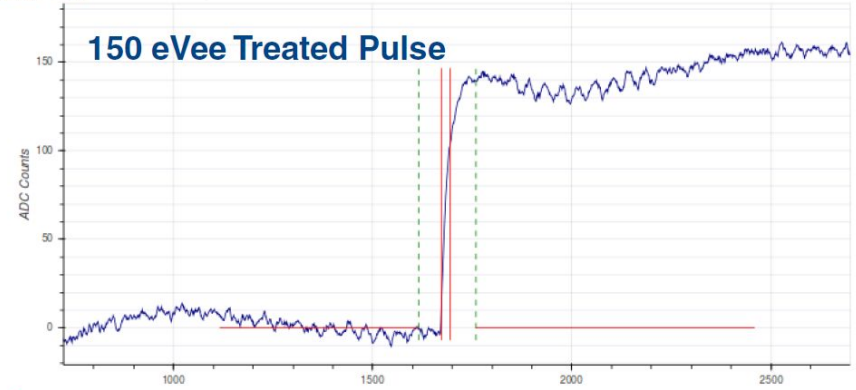
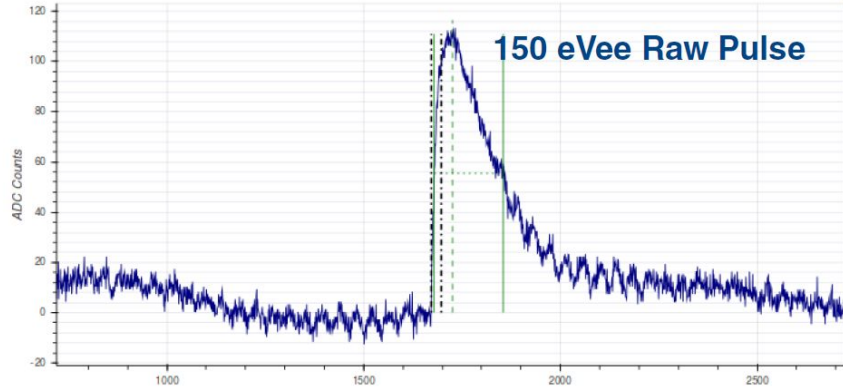
$$W_{\text{Ne}} = 36\text{eV}$$

large statistical fluctuations

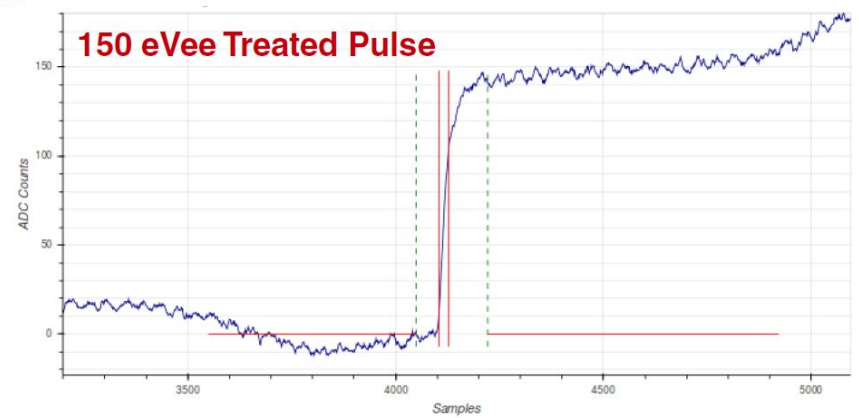
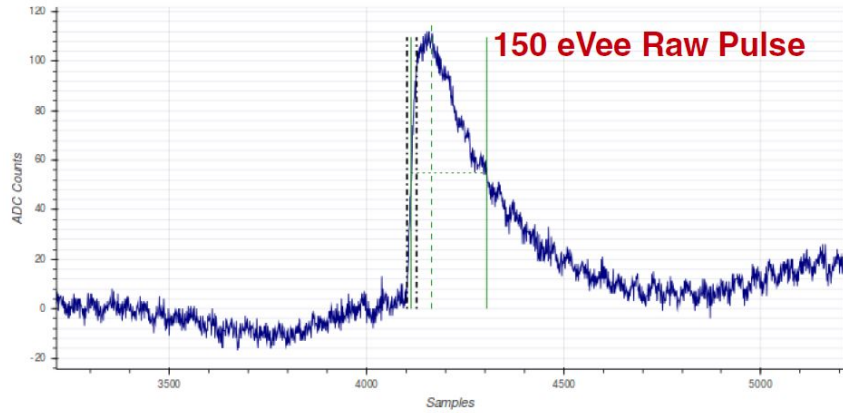


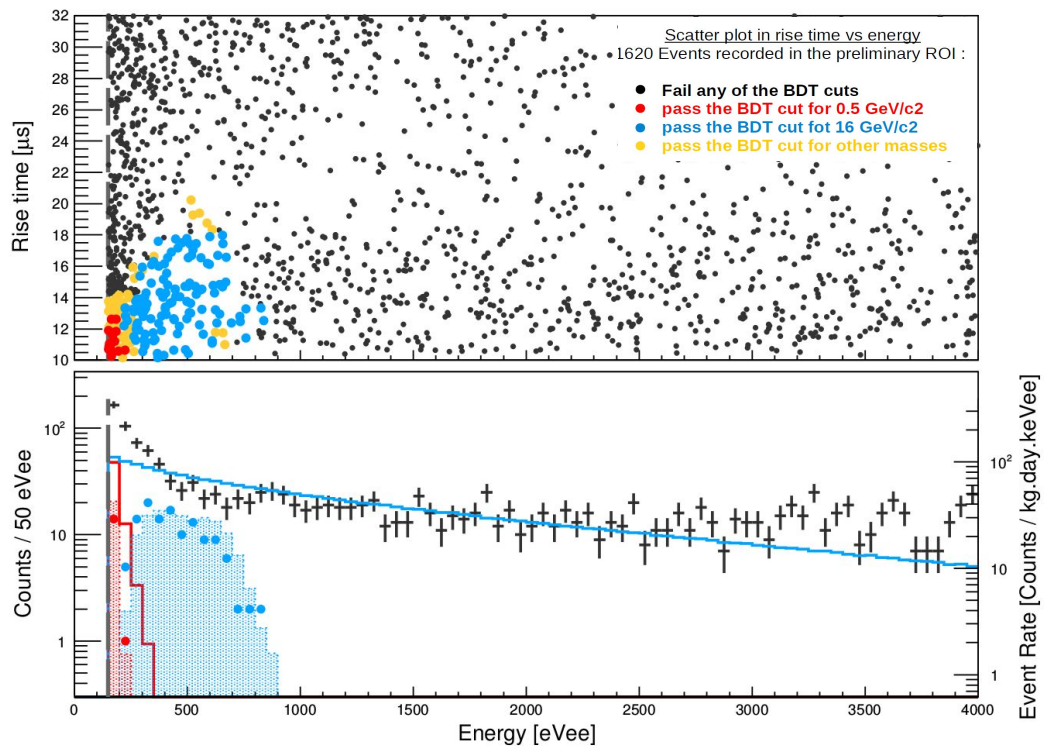


Simulation



Data

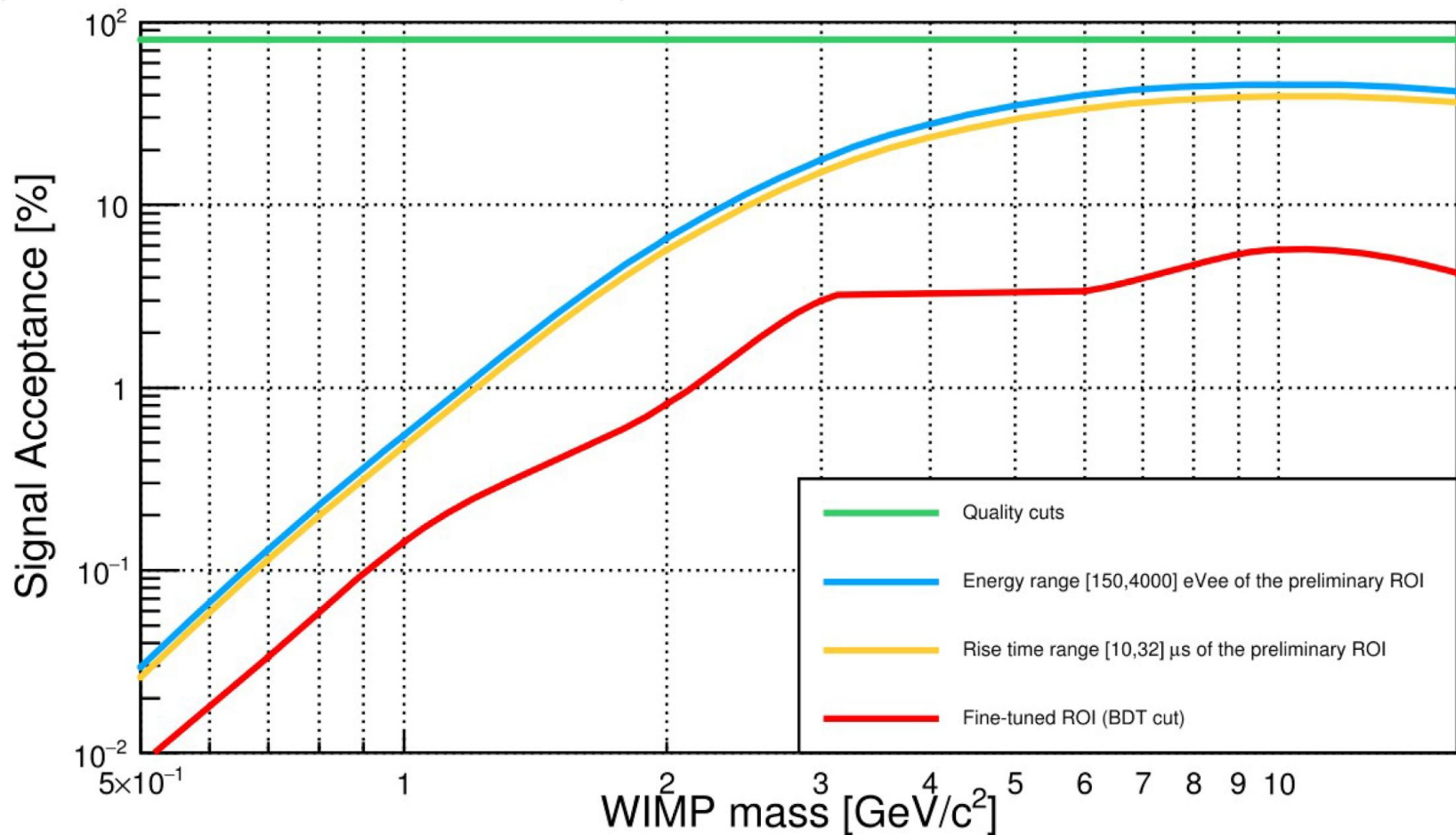




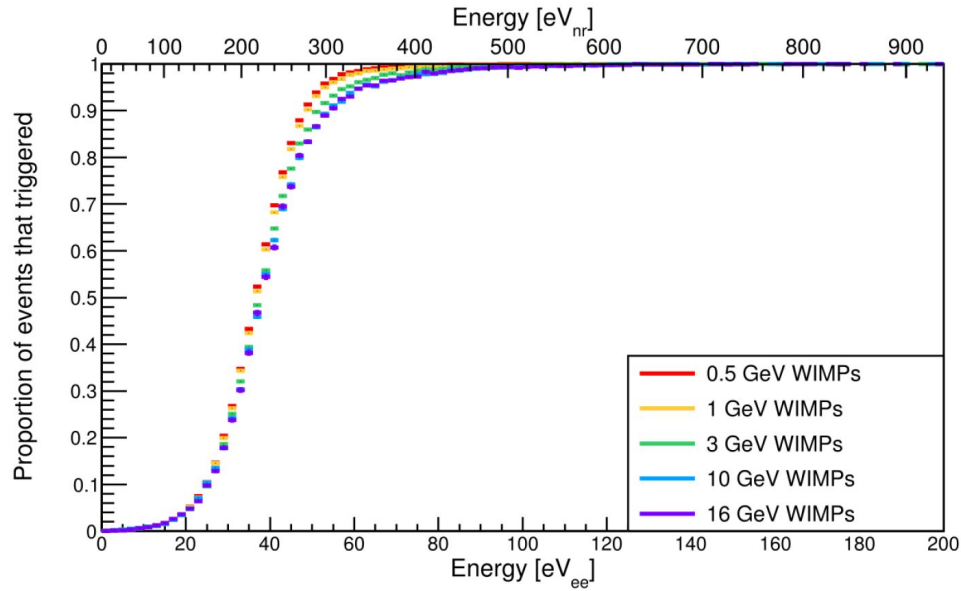
Top panel: distribution of the 1620 events recorded during the physics run in the preliminary ROI. Events that fail (resp. pass) the BDT cut for any of the WIMP masses are shown in black (resp. colour) dots. Events accepted as candidates for 0.5 GeV/c² and 16 GeV/c² WIMP masses are shown in red and blue, respectively, while for intermediate WIMP masses, candidates are shown in yellow.

Bottom panel: the energy spectrum of events recorded during the physics run in the preliminary ROI is indicated by the black markers. Energy spectra of 0.5 GeV/c² and 16 GeV/c² WIMP candidates are shown in red and blue dots. The energy spectra before and after the BDT cut of simulated 0.5 GeV/c² (resp. 16 GeV/c²) WIMPs of cross section $\sigma_{\text{excl}}=4.4 \times 10^{-37} \text{cm}^2$ (resp. $\sigma_{\text{excl}}=4.4 \times 10^{-39} \text{cm}^2$) excluded at 90% (C.L.) are shown in unshaded and shaded red (resp. blue) histograms, respectively.

Proportion of simulated WIMPs that pass a successive set of cuts vs the WIMP mass



Analysis threshold set @ 150 eVee far above the trigger threshold of ~35 eVee (100% trigger efficiency @ 150 eVee)

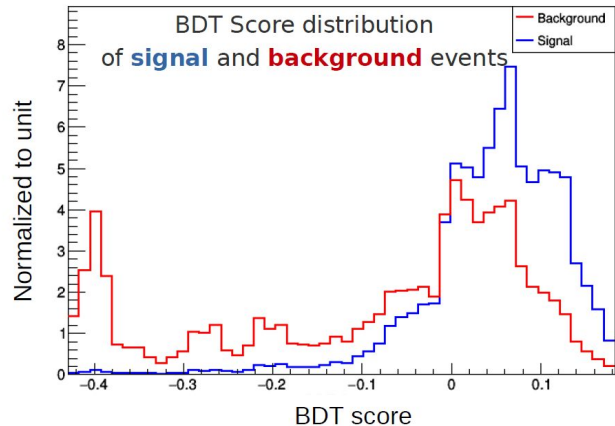
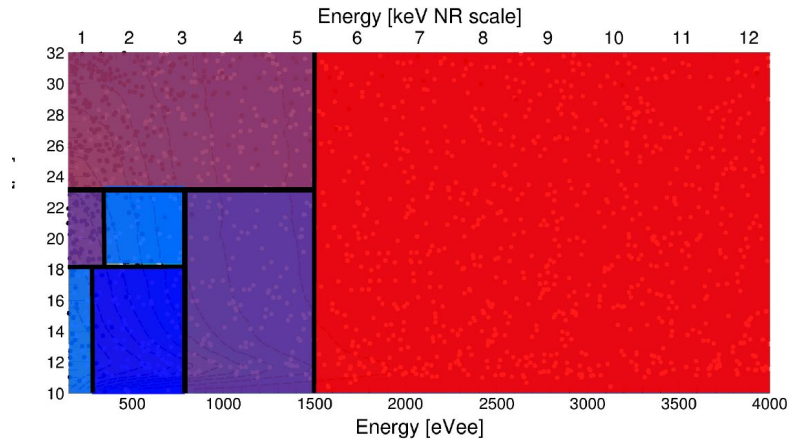


Proportion of events that trigger when pulses are added on top of a baseline vs the energy of the pulse alone

Trigger efficiency derived from simulated WIMP events of various masses to point out its dependence with the WIMP mass.

The trigger algorithm performs slightly better for single PE events

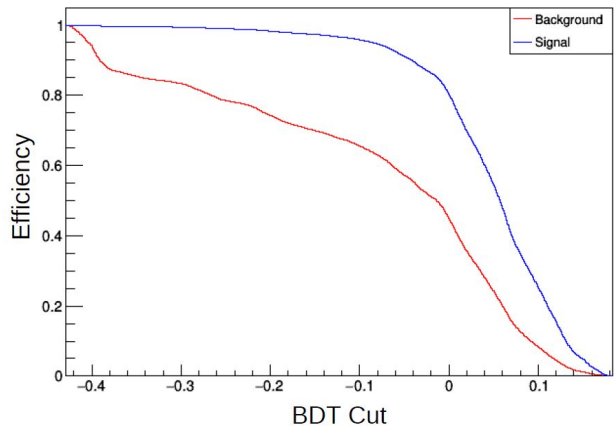
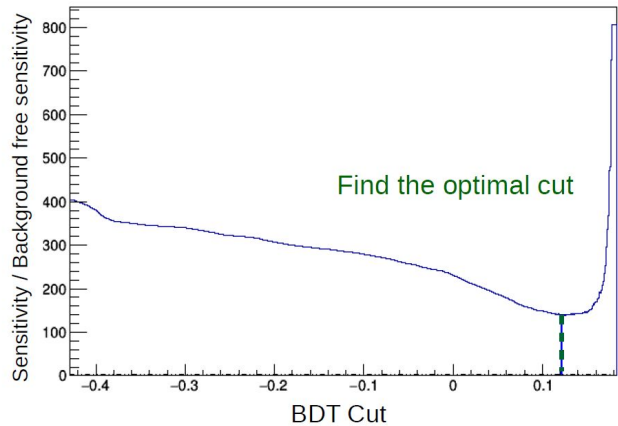
For 0.5 GeV WIMPs : mostly single PE events VS For higher WIMP masses : single & multiple PE events



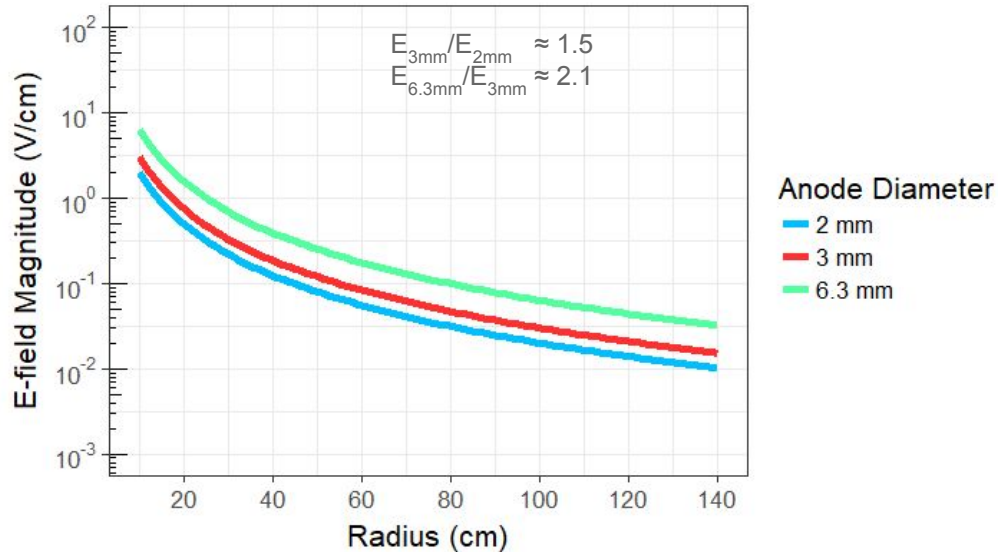
Background like
low BDT Score



Signal like
high BDT Score



The weak electric field



Comparison of E-field magnitude for different anode diameters (HV=2000 V)

AIM:

1. Operation in high pressure
2. Build larger volume detectors

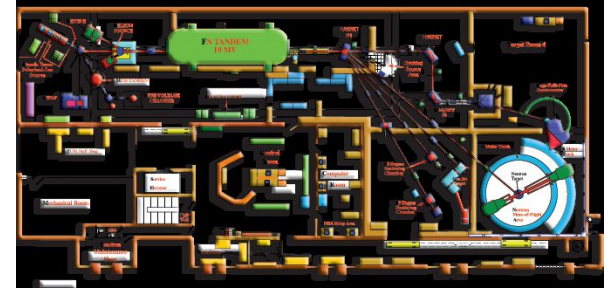
Conundrum:

Both Gain and Drift time are a function of E/P

$$\ln M = \int_{E^{(1)}}^{E^{(2)}} a(E/P) \frac{dE}{E}$$

$$v_{\text{drift}} = \mu \frac{E}{P}$$

Quenching factor measurements at TUNL



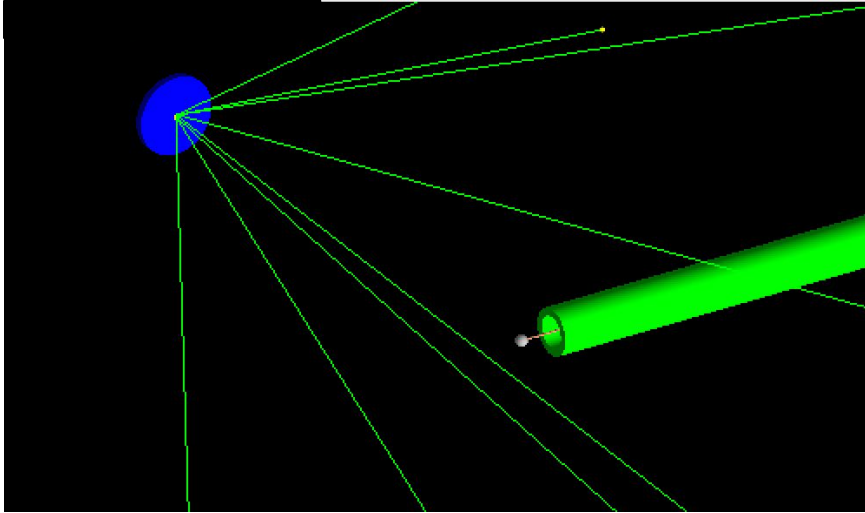
Why a spherical detector ?

Answer:

- **It is a geometry that permits the construction of robust, large volume detectors that can sustain high pressure with minimal material.**
- **The simplicity of the design permit a construction solely by radiopure materials**
- **The configuration of the electric field provide a handle for background rejection, through event discrimination and volume fiducialization**
- **The low capacitance even for large volumes provides single electron detection threshold**

An illustration of the method

The Geant4 simulation



The setup

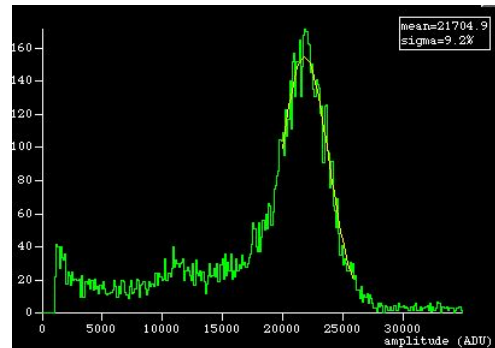
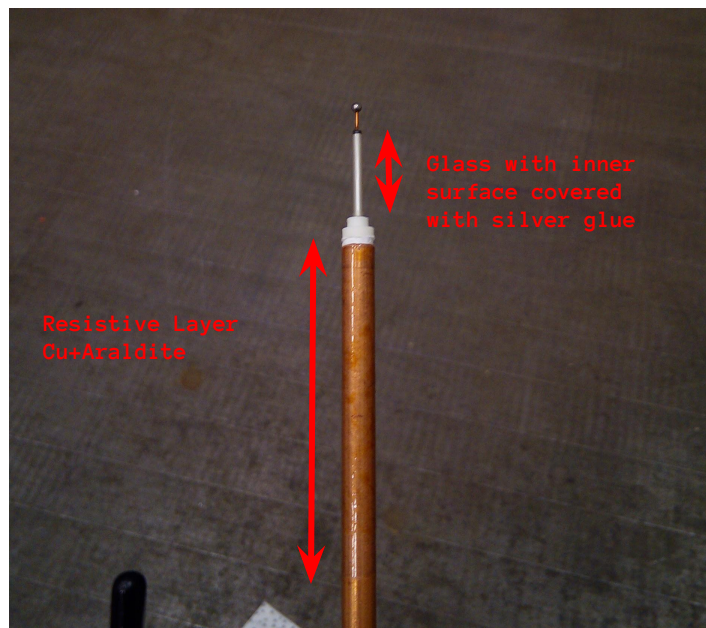
- SPC Φ 30cm
- Anode Φ 3 mm
- Gas Mixture He+10%CH₄ at 1 bar
- Copper rod include along with the wire
- **Fe55 X-ray source inside the detector (shielded)**

Low energy electromagnetic interactions enabled along with fluorescence models

Metallized glass umbrella

He + 29.7% Ar + 2.% CH₄ 700 mbar
HV1=1650 V, HV2= 0 V

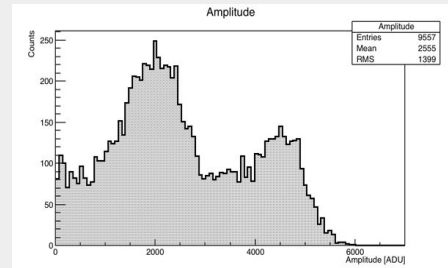
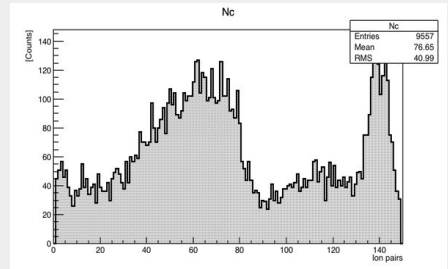
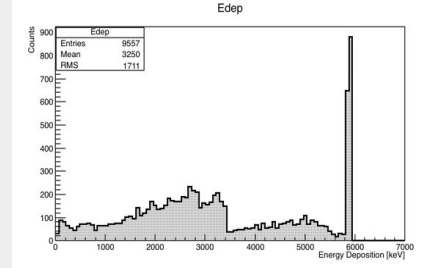
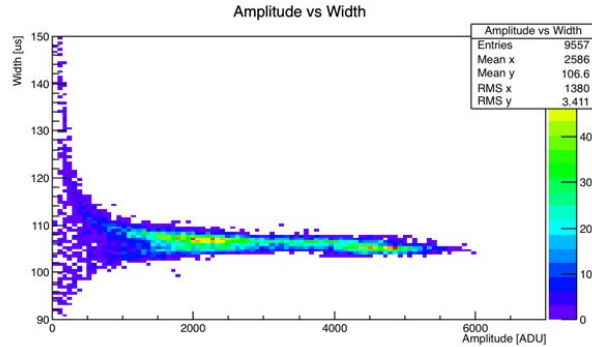
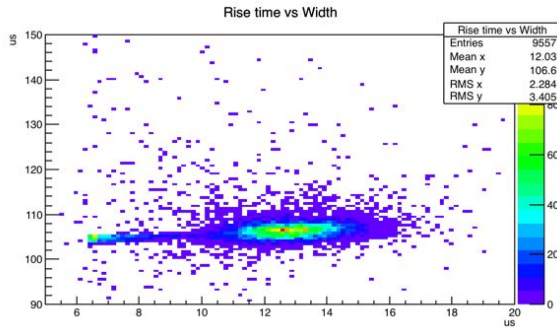
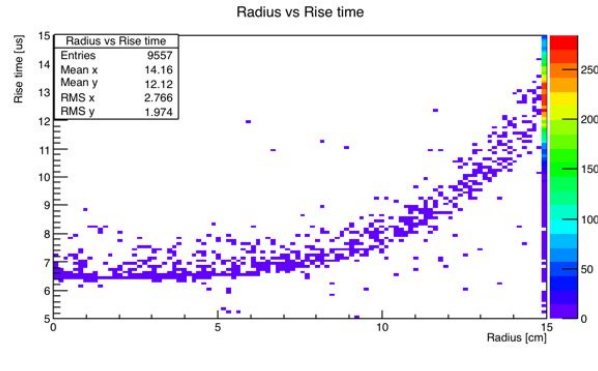
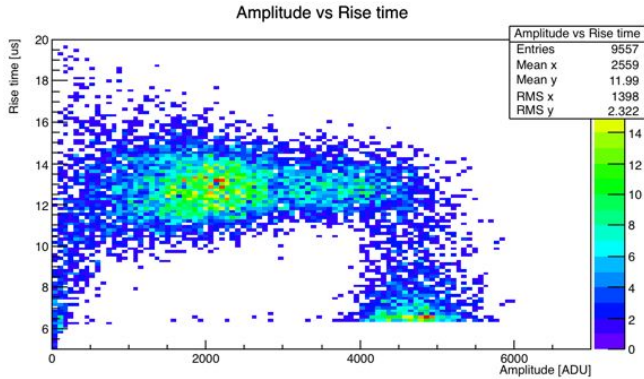
First results - Stability in high gain - Grounded umbrella



An illustration of the method

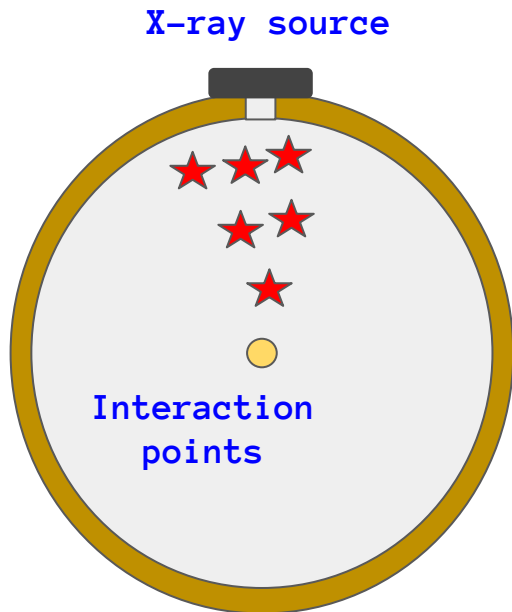
Assumed an $\tau=100 \mu\text{s}$ for our preamp with $g=0.45\text{mV/fC}$ and 50 ADU/mV 2800 V applied on Φ 3mm anode

From the initial interaction to the detector response



Background rejection capabilities-A

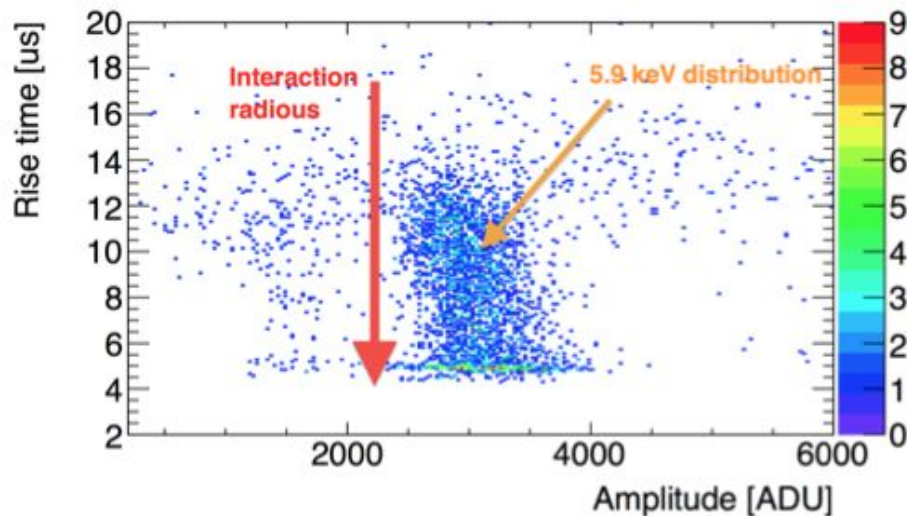
Fiducialization



Primary e- drift time dispersion

$$\sigma(r) \propto (r/r_{\text{sphere}})^3$$

5.9 keV X-rays line



Rise time $\rightarrow \Delta t$ between 90% - 10% of pulse height